(56)

NASA CONTRACTOR REPORT

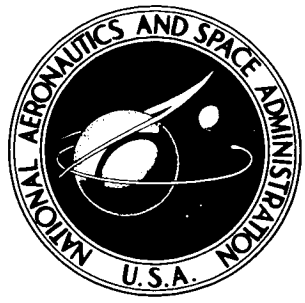

NASA CR-66301
NVR-5014

THE DESIGN AND DEVELOPMENT OF RADIO-FREQUENCY TRANSPARENT OMNIDIRECTIONAL ENERGY-ABSORBING ELEMENT SYSTEMS

by Ronald H. Smith

Prepared under Contract No. NAS 1-5329 *by*
NORTHROP CORPORATION
Newbury Park, Calif.
for

NATIONAL AERONAUTICS AND SPACE ADMINISTRATION • WASHINGTON, D.C. • JANUARY 1967

FINAL REPORT

THE DESIGN AND DEVELOPMENT OF RADIO-FREQUENCY TRANSPARENT OMNIDIRECTIONAL ENERGY-ABSORBING ELEMENT SYSTEMS

NVR-5014

January, 1967

NASA CR-66301
NVR-5014

FINAL REPORT
THE DESIGN AND DEVELOPMENT OF RADIO FREQUENCY TRANSPARENT, OMNIDIRECTIONAL, ENERGY-ABSORBING ELEMENT SYSTEMS

By

Ronald H. Smith

Prepared Under Contract No. NAS 1-5329
NASA Langley Research Center
Langley Station, Hampton, Virginia

NORTHROP CORPORATION, VENTURA DIVISION

1515 Rancho Conejo Boulevard
Newbury Park, California 91320

THE DESIGN AND DEVELOPMENT OF RADIO-FREQUENCY TRANSPARENT, OMNIDIRECTIONAL, ENERGY-ABSORBING ELEMENT SYSTEMS

ABSTRACT

The principal objectives of the program were the development, design, and fabrication of three types of RF transparent honeycomb, composite, and frangible tube element omnidirectional landing systems. Additionally the design and fabrication of a 1.5 foot diameter spherical test vehicle which was to be protected by these landing systems was required.

RF transparent filament-wound frangible tube tests on 1, 2, and 3 inch internal diameter were also specified to provide additional design data. Additional design information for the other element types was to be found in related literature.

The filament wound tubes proved too inefficient and 2 and 3 inch diameter glass fabric reinforced plastic tube tests were substituted. A franging force of 22 300 pounds for an efficiency of 16 800 foot pounds per pound was obtained with the 3 inch tubes. It was necessary to conduct limited nylon phenolic honeycomb and frangible tube anisotropy tests to provide design data. Lightweight 1.0 inch tube franging dies were also developed with a weight one sixth that of steel dies.

A sandwich shell spherical test vehicle with fiberglas skins and honeycomb/syntactic foam core was designed and fabricated, but the landing systems for each element type were not designed because spherical test segments for each element type developed instability after 2 inches of stroke and would have required more segment development effort.

FOREWORD

The final report, prepared in accordance with the requirements of Contract No. NAS 1-5329, covers analysis, design and experimental tests, including the fabrication of a test vehicle, performed during the period of 6 July 1965 through 18 November 1966. The work was sponsored by the National Aeronautics and Space Administration, Langley Research Center, with technical guidance provided by NASA Project Monitor, Mr. J. McGehee.

This program at Northrop Ventura was under the cognizance of Mr. W. R. Stoeltzing, Project Manager, and Mr. R. H. Smith, Project Engineer, assisted by Mr. R. L. Ranes. Acknowledgement is extended by the author to H. Caseldine, W. F. DeMario, and S. Bush in the design, fabrication and testing phases of the program.

CONTENTS

ILLUSTRATIONS

TABLES

SUMMARY

A program was conducted to develop, design, and fabricate three types of RF transparent omnidirectional energy absorbing landing systems for a 1.5 foot diameter instrumented test vehicle. Elements of honeycomb, composite and frangible tube type were specified for the landing systems.

Design data for each of the specified elements was to be obtained from the previous program[1] and from other literature, except for tests which were to be conducted on filament wound RF transparent tubes of 1, 2, and 3 inches in diameter to provide additional design data. Preliminary unsatisfactory test results for filament wound tubes resulted in the substitution of woven glass fabric reinforced plastic tubes. Franging forces as high as 22 300 pounds were obtained for one of the woven fabric 3 inch tubes with an efficiency of 16 800 foot pounds per pound without including die weight.

The stringent 20 pound weight limitation for the landing system could not be met for the frangible tube type unless lightweight dies were developed. Pour molded and reinforced epoxy dies developed and tested were under strength, but a pressure molded phenolic die with chopped glass fibers as reinforcement achieved a 28 000 psi strength for a weight which was one sixth that of the steel dies.

Anisotropy data for frangible tubes and non-metallic honeycomb elements was not available in the literature, therefore a limited test program for these properties was conducted.

The materials and elements design data was used in the evaluation of spherical and polyhedron shaped landing system preliminary design configurations. Trade-off configuration selection studies were conducted between weight, developed crushing force, and energy absorbed. The selected configurations for each type of honeycomb, composite, and frangible tube element system, consisted of 80 elements evenly spaced over the surface of the inner shell. Each element had

its axis aligned with the center of the sphere, and the spherical outer shell attached to the outer ends of the elements.

Three spherical static test segments of each element type and of equal weight were tested to determine energy absorbing efficiency. The honeycomb elements followed the calculated load-deformation curve but both the composite and frangible tube elements were considerably above the calculated curve up to 2 inches of stroke. Beyond 2 inches of stroke, in each case, the first circle of elements collapsed and the outer shell was crushed. It was determined that additional base support was required for the elements with some corresponding weight penalty.

The unsatisfactory segment test results prevented the design and development of an approved landing system until additional segment tests with stabilized elements can be successfully conducted.

The spherical test vehicle was designed and fabricated as two hemispherical sandwich shells with fiberglas skins and with a joining girth band. The core of the sandwich was made from nylon phenolic filled with syntactic foam. This high crushing strength core material was tested to more than 100 percent above landing impact loads with no permanent deformation. The fabricated test vehicle weighed 20 pounds.

INTRODUCTION

The design and development of an effective impact energy absorbing landing system for the protection of instrumented payloads during planetary exploration landings, is complicated by the lack of knowledge about the composition and structure of the atmospheres and landing surfaces of the planets. Instrumentated payloads which transmit data to the earth control center but which are not required to be oriented after landing, are most reliably protected by an omnidirectional impact absorbing landing system which is required to also be RF transparent.

The principal objectives of this program were the development, design, and fabrication of an instrumented payload test vehicle, and three types of RF transparent omnidirectional impact absorbing landing systems. The specific design requirements were for a 1.5 feet diameter spherical test vehicle of 25 pounds maximum shell weight, to contain 5 pounds of instrumentation and to be protected by omnidirectional landing system with a combined vehicle weight of 50 pounds. The protection system was required to limit impact deceleration to a maximum of 1000 earth g-units on impacting with horizontal and vertical velocity components of 100 feet per second in each direction. Additional requirements were for the landing systems and test vehicle to be fabricated as two hemispheres with provisions for joining the two sections. The test vehicle shell was also required to resist permanent deformation when subjected to loads 100% greater than the landing system design impact loads.

A preliminary design investigation was made of omnidirectional landing systems of spherical and polyhedron shapes. Candidate landing system design concepts were established for each of the three types of honeycomb, composite, and frangible tube element systems.

A test program was conducted on frangible tubes in accordance with the specific requirements that 1, 2, and 3 inch internal

diameter filament-wound tubes of RF transparent material be investigated. Preliminary test results indicated such low franging stress levels were obtained that the fabrication and testing of 2, and 3 inch diameter tubing of glass fiber fabric reinforced plastic was substituted with improved results.

Design information for honeycomb and composite elements was specified to be obtained from the previous elements test program and other literature available on the subject. Information was not found on the anisotropy properties applicable to the omnidirectional landing system design requirements, therefore a limited test program was conducted on honeycomb and frangible tube elements to obtain anisotropy values.

Preliminary calculations indicated that the frangible tube design concept would not be competitive with honeycomb or composite elements unless lightweight dies were developed. Although is was not a specific requirement of the program, lightweight plastic die tests were conducted and a pressure molded plastic die design was developed.

The materials and elements design information was utilized in a parametric analysis of candidate landing system where the developed crushing force, energy absorbed, and weight were the trade-off parameters. Spherical landing systems for each of the honeycomb, composite and frangible tube types were selected in the evaluation. Static testing of spherical test segments were conducted for each selected design type. Each type of test segment provided more efficient test results for the first 2 inches of stroke than was calculated, then a rapid drop in load caused by collapse of the elements occurred.

A spherical test vehicle based on the use of nylon phenolic filled with syntactic foam as a core material for the sandwich shell was designed and fabricated. Since satisfactory performance of the spherical test segments was not obtained, design and fabrication of the landing systems was not approved.

SYMBOLS

A_C = Cross-Sectional Area of Removed Corner Elements (sq. in.)

A_E = Cross Sectional Area Of Basic Triangular Elements (sq. in.)

A_E' = Cross Sectional Area of Hexagonal Elements (sq. in.)

A_{IS} = Surface area of inner shell (sq. in.)

a = Length of side of a polyhedron (in.)

b = Height of hexagonal cross-section (in.)

E_c = Modulus of elasticity in compression (psi)

E_{sp} = Specific energy (ft-lb/lb)

E_x, E_y = Compressive modulus of elasticity of reinforced plastic in direction of warp and 90° to warp, respectively (psi)

F_f = Franging stress (psi)

F_{cu_x}, F_{cu_y} = Compressive strength of reinforced plastic in direction of warp and 90° to warp, respectively (ksi)

F_{cy} = Compressive yield stress (ksi)

F_{su} = Shear strength (ksi)

F_{su_e}, F_{su_i} = Transverse shear strength, interlaminar shear strength respectively (ksi)

F_{tu} = Tensile strength (ksi)

F_{tu_x}, F_{tu_y} = Tensile strength of reinforced plastic in direction of warp and 90° to warp, respectively, (ksi)

G = Shear modulus (psi)

Symbols (Continued)

h	= Total element length (in)
	= Height of base area (in)
	= Sandwich shell thickness (in)
h_{Eff}	= Effective element stroke (in)
h_c	= Height of corner triangular section (in)
M.S.	= Margin of Safety
P	= Force (lb)
P_{CR}	= Collapse buckling pressure of a spherical shell (psi)
P_{TU}	= Burst pressure of a spherical shell (psi)
R	= Shell radius (in)
r	= Die Radius (in)
R_I	= Inner radius of shell (in)
R_O	= Outer radius of shell (in)
R_o	= Distance from landing system center to impact surface (in)
	= Landing system radius (in)
s	= Length of side of an element (in)
s_c	= Length of side of corner element (in)
t	= Tube or shell thickness (in)
t_f	= Sandwich facing thickness (in)
V	= Volume (cu.in.)
W_{CC}	= Weight of composite core (lb)
W_E	= Weight of element (lb)

Symbols (Concluded)

W_{80E} = Weight of 80 elements (lb)

W_{IS} = Weight of inner shell skin (lb)

W_J = Weight of girth band joint (lb)

W_{LS} = Weight of landing system (lb)

W_{OS} = Weight of outer shell skin (lb)

W_{TV} = Weight of test vehicle (lb)

μ_x, μ_y = Poisson's ratio of reinforced plastic in direction of warp and 90° to warp, respectively

ϕ = Apex angle of cone with impact surface as base

ρ_p = Density of fiberglas (lb/cu.in.)

PRELIMINARY DESIGN

The design approach, which has been used in establishing an effective impact energy absorbing landing system for the protection of payloads when landing on the unknown surfaces of planets, has been based on four general design objectives. The landing system will provide adequate omnidirectional energy absorbing capability, the impact shock level will be below specified limits, the configuration will be the lightest weight, and will be producible.

Detail design requirements which have been applied to the landing systems and the test vehicles are as follows:

Design Criteria.

1. Environment - room temperature and pressure test conditions.
2. Materials - efficient as energy absorbers and RF transparent after crushing.
3. Test Vehicle Geometry - 18 inches external diameter; designed as two hemispheres with provisions for joining.
4. Landing System Geometry - designed as two hemispheres with provisions for joining and attaching to the test vehicle.
5. Impact Velocity - 100 feet per second vertically
   100 feet per second horizontally.
6. Impact Shock - 1000 Earth G's maximum.
7. Weights - Total Impacting Vehicle 50 pounds
   Test Vehicle 25 pounds
   Instrumentation 5 pounds

8. Required Landing System Types - Honeycomb
Composite
Frangible Tubes

9. Test Vehicle Strength - The test vehicle shall be of adequate strength to resist permanent deformation under loads one hundred percent greater than the landing system impact loads.

Preliminary Calculations.

Landing System Weights - When the weight of the test vehicle and the instrumentation is subtracted from the total impacting vehicle weight a landing system weight of 20 pounds is obtained. This weight limitation has been rigidly held as a design parameter throughout the program.

Energy Absorption - A specified vehicle total weight of 50 pounds and a landing impact shock limitation of 1000 g's establishes the following upper limit on landing impact force:

$$P = 50{,}000 \text{ pounds}$$

If this total maximum force was absorbed by the crushing of one element as a steady load, the stroke required to absorb the energy of 50 pounds impacting at 100 feet per second both horizontally and vertically would be:

$$h_{Eff.} = 3.725 \text{ inches}$$

This is considered to be an effective stroke which for honeycomb materials is close to eighty percent of the actual length. The actual length for an eighty percent stroke would be:

$$h = 4.66 \text{ inches}$$

The actual length represents the minimum thickness for an omnidirectional impact attenuation system of any material which had an eighty percent stroke efficiency.

Geometry Considerations. - The geometry characteristics of an omnidirectional impact attenuation system are illustrated in figure 1. Figure 1a shows a high density energy absorbing system with a thickness, h, of 4.66 inches if a single element absorbs all of the impact and has an eighty percent stroke efficiency. Figure 1b shows a landing system of low density material with a landing system which is much thicker. If the landing impact is absorbed by a series of elements or by a continuous material such as layers of honeycomb, then the contact cone area with the apex angle ϕ is significant. In the high density configuration very little of the material at the extremes of the cone angle is at much of an angle to the load. The low density configuration shows that the material at the extreme of the cone angle is being bent or sheared rather than crushed.

Practical preliminary design considerations for landing systems which completely enclose the test vehicle require that polyhedron as well as spherical shaped systems be evaluated.

Polyhedron Shapes - A regular polyhedron is an enclosing shape composed of a repeating pattern of identical face shapes. The number of regular polyhedrons is limited to five as shown in figure 2. This figure shows that the regular polyhedron with the maximum number of faces is the icosahedron, which has twenty triangular faces and twelve vertices. The dodecahedron which is next to the icosahedron has twleve pentagonal faces and twenty vertices. The icosahedron can be modified by truncating the vertices, and the truncated icosahedron has twelve pentagonal faces and twenty hexagonal faces. This semi-regular polyhedron is compared with other polyhedrons of this class in figure 3.

Spherical Shapes - The division of spherical shapes into regular or semi-regular faces is presented in figures 4 and 5. Figure 4 shows the division of a spherical surface into twenty triangular shaped elements by the projection of an icosahedron shape on its surface. The actual projection of the triangular shapes of the icosahedron produces convex sides on the sphere as shown. Further division of

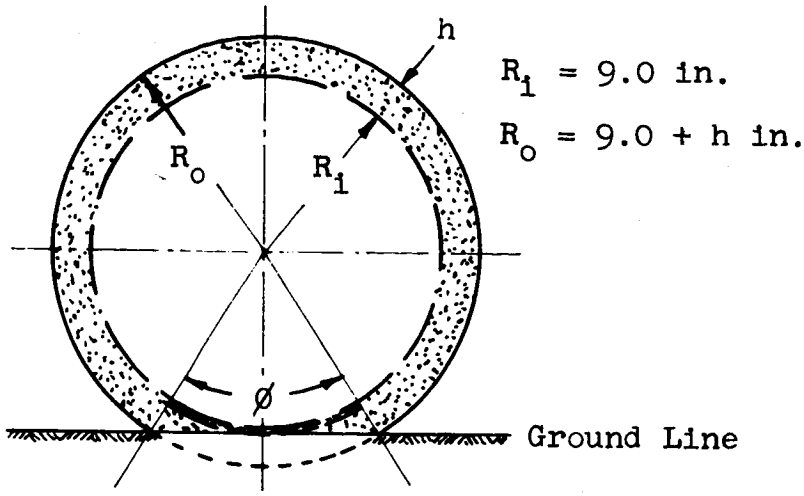

a. High Density Landing Impact Absorbing Material

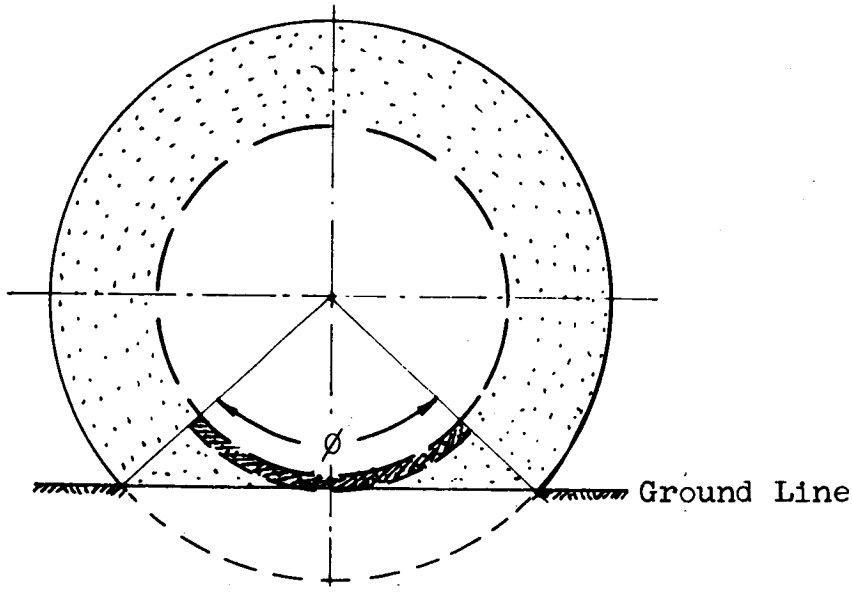

b. Low Density Landing Impact Absorbing Material

Figure 1. Characteristics Of Spherical Omnidirectional Impact Absorbing Landing Systems.

Polyhedron	Surface Area/a^2	Volume/a^3	a/R
Tetrahedron	1.7321	.1179	4.8970
Cube	6.0000	1.0000	2.0000
Octahedron	3.4641	.4714	2.4495
Dodecahedron	20.6457	7.6631	.89805
Icosahedron	8.6603	2.1817	1.3232

where "a" is the length of one side and "r" is the radius of an inscribed sphere.

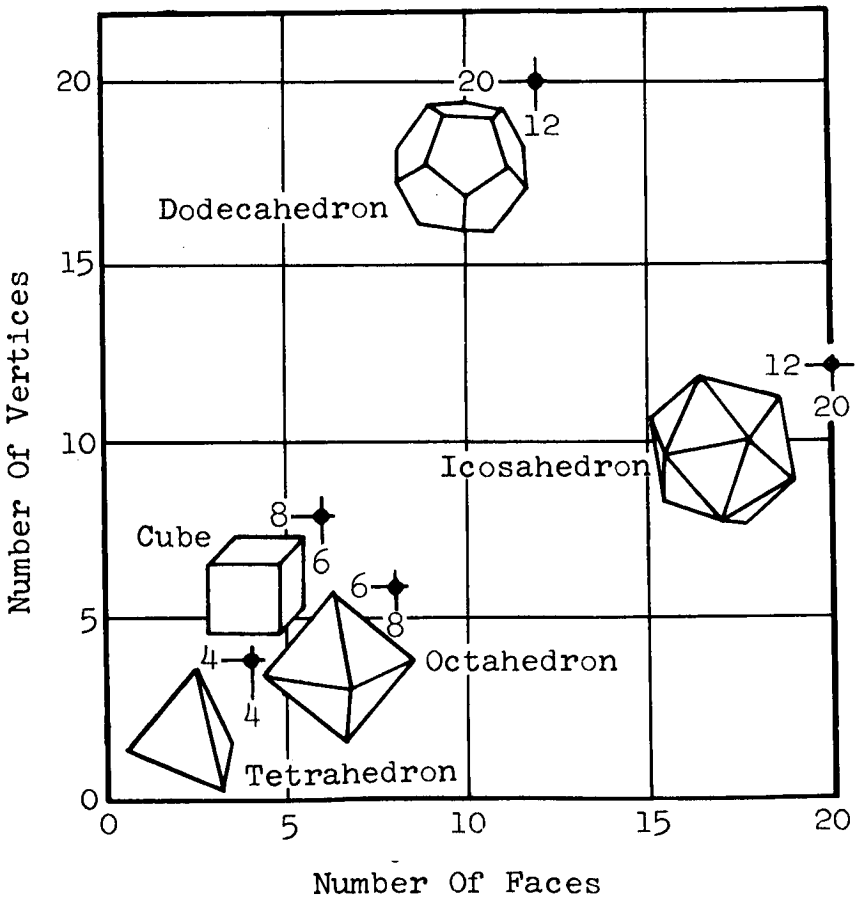

Figure 2. Relationship Of Number Of Faces To Number Of Vertices For Regular Polyhedrons.

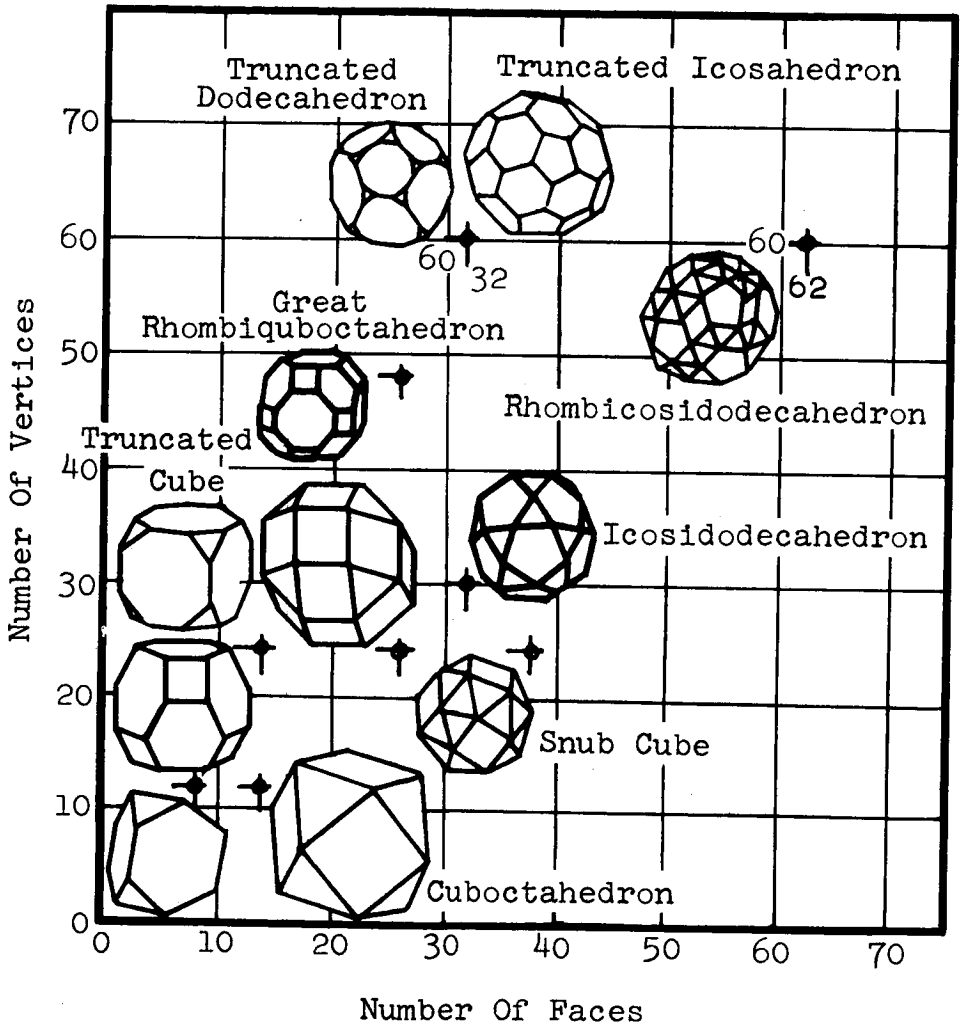

Figure 3. Relationship Of Number Of Faces To Number Of Vertices For Semi-Regular Polyhedrons.

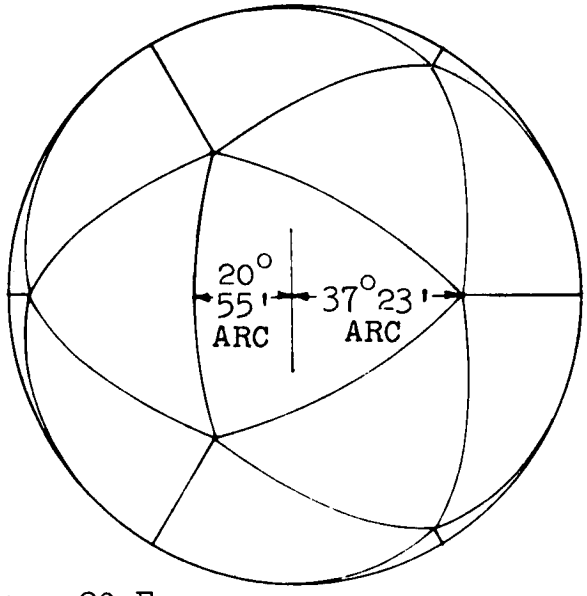

a. 20 Faces

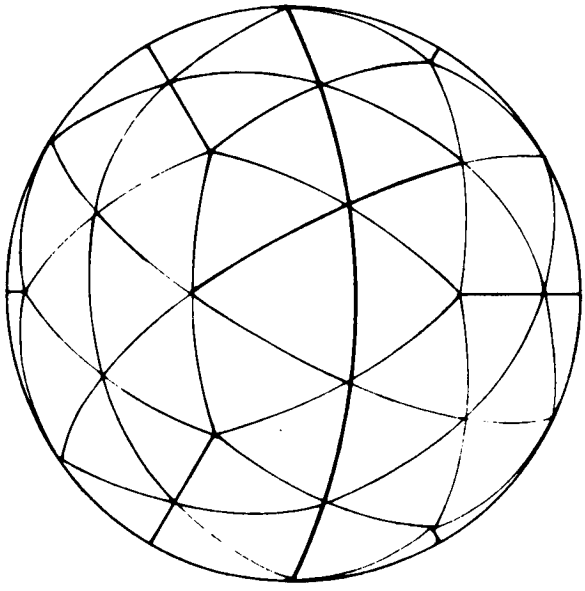

b. 80 Faces

Figure 4. Division Of Spherical Surface Into Regular Triangular Faces Based On Projection Of The Icosahedron Faces On The Surface.

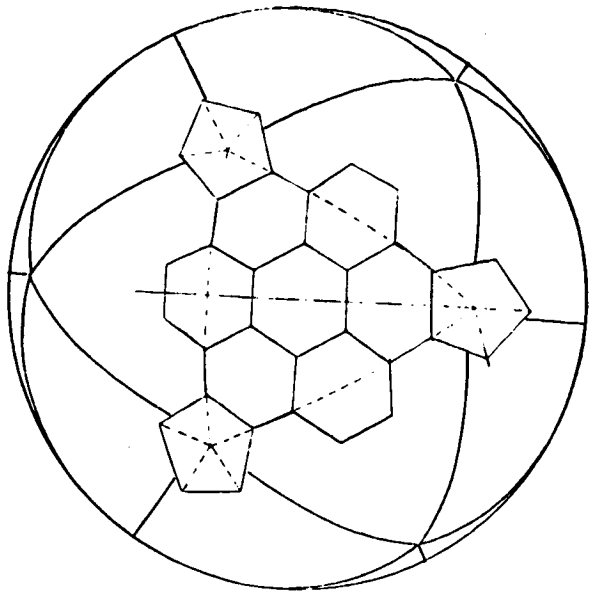

a. 122 Faces (110 Hexagons, 12 Pentagons)

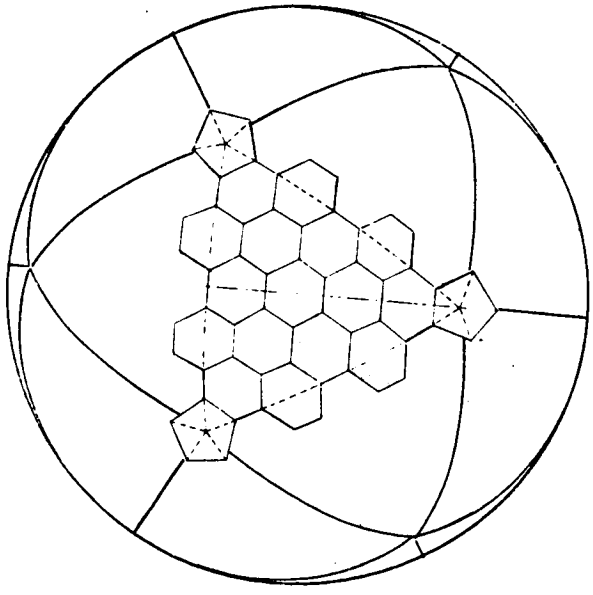

b. 272 Faces (260 Hexagons, 12 Pentagons)

Figure 5. Division Of A Regular Polyhedron Spherical Surface Into Additional Hexagonal And Pentagonal Faces.

the basic icosahedron pattern has been used to produce the 80 faces of figure 4b and the 122, and 272 faces of figure 5.

Landing System Configurations. - The basic requirement for the landing system is that it provide omnidirectional protection for the spherical test vehicle, which can be achieved by completely covering the test vehicle with spherical or polyhedron shaped landing system configurations. Concepts for spherical shaped systems are shown in figure 6 and polyhedron shaped systems are shown in figure 7.

Spherical - The spherical shaped landing system configurations shown in figure 6 consist of a honeycomb or composite layered construction, figure 6a, contoured honeycomb or composite rectangular segments, figure 6b, evenly spaced radially arrayed frangible tubes, figure 6c, and contoured triangular segments, figure 6d.

The spherically layered construction is a producibility problem, because the thickness of the layers is controlled by the cell size and the degree of double curvature to which the layers are stretch wrapped. The added weight of the plies between the layers contributes significantly to the total landing system weight because a minimum of two plies is required. The contoured rectangular segments provide the greatest stability for the landing system elements because they are interlocked. This type of construction would be best for resisting impact with a high horizontal velocity. The practical fabrication of the contoured elements would pose a significant problem, since weight restrictions limit the width of the elements to narrow strips. The radial frangible tube configuration requires the consideration for anchoring the tubes at each end, and does not ensure that impact with high horizontal velocity will not knock the tubes over. The contoured triangular segment configuration can be fabricated from a repeating pattern of triangular elements of constant cross section which could be stamped out; but a method for providing the end contour, which is not involved, is required.

Icosahedron - The icosahedron configuration concept shown in figure 7a consists of a series of twenty honeycomb or composite

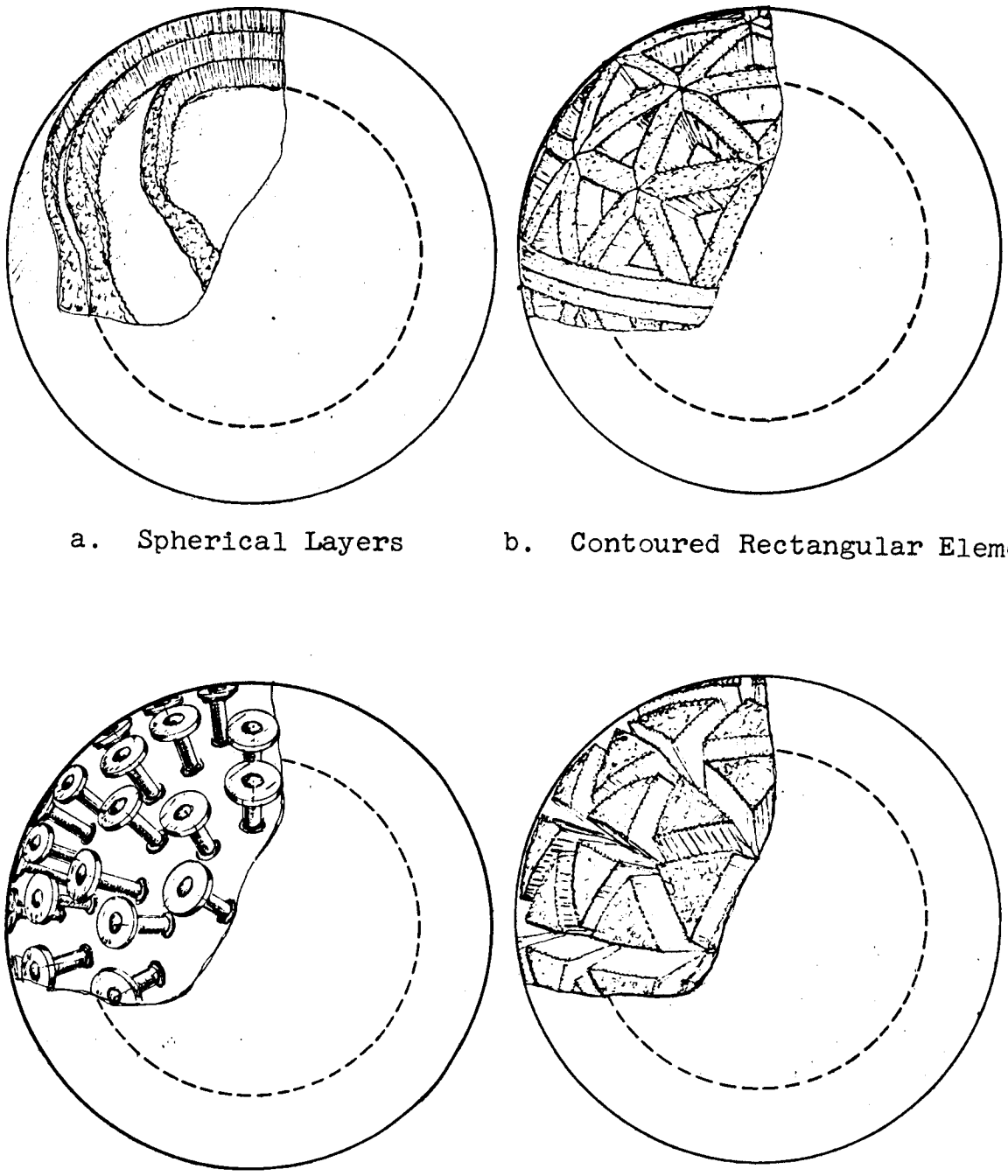

a. Spherical Layers

b. Contoured Rectangular Elements

c. Frangible Tubes And Dies

d. Contoured Triangular Elements

Figure 6. Spherical Landing System Configuration Concepts.

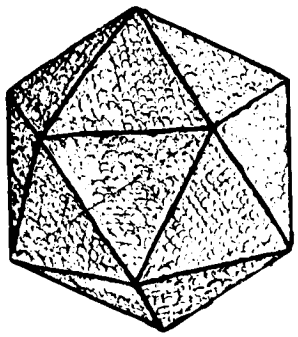

a. Icosahedron Shapes

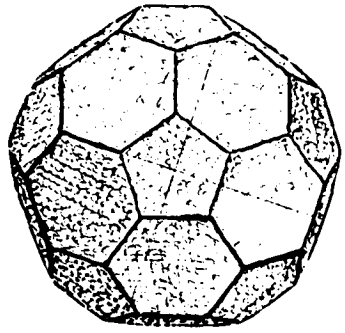

b. Truncated Icosahedron Shapes

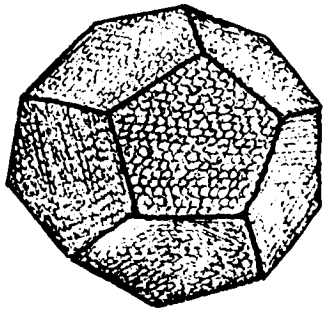

c. Dodecahedron Shapes

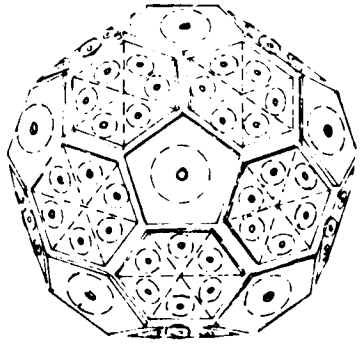

d. Truncated Icosahedron Frangible Tubes

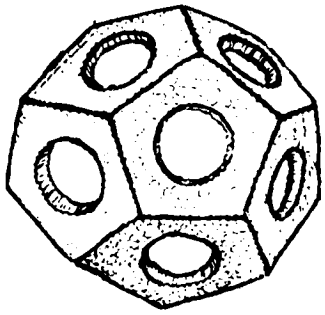

e. Lightweight Dodecahedron

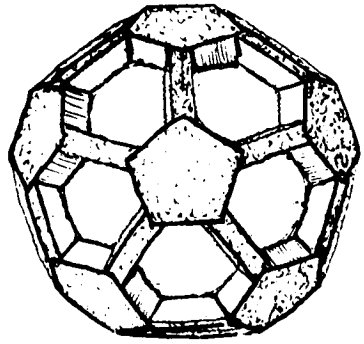

f. Lightweight Truncated Icosahedron

Figure 7. Polyhedron Landing Systems Configuration Concepts.

triangular section truncated pyramids which butt together and completely enshroud the test vehicle. Fabrication of these pyramid elements would require a fixture to ensure that each surface is cut to close tolerances.

Dodecahedron - The dodecahedron configuration concept is shown in figure 7c and 7e and consists of twelve honeycomb or composite, pentagonal section, truncated pyramids which butt together and form a complete protection for the test vehicle.

Truncated Icosahedron - The truncated icosahedron is shown in figure 7b, 7d and 7f and consists of twenty hexagonal section and twelve pentagonal section truncated pyramid honeycomb or composite elements in figure 7b. Figure 7d presents a configuration which uses twelve large frangible tubes one each on the pentagonal faces, and 120 small frangible tubes, 6 each on each hexagonal face. These tube franging elements support an outer sandwich skin element which is either pentagonal or hexagonal. The light weight configuration in figure 7f has twelve constant section pentagonal elements of honeycomb or foam joined by a total of thirty constant section rectangular elements.

MATERIALS AND ELEMENTS EVALUATION

Design information for each of the three honeycomb, composite, and frangible tube, omnidirectional impact attenuation landing systems was specified to be determined from the previous program,[1] from other literature, or from the additional tube franging tests on 1.0, 2.0 and 3.0 inch diameter filament wound tubes conducted in this program.

The omnidirectional impact attenuation requirements for these three landing systems place emphasis on establishing the anisotropy characteristics which are directly applicable to design concepts.

The specified weight limitations of 20 pounds maximum for each of the three landing systems limit material selections to those RF transparent materials with high specific energy absorption capability. In the previous program preliminary tests were conducted on light-weight franging dies with limited success. The rigid landing system weight restrictions establishes that the franging dies must be light-weight or the particular tube franging system would not meet the weight limitations, but the development of light-weight dies is not a specified requirement.

Each of the three energy absorbing element systems will be evaluated in order to establish sufficient design information to ensure the development of landing systems with reliable performance.

Frangible Tubes. - Frangible tube tests conducted in the previous program were limited to 1.0 inch internal diameter tubes fabricated by hand wrapping and later machine wrapping "E" glass fabric reinforcement in a "B" stage epoxy resin condition. Variations in tube performance were made by changing the number of plies and by using 181 bi-directional fabric or 143 uni-directional fabric. The 143 uni-directional fabric with maximum strength oriented in the longitudinal or "finger" direction of the tube achieved the greatest efficiency with franging stress levels as high as 25 000 psi, however, this configuration has a tendency to split, which was not true of the more reliable but less efficient 181 bi-directional fabric. A preliminary

plan for establishing tube wall thickness and die radii was based on the 181 fabric tube test results which indicated a target design stress level of 20 000 psi for tube franging could be used.

Material Evaluation. - This program specified that additional tube franging tests were to be conducted on RF transparent filament wound tubes in diameters of 1.0, 2.0, and 3.0 inches and at loading rates of one inch per inch. Preliminary tests were conducted using a 54° spiral wrapped "E" glass filament wound tubing and an epoxy resin system. The internal diameter of the tubing measured 2.095 inches, and wall thicknesses which gave a range of tubing to die radius ratios were machined to .063, .080, and .100 inches thickness. Short lengths of the tubing in each wall thickness were crushed to determine maximum compressive crippling strengths, and longer lengths, close to estimated tube franging landing system application requirements were franged on dies. Test results were 8 430 pounds, or 19 800 psi crushing strength and 2 800 pounds or 6 580 psi franging strength for the .063 thick tube, and 3 000 pounds franging strength for the .080 tube. At this stage of the program the further testing of spiral wrapped filament wound tubing was stopped due to the extremely low efficiency. Figure 8 shows the franging sequence in a 2.0 inch diameter spiral wrapped tube, which indicates that finger forming does not occur with this method of construction and may be the cause for the low franging force.

A different filament wound tube fabrication approach was also tried using "B" stage epoxy resin filled non-woven filament tapes of new high strength "S-994" glass on the tape wrapping machine. A strength comparison of woven fabric reinforcements in the conventional "E" glass with fabrics in the high strength "S-994" glass can be made in Tables I and II respectively. A significant improvement in tensile and compressive strength is shown for the "S-994" glass but a significant reduction in interlaminar shear is noted. The "S-994" material is supplied as single layer, non-woven parallel filaments held together by the "B" stage epoxy resin. The material is produced as

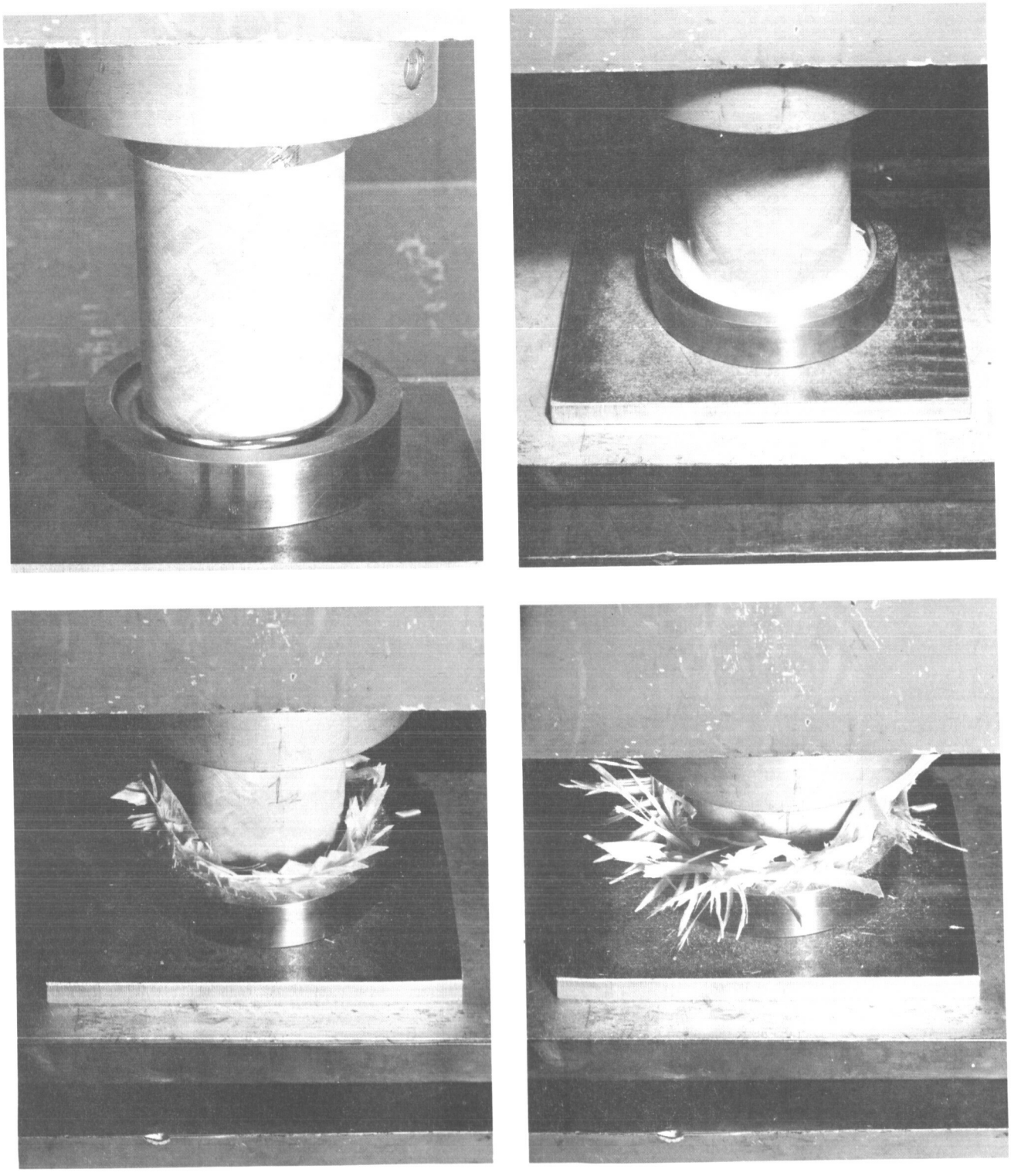

Figure 8. Typical 2.0 Inch I.D. Tube Fragmenting Sequence For Specimens of Epoxy Resin and "E" Glass Filament Wound Reinforcement.

TABLE I. MIL-HDBK-17 DATA (WET)
MECHANICAL PROPERTIES OF "E" GLASS AND EPOXY RESIN SYSTEM
AND DATA FOR ALUMINUM TUBING FROM MIL-HDBK-5

Fabric Weave	$\frac{E_x}{10^6}$ (psi)	$\frac{E_y}{10^6}$ (psi)	$\frac{\sqrt{E_x E_y}}{10^6}$ (psi)	$1-\mu_x\mu_y$	F_{cu_x} (ksi)	F_{cu_y} (ksi)	F_{tu_x} (ksi)	F_{tu_y} (ksi)	F_{su_i} (ksi)	F_{su_e} (ksi)	$\frac{G}{10^6}$ (psi)
181	3.28	3.14	3.21	0.980	45	38.2	45	42.4	6.79	14.0	0.810
143	5.12	2.08	3.26	0.972	60	26.3	85.0	10.2	3.69	7.86	0.590
2024-T3 Aluminum	$E_c = 10.7$			0.889	$F_{cy} = 42$		$F_{tu} = 64$		$F_{su} = 39$		4.0

TABLE II. MECHANICAL PROPERTIES OF S(994) GLASS AND EPOXY RESIN SYSTEM

181	Wet	3.88*	3.48			61.1*		88.0*		4.26*		
	Dry	4.01*	3.37	3.68	0.980	62.1*	52.7	87.2*	8.21	3.95*	18.27*	0.810
143		6.25	2.23	3.735	0.972	81.8	36.3	130.0		2.15	10.26	0.590

The values shown in the table not marked * were ratioed from MIL-HDBK-17 values; i.e.,

$$E_{x_{143(S)}} = E_{x_{181(S)}} \frac{E_{x_{143(E)}}}{E_{x_{181(E)}}}$$

tape or sheet and can be stacked in parallel or cross-laminations as required. Tensile, compressive and flexure test coupon specimens were fabricated and tested prior to tube fabrication, and established that material strengths were within rated strength limits. Tubes in 2.0 inch internal diameter size were tape wrapped using the machine wrapping process described in the previous program. A total of eight plies were used in each tube specimen in various combinations of hoop or longitudinal layup for three tubing specimens as follows:

Specimen	Hoop Layer	Longitudinal Layer
1	1, 2, 8	3, 4, 5, 6, 7
2	1, 2, 7, 8	3, 4, 5, 6
3	1, 3, 5, 7	2, 4, 6, 8

The wall thickness of the tubing when fabricated was in the range of .060 to .068 inches. Crushing load for short tube lengths ranged from 2 400 pounds to 2 800 pounds with similar low franging load levels regardless of the variation in layer orientation. The franging sequence for this method of filament wound fabrication is shown in figure 9. This figure shows that finger forming did occur but that the fingers showed complete delamination between layers.

Table II showed that interlaminar shear strength was lower for this high strength material than the "E" glass. It was concluded that further testing of filament wound construction was delaying the program effort and would not provide efficient test results, therefore filament wound tube franging was abandoned.

Diameter Evaluation. - The previous program had demonstrated that "E" glass 181 glass fabric reinforced plastic tubes with an epoxy resin system would frange at stress levels near 20 000 psi at most efficient thickness to radius ratio. A continuation of the woven fabric reinforced tube franging evaluation was made in this program, using the machine wrapped fabrication and testing procedures identical to the 1.0 inch tube program, for 2.0 inch and 3.0 inch internal diameter tubing. Figure 10 shows a comparison of franged

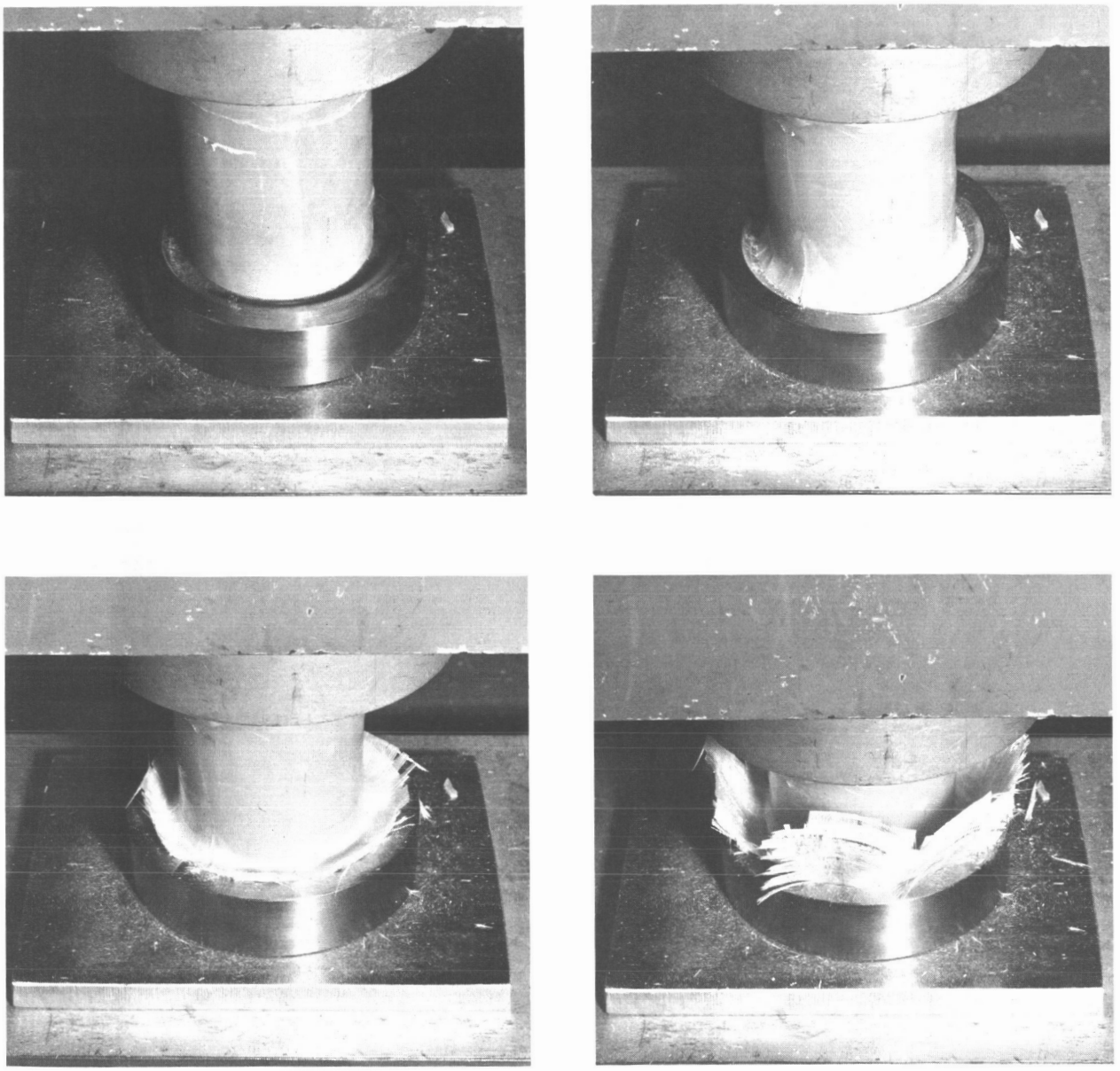

Figure 9. Typical 2.0 Inch I.D. Tube Fragmenting Sequence For Specimens of Epoxy Resin and "S-994" Glass Filament Tape Reinforcement Laminations.

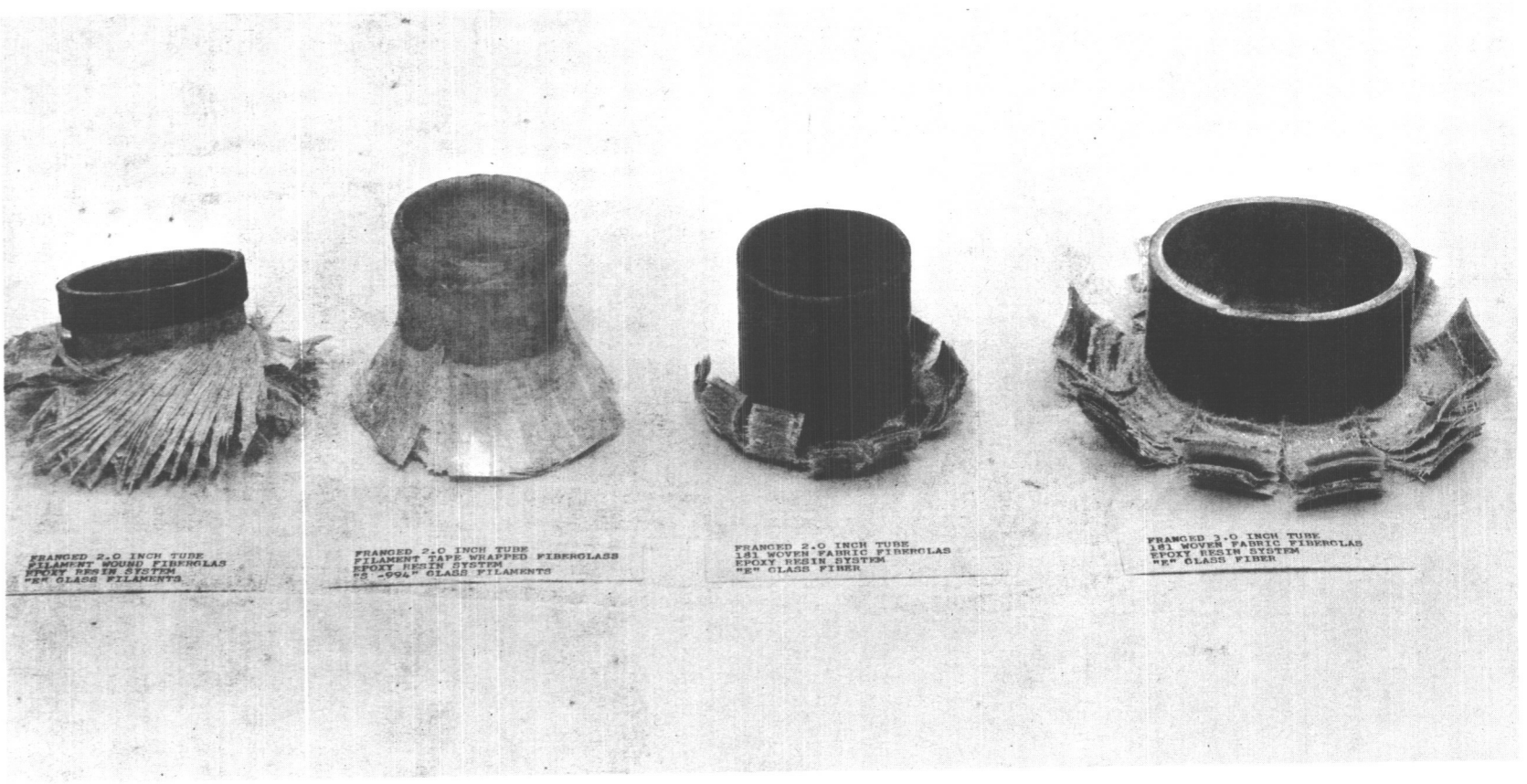

a. "E" Glass Filaments

b. "S-994" Glass Tape

c. "E" Glass Fabric

d. "E" Glass Fabric

Figure 10. Typical Franged 2.0 Inch and 3.0 Inch Diameter Tube Fabricated With Epoxy Resin and Glass Fiber Reinforcements Noted For Each Specimen.

spiral wrapped and tape wrapped filament wound 2.0 inch tubes with the 2.0 inch and 3.0 inch woven fabric tubes. Both the woven fabric tubes have distinct finger forming characteristics that are similar to the 1.0 inch tubes of the previous program. The results of the 2.0 inch woven fabric tube tests are presented in Table III, and the 3.0 inch tube test results are presented in Table IV. The test objectives were to approach a franging stress level of 20 000 psi as obtained in the 1.0 inch tubes, and thus provide franging force levels with the number of plies chosen which would be applicable to some of the preliminary design configurations discussed for frangible tube landing systems. It was determined that the range of maximum efficiency for the 2.0 inch tubes was for t/r's between .480 and .560 and the highest stress levels were close to but below 10 000 psi. The specific energy for the most efficient tubes, neglecting die weight, did exceed the 10 000 ft-lb/lb limit specified in the previous program.

Initial tests of the 3.0 inch diameter tubes resulted in extensive full length tube splitting as recorded in Table IV. Additional tests fragmented and achieved stress levels as high as 13 400 psi with the highest franging force reaching 22 300 pounds. The most efficient thickness die radius ratio ranged from .527 to .636, and the highest specific energy was 16 800 ft-lb/lb which was also considerably above the 10 000 ft-lb/lb objective of the previous program, again neglecting die weight. The load displacement graph for the most efficient 3.0 inch tube tested is shown in figure 11. This graph is typical for the 2.0 and 3.0 inch diameter woven fabric reinforced tubes. The graph shows that an initial rapid buildup of force occurs until the tube suddenly splits into "fingers" of considerable length. This splitting action is shown as a load relief and the load stays approximately level until further franging, or finger forming occurs. The 2.0 and 3.0 inch tubes had a tendency to split the total length of the tube before franging action was noticed. An examination of these split tubes showed no defects in fabrication which could explain this tendency.

TABLE III. TEST RESULTS FROM 2.0 INCH DIAMETER TAPE-WRAPPED TUBES OF EPOXY RESIN WITH 181 GLASS FABRIC

No. of Plies	r(in)	t/r	P_{ave} lb	F_f psi	$E_{sp} \times 10^{-3}$ ft-lb/lb
8	0.20	0.380	3300	6940	9130
8	0.20	0.390	3300	6740	8900
8	0.20	0.400	2800	5580	7940
8	0.20	0.380	2600	5450	7450
8	0.20	0.375	3100	6580	9130
8	0.20	0.385	2850	5790	8800
8	0.20	0.410	2800	5440	8730
8	0.20	0.395	2900	5850	8250
8	0.22	0.363	3800	7580	9630
8	0.22	0.354	3100	6330	8500
8	0.22	0.359	3000	6050	8520
8	0.22	0.349	2700	5580	6730
8	0.22	0.363	2900	5780	7530
8	0.22	0.373	2600	5050	7270
8	0.22	0.355	2800	5710	8480
8	0.22	0.359	2900	5850	7720
8	0.22	0.359	3000	6050	7950
11	0.20	0.540	3700	5440	7390
10	0.20	0.515	3100	4780	6430
10	0.20	0.520	3100	4730	6500
11	0.20	0.560	5600	7940	11500
10	0.20	0.520	5500	8400	11800
11	0.20	0.545	6400	9360	13800
10	0.20	0.525	5100	7720	9920
11	0.20	0.540	5700	8370	11800
11	0.20	0.525	5800	8770	11750
10	0.22	0.455	4700	7490	10150
10	0.22	0.478	4300	6500	9520
11	0.22	0.492	5100	7500	10100
11	0.22	0.486	5000	4720	10430
10	0.22	0.468	4900	7550	10140
10	0.22	0.476	4800	7250	9150
14	0.22	0.637	5000	7640	11400
11	0.22	0.492	6700	9850	12000
11	0.22	0.487	5500	8170	10820

TABLE IV. TEST RESULTS FROM 3.0 INCH DIAMETER TAPE WRAPPED TUBES OF EPOXY RESIN WITH 181 GLASS FABRIC

No. of Plies	r in	t/r	P_{ave} lb	F_f Ave psi	E_{sp} ft-lb / lb	Remarks
15	.33	.471	--	--	--	Tube Split
15	.33	.461	10 000	10 500	9 110	
15	.33	.471	--	--	--	Tube Split
15	.33	.467	--	--	--	Tube Split
16	.33	.476	8 900	9 050	10 180	
16	.33	.500	8 800	8 500	9 370	
15	.30	.493	--	--	--	Tube Split
14	.30	.482	--	--	--	Tube Split
	.30	--	--	--	--	
14	.30	.477	8 700	9 700	10 300	
18	.30	.597	9 500	8 450	9 300	
18	.30	.601	--	--	--	Tube Split
18	.30	.587	--	--	--	Tube Split
18	.30	.608	--	--	--	Tube Split
18	.30	.587	--	--	--	Tube Split
18	.30	.597	--	--	--	Tube Split
19	.300	.636	21 600	11 900	16 300	Fragmented
20	.300	.670	15 500	8 600	5 020	Fragmented
19	.300	.627	12 900	7 300	9 550	Fragmented
18	.300	.586	13 700	8 260	8 220	Fragmented
18	.300	.600	18 900	11 100	12 900	Fragmented
18	.300	.593	12 700	7 560	9 220	Fragmented
19	.300	.633	22 300	12 500	15 700	Fragmented
19	.300	.623	21 500	12 200	16 800	Fragmented
19	.330	.564	20 900	11 900	15 400	Fragmented
18	.330	.539	19 000	11 350	12 600	Fragmented
17	.330	.527	22 000	13 400	15 400	Fragmented
19	.330	.583	19 600	10 800	15 900	Fragmented
19	.330	.570	18 000	10 180	11 500	Fragmented
18	.330	.561	13 000	7 470	9 460	Fragmented
17	.330	.513	18 000	11 320	14 740	Fragmented
17	.330	.518	20 500	12 720	13 900	Fragmented
17	.330	.533	13 000	7 850	8 930	Fragmented

Epoxy Resin System
181 "E" Glass Fabric
.187 (19 ply) in. Thickness
t/r = .623
Average Force $\overline{P}$ = 21,500 lb.
Average Stress $\overline{F}_f$ = 12,220 psi
Specific Energy E_{sp} = 16,800 ft-lb/lb

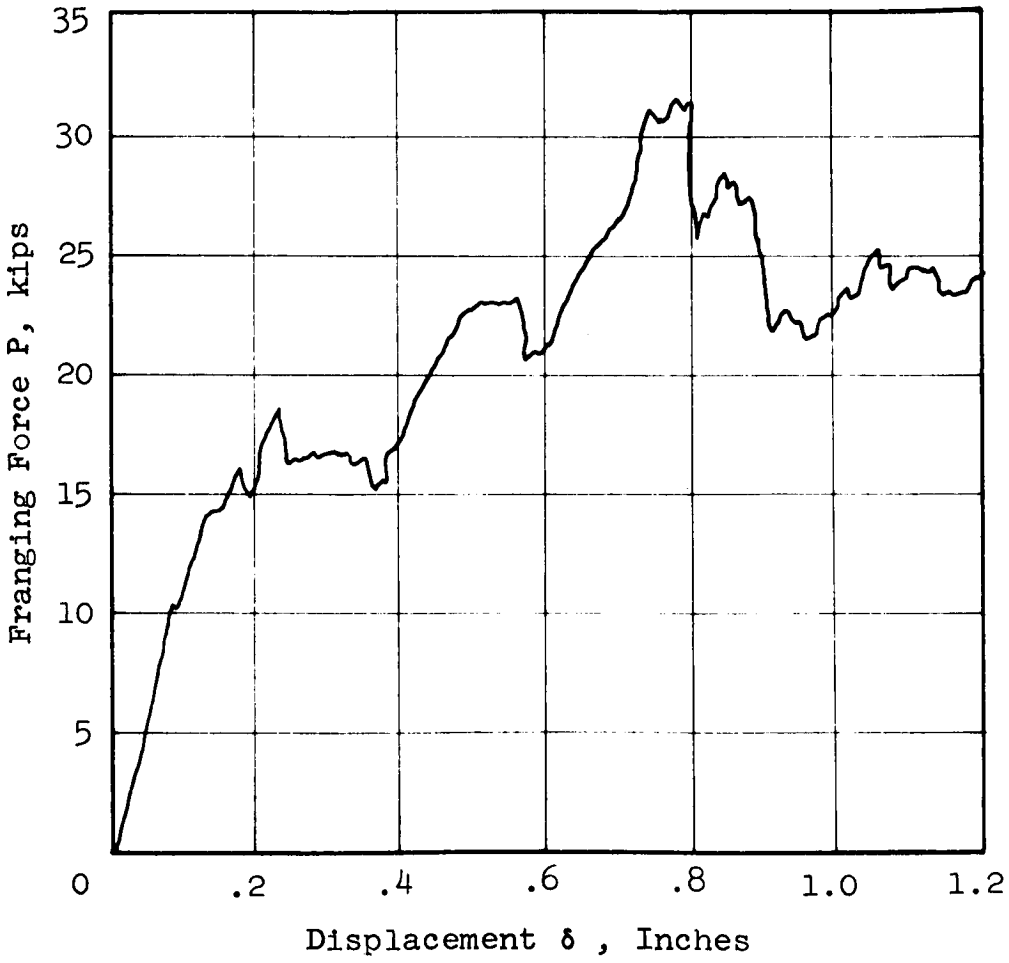

Figure 11. Typical Load Displacement Graph For 3.0 Inch I.D. Fabric Glass Fiber Reinforced, Epoxy Resin System Tube Fragmented Over A Steel Die.

Die Development. - The 2.0 inch and 3.0 inch mild steel dies used in the test program for filament wound and woven fabric tubes are shown in figure 12. No attempt was made to remove weight by drilling holes in the center of the steel dies since steel die weights would be excessively heavy. Figure 12 also shows some rubber molds which were made of these large dies in preparation for casting light-weight epoxy dies for further testing; however, the poor franging performance of the larger tubes stopped further consideration for dies in this size range.

The successful development of all three specified honeycomb, composite, and frangible tube element landing system significantly depends on meeting the weight limitation of 20 pounds for this system. This limitation is particularly severe for the tube franging system because the weight must include die weights.

The previous program effort does not provide design information for light-weight dies, and no design information is available from other literature. The initial tube franging program conducted by McGehee[2] on aluminum tubes does not consider die weight in the calculation of specific energy. The previous program[1] also ignores die weight in the specific energy calculations for RF transparent tubes, however, it was recognized that steel dies would be too heavy in an energy absorbing systems application and preliminary light-weight die tests were conducted.

The die development approach which was undertaken was to review the inadequacies of the 1.0 inch cast epoxy dies which were tested in the previous program. The bearing strength of the cast material proved to be critical, and caused die choking; also the die rim tended to fracture. An identical fabrication procedure for cast epoxy dies, as described in the previous program, was used with inner and outer rim fiberglas tube reinforcements added to the mold before the epoxy material is poured. Figure 13 compares the original steel die with three reinforced cast epoxy dies. The steel die weighs .312 pounds and the epoxy dies are one sixth of this weight.

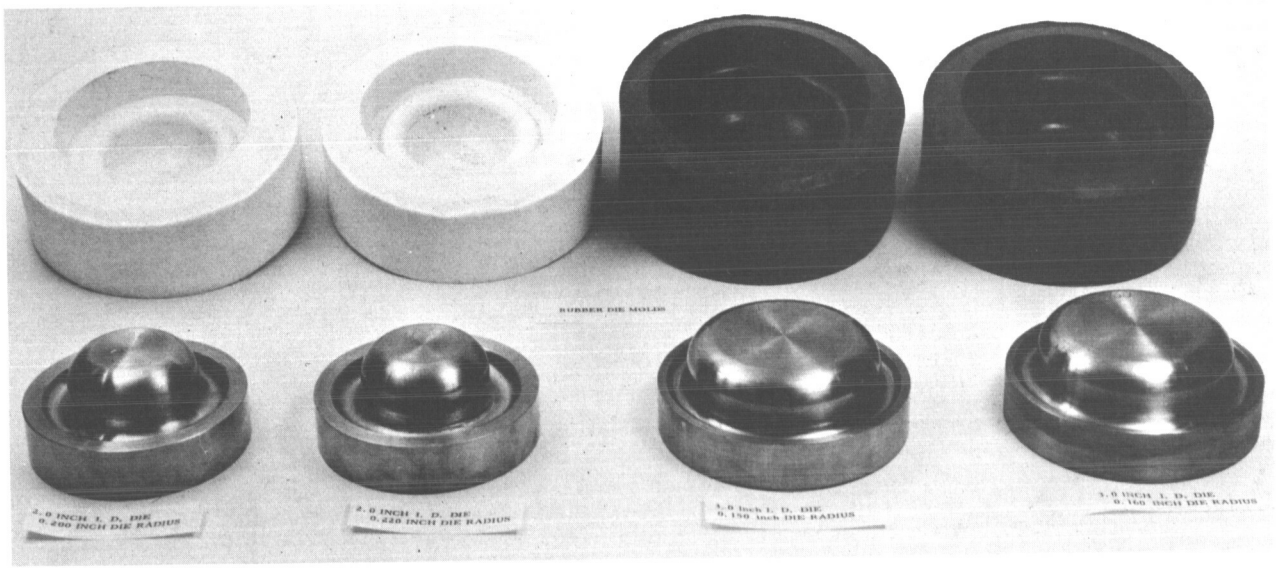

Figure 12. Typical Mild Steel 2.0 Inch and 3.0 Inch Diameter Fragmenting Dies and Rubber Molds For Fabrication of Plastic Dies.

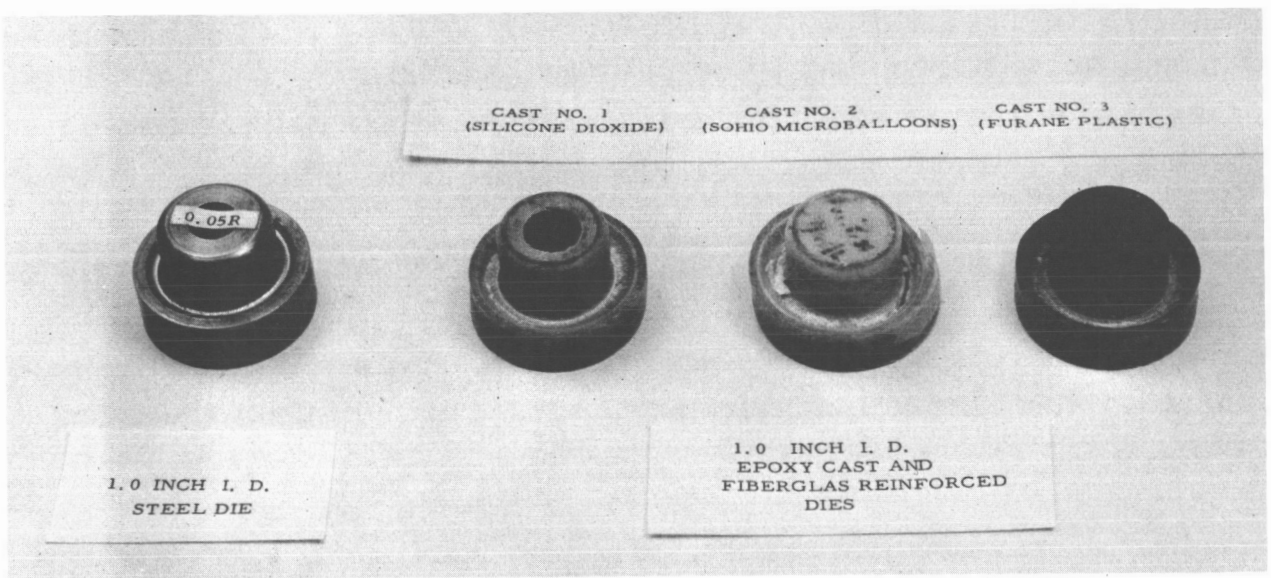

Figure 13. Typical 1.0 Inch Diameter Fragmenting Dies of Mild Steel and Cast Epoxy With Glass Fiber Plastic Tubular Reinforcements.

Cast Number 1 die has a silicone dioxide filler in the epoxy material and this mixture resulted in a die weight with reinforcement of .049 pounds. The compressive strength of the epoxy with filler was 16 000 psi which caused some tube choking. Cast Number 2 die consisted of an epoxy resin mixed with microballoons which exhibited a compressive strength of 10 000 psi. This low strength caused severe choking and failure of the outer rim reinforcement as shown in figure 13. Cast Number 3 die was fabricated using a commercial epoxy and filler mixture. A similar performance and strength to Cast Number 1 die was obtained with Cast Number 3 but the die weight was higher, which was .056 pounds. Since a target compressive franging stress level of 20 000 psi was planned for franging of the 1.0 inch tubes, it was determined that a compressive strength above this value should be used for die material. Low cost cast epoxy dies were considered to be inadequate, but a matched die molding material Military Specification MIL-M-19833, Type GDI-30 which recently became commerically available, had properties which could meet weight and strength requirements. The dies which were successfully developed using this phenolic molding compound with chopped glass fibers as fill material are shown in Sketch SK 78056. This die required the design and fabrication of matched die metal molds which were used in a heated molding press. The die material requires a molding pressure in compression between 200 to 2000 psi at temperatures between 290 to 340 degrees F, with a cure time of 2 minutes. The mechanical properties of the material are a flexural strength of 20 000 psi, a compressive strength of 28 500 psi, and an Izod impact strength of 8.0 ft/lb/inch notch.

Sketch SK 78056 shows that the dies are contoured to fit spherical test vehicle dimensions, and that the die diameter is 1.8 inches compared with the 1.5 inch steel die. The diameter of the die and the internal hole size were calculated to give compressive loading stresses due to the franging action of a 1.0 inch tube which were below the specified limits for the spherical test vehicle shell. Die weight was .040 pounds which is lighter than the lightest cast reinforced epoxy resin die fabricated. Tube franging action with

the matched die molded dies was as good as that obtained with the steel dies and the franging groove of the die remained polished and underformed after each test. No deformation or cracking of any part of the die was experienced in franging or crushing tests against representative test vehicle shell material.

Anisotropy Tests. - Each of the three specified landing systems are required to completely surround the test vehicle and to provide omnidirectional energy absorbing capability. Consideration for the frangible tube landing system requires that design information on the franging of tubing under loading conditions which are not parallel to the tube axis be available. A test program was conducted on paired 1.0 inch tubes which were mounted at selected angles to the direction of load axis as shown in figure 14. The support for the tubes was provided by wooden blocks as shown, and the angle of the tubes to the direction of load could be varied. The franging force displacement graph indicates that franging action can be expected up to 15 degrees from the direction of load application before the steel die was pressed into the wood fixture, and caused one tube to fracture. The preliminary design information shown in figure 14 provided the limited anisotropy data used in calculating expected energy absorption and limiting force characteristics for the frangible tube segment tests.

Honeycomb. - The use of RF transparent honeycomb elements is specified as one of the required landing systems, therefore preliminary data was required which would establish the initial choice of the cell size, material, and density of the most suitable honeycomb, and solid height after crushing, or effective stroke. Figure 15 is presented with an accumulation of design information on the average crushing strength versus density of nylon phenolic (NP) and heat resistant phenolic (HRP) honeycomb for several cell sizes. The design data on the effective stroke versus density for the same materials is presented in figure 16. This design information was obtained from the previous program,[1] figure 32, the materials producer, and from the literature.

1.0 in. I.D. Tubes
Epoxy Resin System
181 "E" Glass Fabric
.04 (4 Ply) in. Thickness
t/r = .467
Average Franging Force
For One Tube Axially Loaded $\overline{P}$ = 2,200 lb.

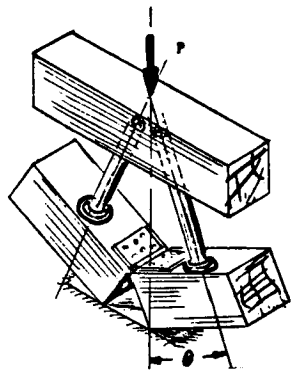

——— Both Tubes Franging
—·— One Tube Fractured
..... Both Tubes Fractured

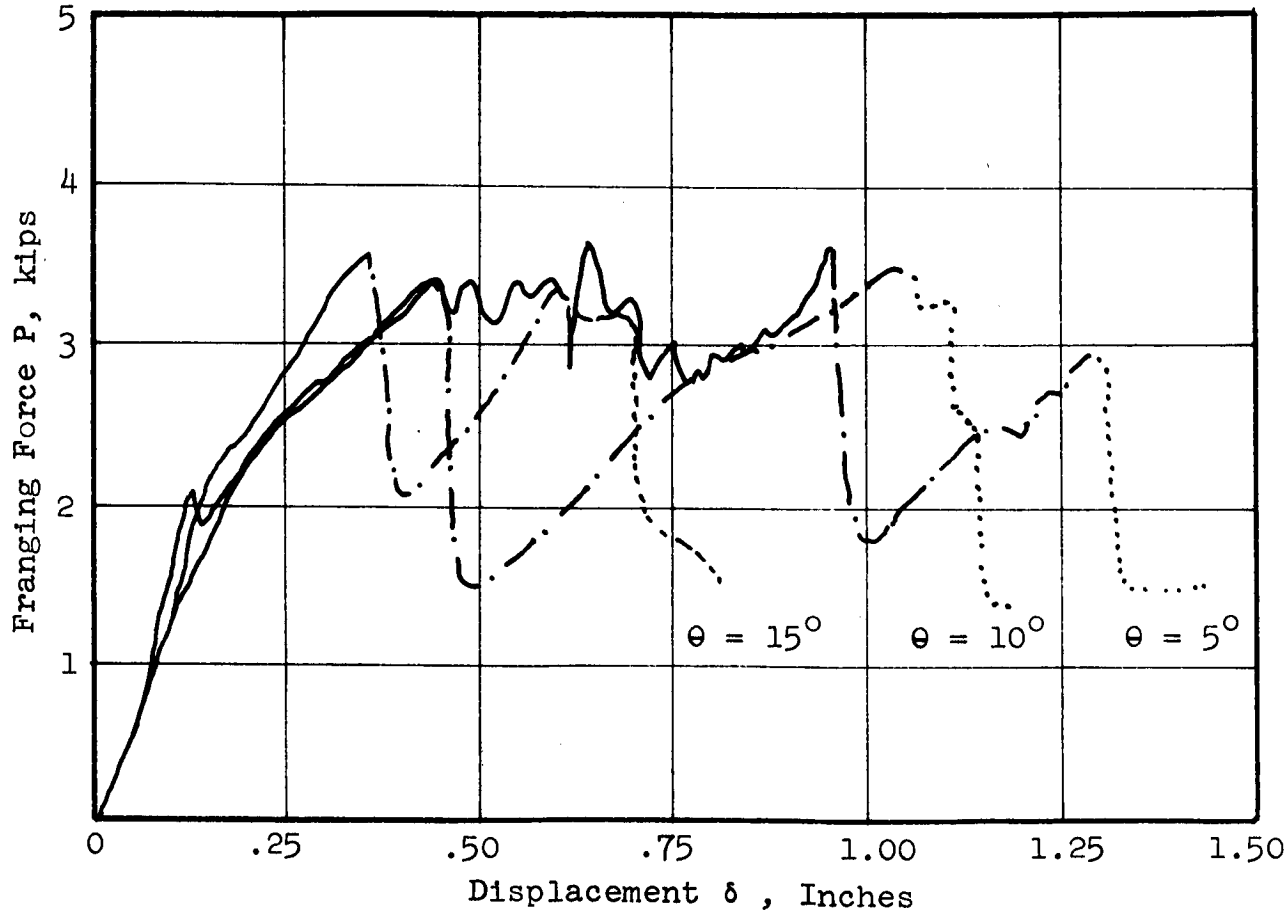

Figure 14. Load Displacement Graph For 1.0 Inch I.D. Tubes Franged At Various Angle To the Tube Axis On Steel Dies.

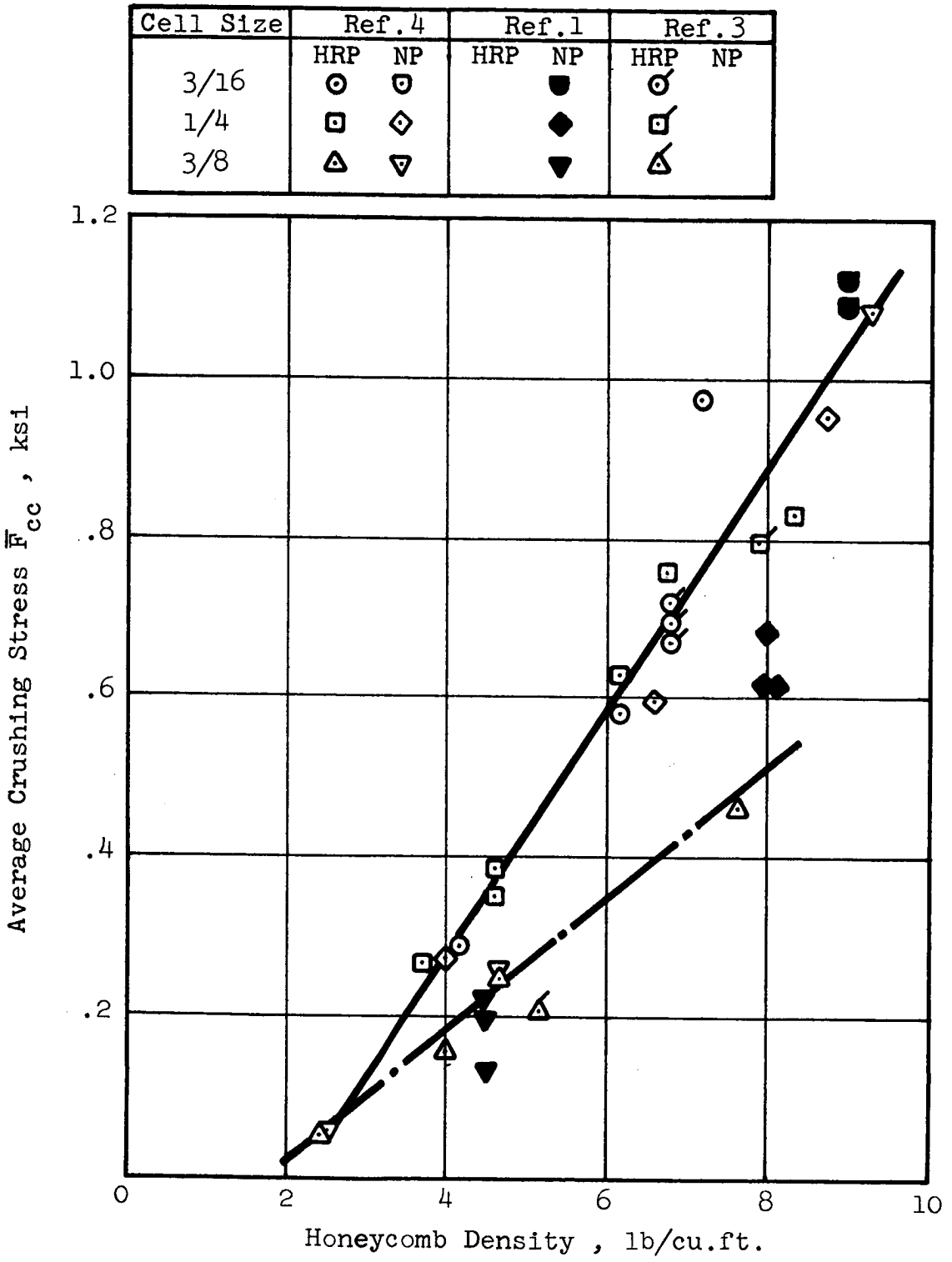

Figure 15. Variation of HRP and NP Fiberglas Honeycomb Average Crushing Stress With Density For Three Cell Sizes.

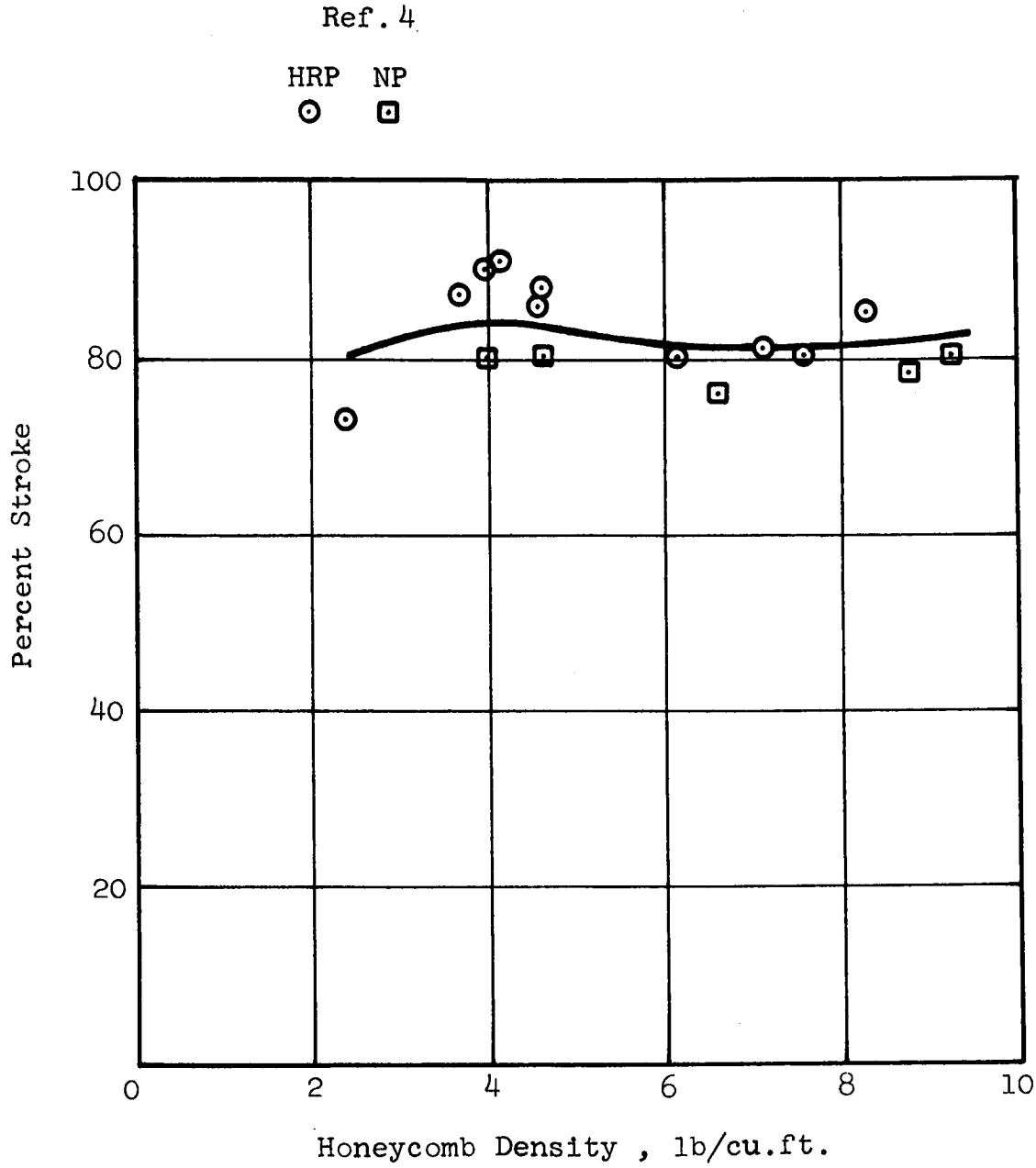

Figure 16. Variation of Useable Stroke With Density For HRP and NP Fiberglas Honeycomb.

The most efficient honeycomb material, cell size, and density, may be determined by the following formula:

$$\text{Specific Energy} = 144 \frac{(\text{Average Crushing Stress}) \times (\text{Effective Stroke})}{\text{Honeycomb Density}}$$

Where the specific energy is in foot pounds per pound, the crushing stress is in pounds per square inch, the effective stroke is in inches per inch, and the density is in pounds per cubic foot. The specific energy for a particular material, cell size and density can be immediately determined in figure 15 by locating the test point on the graph and by determining the slope of a line from the origin to the test point and multiplying the determined value by 144 times the effective stroke.

Figure 16 indicates that the effective stroke is in a scatter band above eighty percent which is independent of material or density, therefore one value can be assumed for preliminary calculations. The specific energy is therefore a direct function of the average crushing stress/density ratio. The most efficient honeycomb element can be determined from figure 15 to be the one with the steepest slope from the origin. Since the line passing through the 1/4 and 3/16 cell size test points does not pass through the origin, then the most efficient elements tested were in these cell sizes and with 9 pound per cubic foot density. Close to this density and in the same cell sizes is the 6.7 pound per cubic foot density honeycomb. The large 3/8 cell size is shown as a separate curve with a much reduced slope efficiency from the smaller cell size line.

Cross-Sectional Shape Evaluation. - Design information which will provide a comparison between several honeycomb element cross-sections was considered useful in determining the significant effect of the element boundary on the crushing strength. Four 1/4 cell size nylon phenolic honeycomb elements were fabricated to equal cross-sectional areas but in different shapes as a square, circle

hexagon, and equilateral triangle. The specimens after crushing are shown in figure 17. Since the honeycomb cell shape is hexagonal, it was considered that the triangular or hexagonal element sections would crush at the highest stress level. The triangle, hexagon, circle, and square sections crushed at 295, 287, 244 and 269 psi respectively. The most efficient element is therefore the triangular section, and the least efficient is the circular section.

Stacked Layers Evaluation. - The practical fabrication of honeycomb element landing systems with omnidirectional characteristics requires the consideration for stacked honeycomb layers. The continuous spherical shape honeycomb configuration is one type which cannot be formed without fabricating the double contoured honeycomb surface in layers. Figure 18 provides a crushing force versus displacement comparison between three layers and 6 layers of 1/4 cell size nylon phenolic honeycomb with each layer separated by two plies of 181 fabric and epoxy resin system laminations. The test results show some peaking before each layer followed by a drop in the load carrying capability. The most significant difference between the three layer and six layer configuration is the greater weight of the latter, which tested at a higher average stress, but had a lower specific energy due to the greater weight.

Anisotropy Tests. - A dynamic test program was conducted in 1960 to provide design information on the energy absorption characteristics of 1/4 cell size 5052 aluminum .001P foil honeycomb.[5] The test program crushed circular section elements against inclined surfaces which were contacted when the specimen was impacted at a controlled velocity of 14 feet per second. Specimens during test are shown in figure 19. The crushing action is shown to progress from the impacting end of the honeycomb element. Figure 20 shows the test setup and the curve developed from the tests. This curve which is almost linear represents the crushing of aluminum alloy material which is considered to behave differently from the fiberglas honeycomb materials.

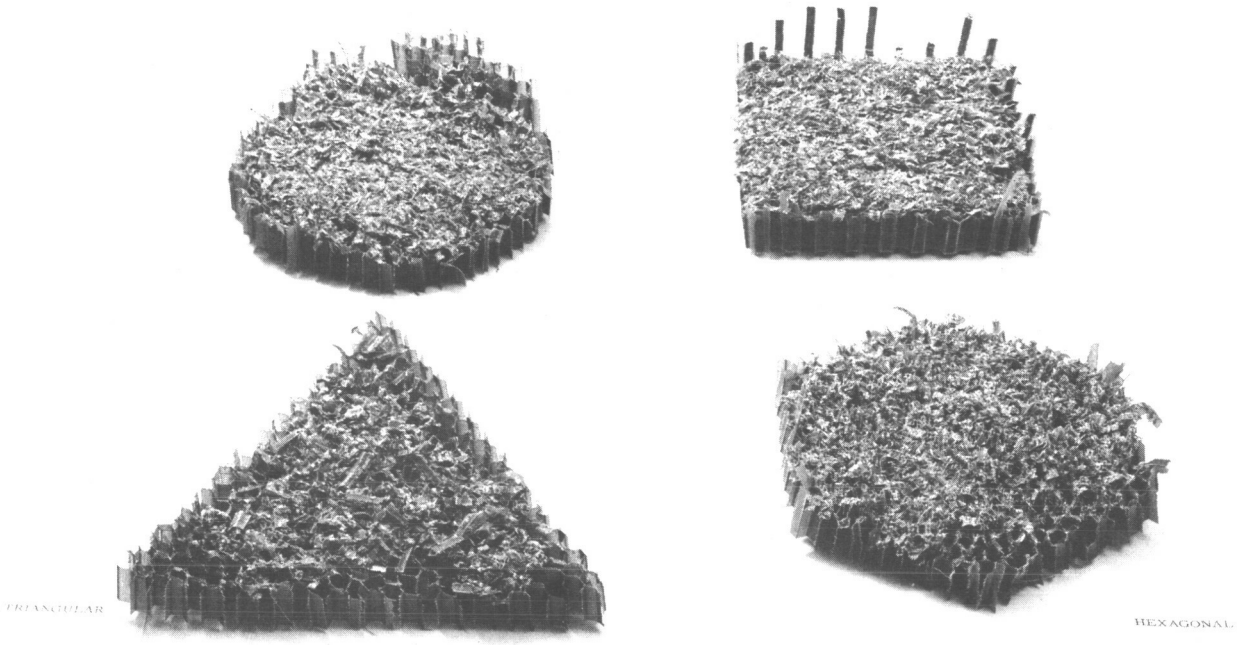

Figure 17. Evaluation of the Effect of Cross-Sectional Shape For Equal Areas On the Crushing Strength of 1/4 Cell Size Nylon Phenolic Honeycomb.

Material:	Nylon Phenolic Honeycomb 1/4 in. Cell Size, 4.2 lb/cu.ft.	
Laminations:	2 Ply 181 Fabric, Epoxy Resin	
Layers:	3	6
Average Stress, F_{cc}:	340 psi	363 psi
Useable Stroke:	84%	84%
Specific Energy, E_{sp}:	5622 ft-lb/lb.	4518 ft-lb/lb.

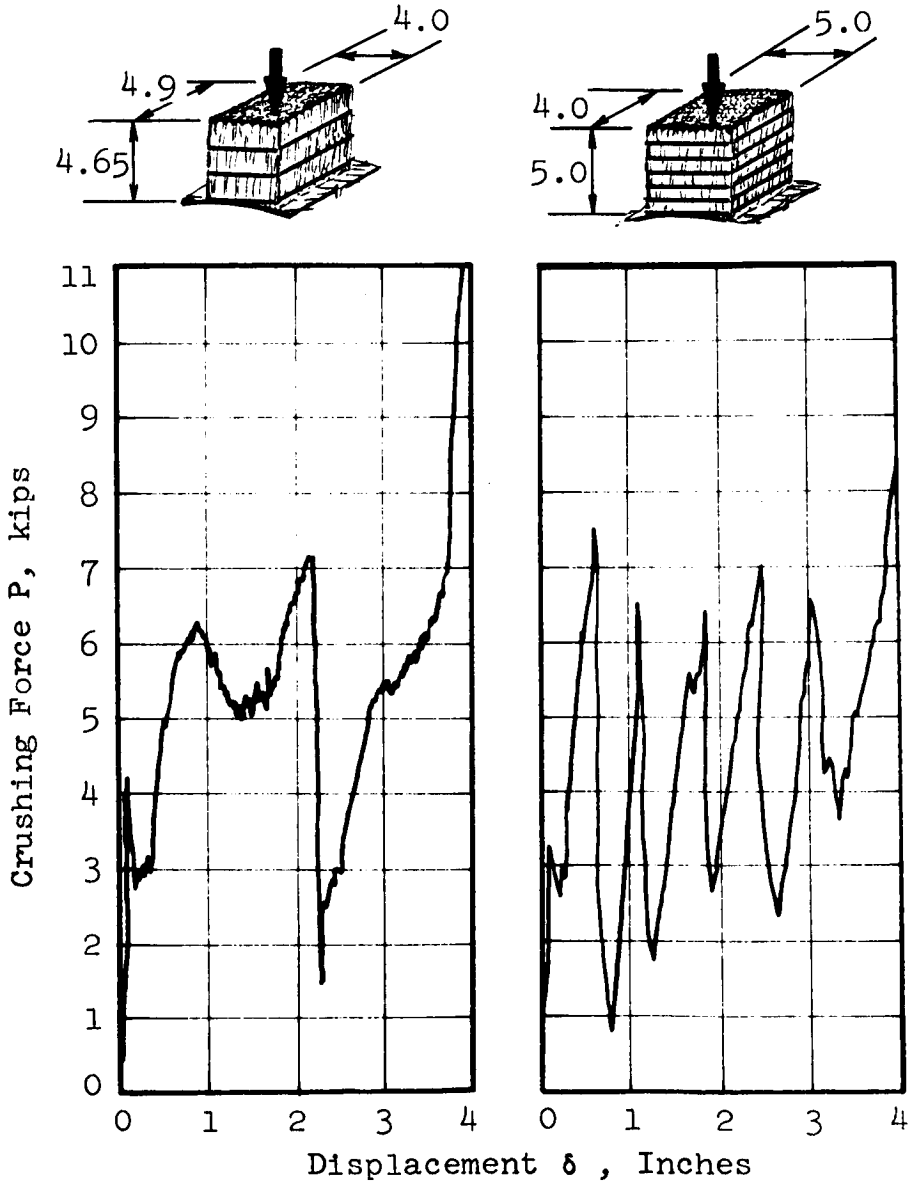

Figure 18. Load Displacement Graph For Nylon Phenolic Honeycomb With Variation In Number and Thickness of Stacked Layers.

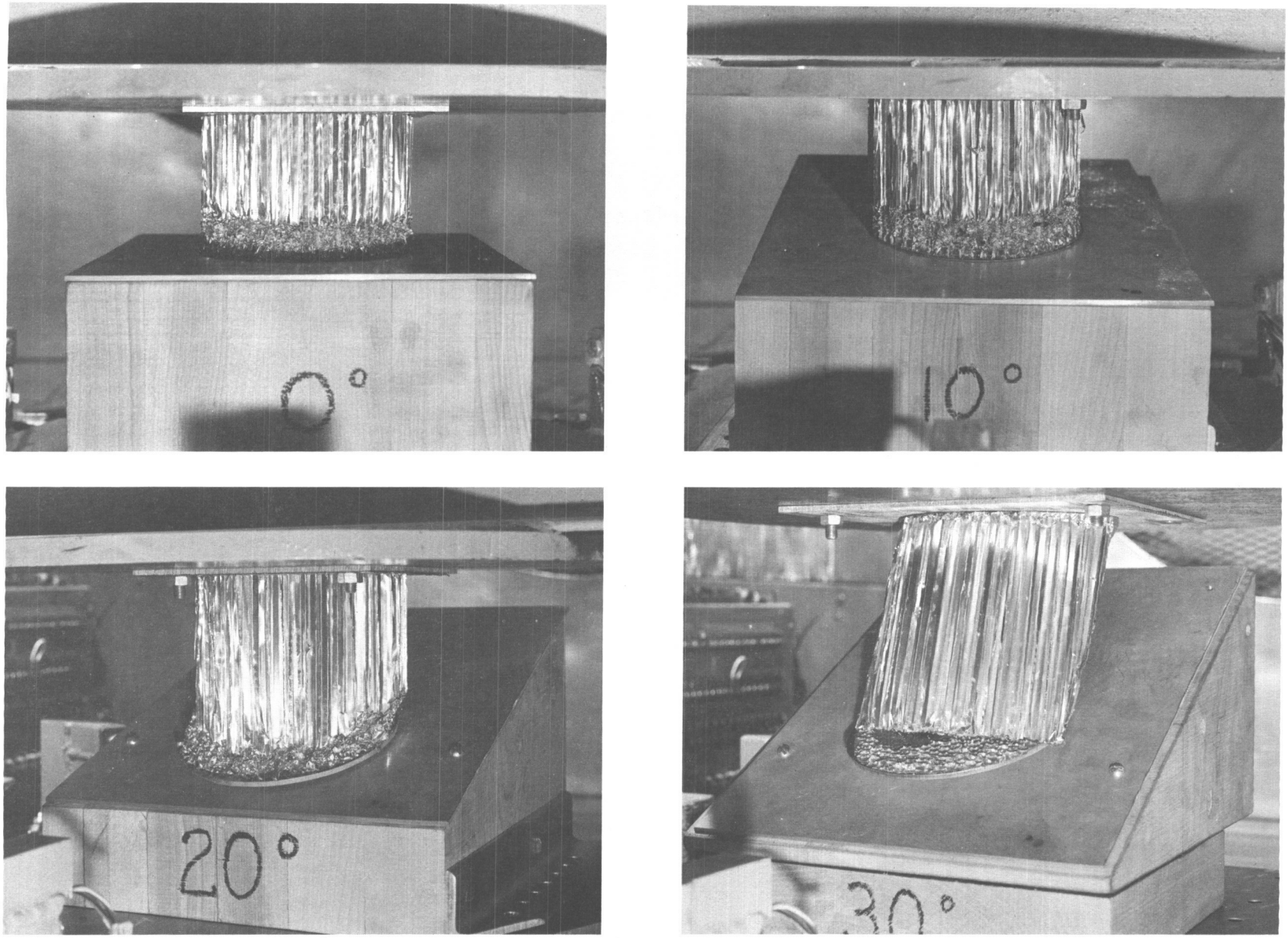

Figure 19. Dynamic Impact Testing At 14 ft/sec Velocity of 1/4 Cell Size 5052 Aluminum .001P Foil Honeycomb, Impacting At Various Angles To the Cell Cross-Section.

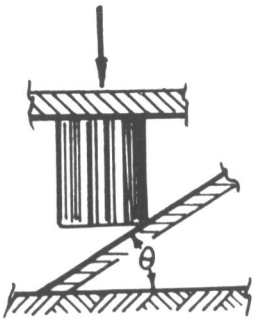

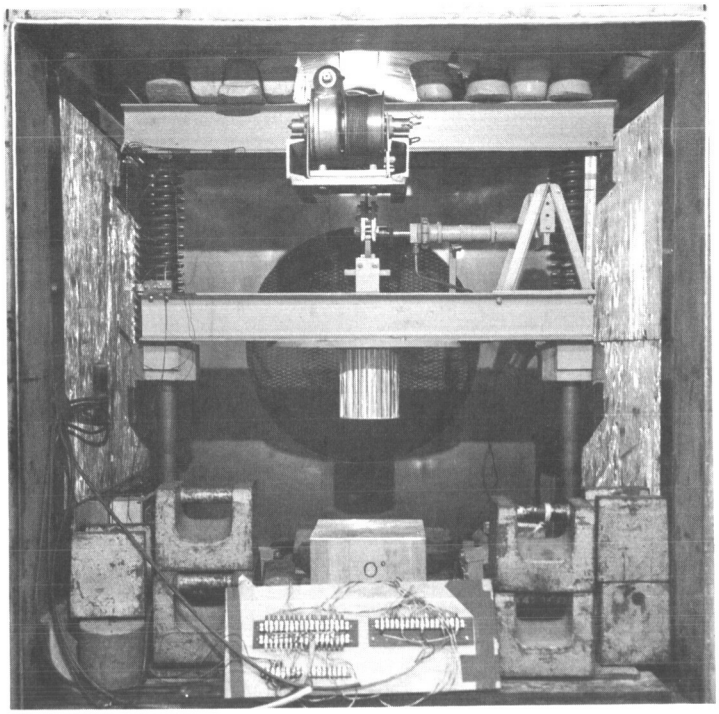

Test Setup

Material: 5052 Aluminum
1/4 Cell .001P

Impact
Velocity: 14 ft/sec
Section Area: 20 sq. in.
Crushing Stress: F_{cc} = 124 psi

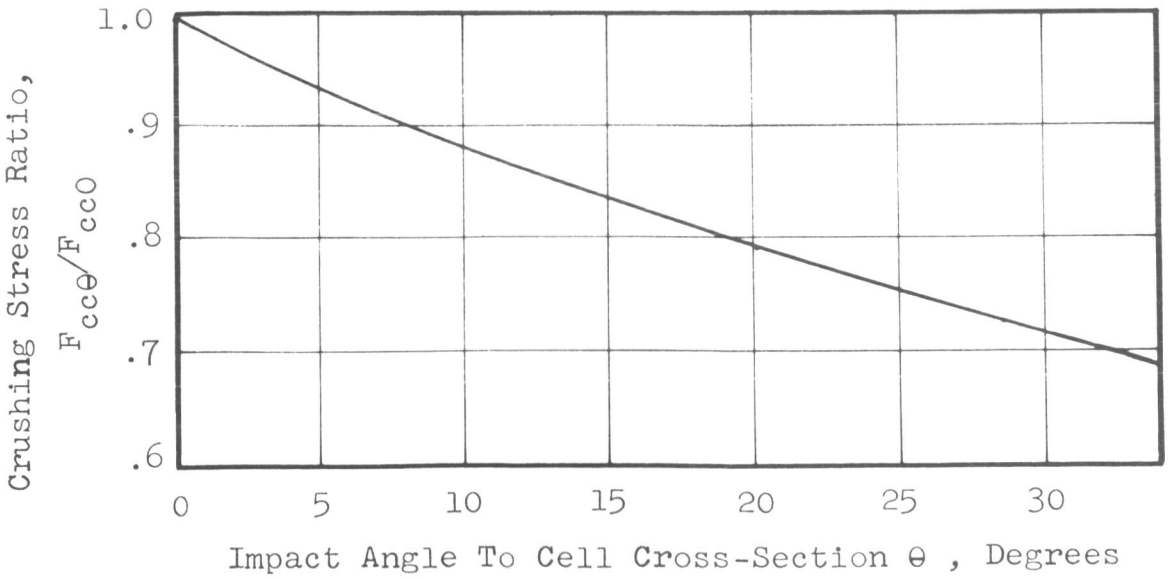

Figure 20. Test Set-Up and Dynamic Impact Test Results For 1/4 Cell Aluminum Honeycomb Impacted At Various Angles To the Cell Cross-Section.

The aluminum anisotropy test results were considered to be unconservative for application to glass fiber reinforced plastic honeycomb elements since it was considered that at higher angles of the load to the cell axis the crushing capability of fiberglas would drop off more rapidly. McFarland[6] has presented an equation for predicting the direct crushing stress of honeycomb, and this equation was modified in Appendix C of the previous program[1] to provide the specific energy capability of honeycomb materials. The modified equation contained a significant shear strength to compressive strength ratio term which can be compared for fiberglas and aluminum using the material strength properties in Table I. The much lower shear strength of the fiberglas is considered to be the reason for predicting an exponential drop off of crushing strength capability with load angle to the cell axis compared to linear for aluminum. A limited amount of testing of nylon phenolic honeycomb was performed since no anisotropy data was available for this material.

Rectangular 4 x 5 x 1.5 inches thick blocks of nylon phenolic in 1/4 cell size were crushed at various angles to the cell axis and the resulting force versus displacement graphs are presented in figure 21. Limitations of the test fixture prevented testing beyond 11.7 degrees at which angle it was determined that the honeycomb crushed at 61 percent of the zero degree load level.

A wooden test fixture which consisted of a semi-circular block of 9.0 inch radius as shown in figure 22 was used to test pairs of three layered elements of 1/4 cell nylon phenolic honeycomb spaced at various symmetrical angles to the load. This two dimensional test approximated the 9 inch radius spherical test vehicle support. The layered elements crushed in a manner previously described for direct crushing tests, with dips in the load curve occurring as the displacement reach each layer level. The effect of reduced shear strength in the nylon phenolic honeycomb as the angle to the cell axis is increased is considered to be the reason for the

1/4 Cell Nylon Phenolic Honeycomb
4.2 lb/cu. ft. Density

Angle, θ (Deg)	0	5.3	8.3	11.7
Average Force, P (lb)	5875	5400	5340	4140
Useable Stroke, (%)	83.4	78	58	72
Specific Energy (ft-lb/lb)	8820	7250	5540	5360
Anisotropy Coeff.	1.0	.82	.63	.61

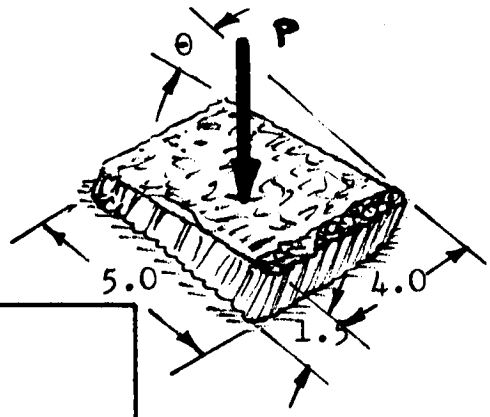

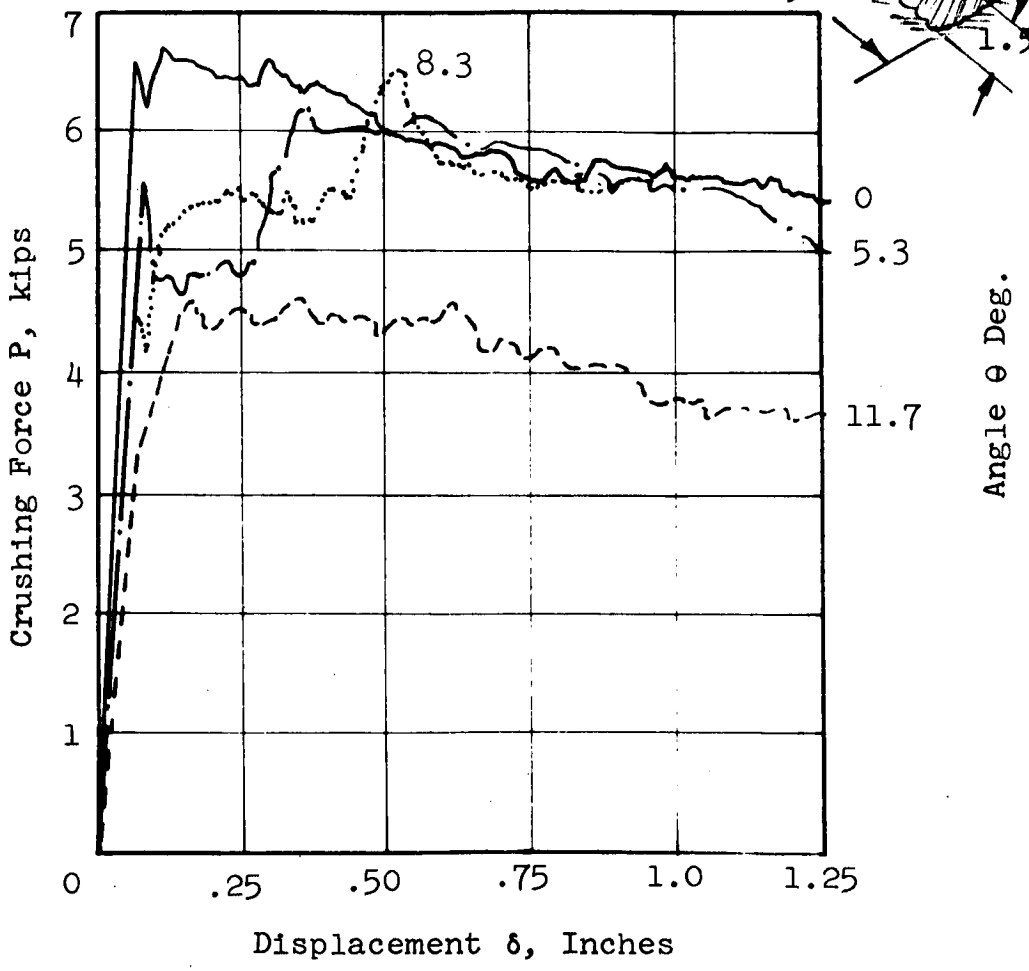

Figure 21. Load Displacement Graph For Nylon Phenolic Honeycomb Crushed At Various Angles To the Honeycomb Cell Axis.

Material: 3 Layers of Nylon Phenolic
1/4 Cell Size, 4.2 lb/cu.ft Honeycomb
5.0 x 4.0 x .46 Block Height
2 Ply 181 Fabric, Epoxy Resin Lamination

Angle θ (deg)	15	20	30
Average Force (lb)	6650	6500	4500
Useable Stroke (%)	91	91	84
Specific Energy (ft-lb/lb)	3370	3250	2120
Anisotropy Coeff.	.50	.49	.36

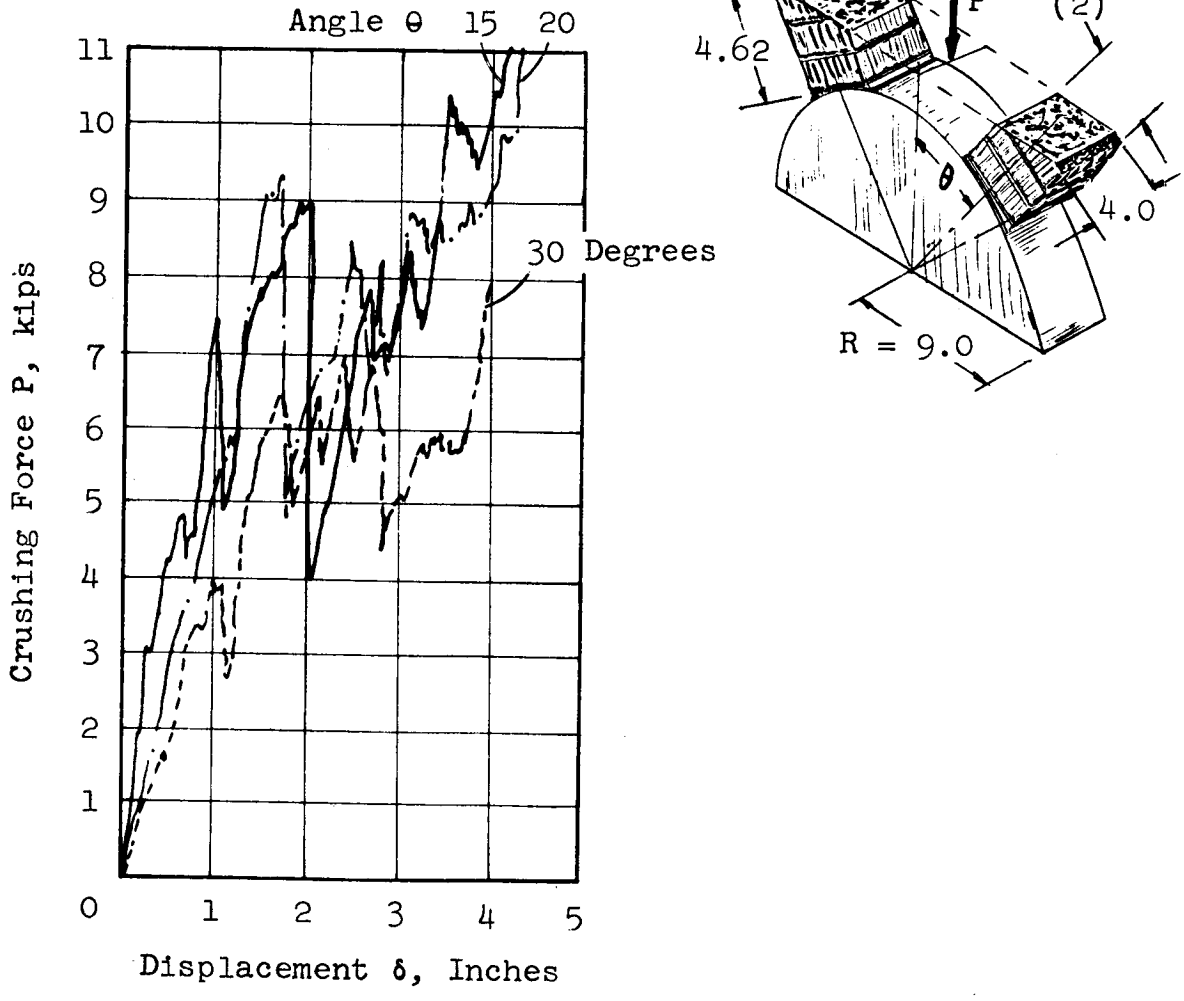

Figure 22. Load Displacement Graph For Two Three Layered Nylon Phenolic Honeycomb Elements Crushed At Various Angles To the Honeycomb Cell Axis.

significant reduction in the load capability shown for the elements tested at a 30° angle.

Additional tests of single layers of 1/4 cell nylon phenolic were performed on the 9 inch radius semi-circular test block as shown in figure 23. The length of the "wrap around" test elements was increased for each test in equal angular increments. The differences in the areas between curves shows the contribution of the added angle increment of length to the total energy absorbed. Beyond 20° there is almost negligible contribution from the element. This test indicates that a design which would consist of a continuous layer of honeycomb material would obtain most of the omnidirectional energy absorption from a cone area, previously identified in figure 1 as ϕ , of 40°.

The single layer wrap around tests were limited to 1/4 cell nylon phenolic elements of 1.52 inches thickness. This thickness was considered to be the upper limit for the practical fabrication of layered honeycomb curved strips in this cell size. The thickness limitation for smaller cell sizes such as 3/16 and for spherically contoured layers was not determined, but the thickness would approach one inch. The practical layered landing system was also tested on the 9 inch radius test fixture as shown in figure 24. Three layers of material provided a 4.5 inch total thickness. The load deformation curve showed a sharp drop due to the collapse of one layer into another layer of the specimen, because a two ply separating layer of 181 fabric and epoxy resin system was planned, but a single layer was fabricated in the test specimen. The limitations on the capacity of the test machine provided the upper boundary for the test curve.

Preliminary configuration analysis included polyhedron shapes as a design approach for providing omnidirectional impact attenuation protection for the test vehicle. The icosahedron is one polyhedron configuration which has been considered as a landing system. This particular shape can impact on one of the triangular

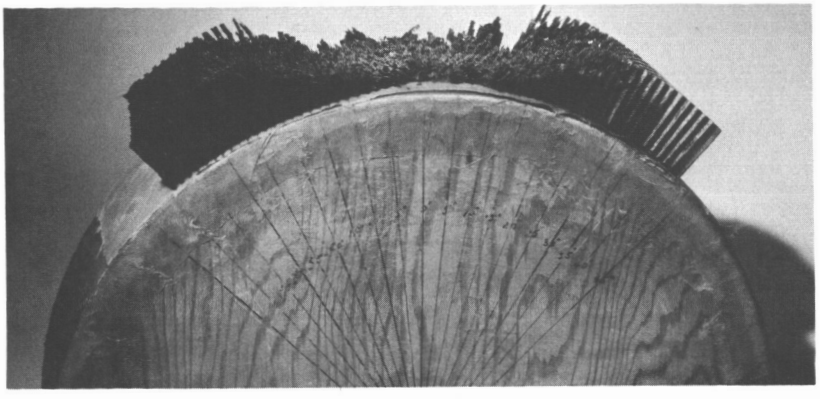

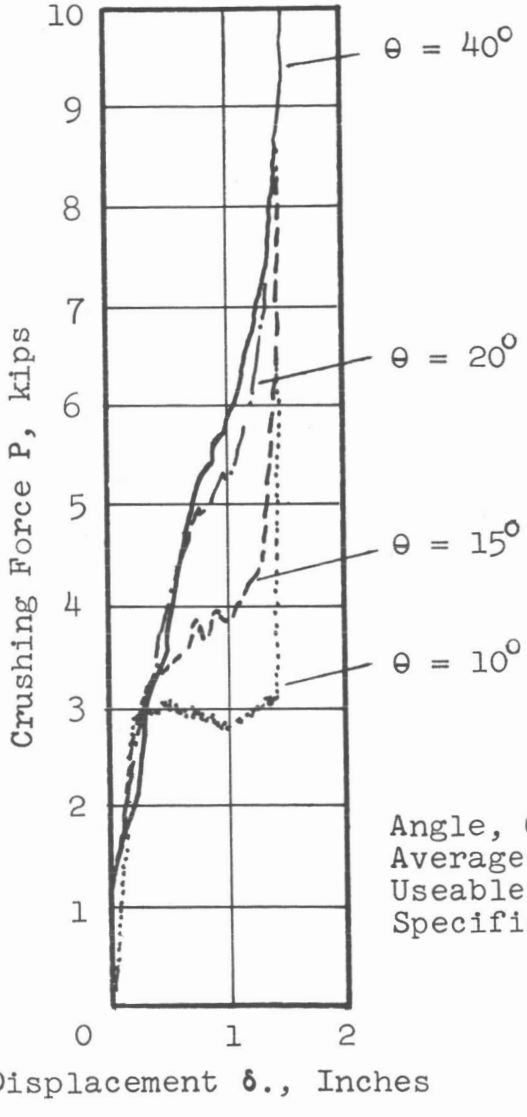

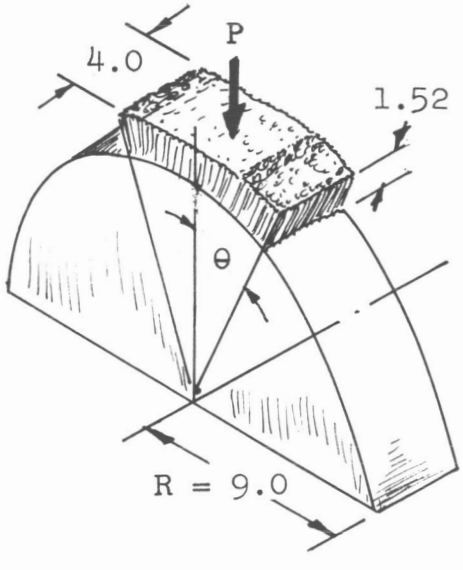

1/4 Cell Size Nylon Phenolic Honeycomb 4.2 lb/cu.ft Density

Angle, θ	10	15	20	40	Deg.
Average Stress	246	322	358	408	PSI
Useable Stroke	92	92	92	86	%
Specific Energy	7240	6340	5270	2720	

Figure 23. Load Displacement Graph For Nylon Phenolic Honeycomb Crushed As Single Layer Curved Elements of Various Lengths.

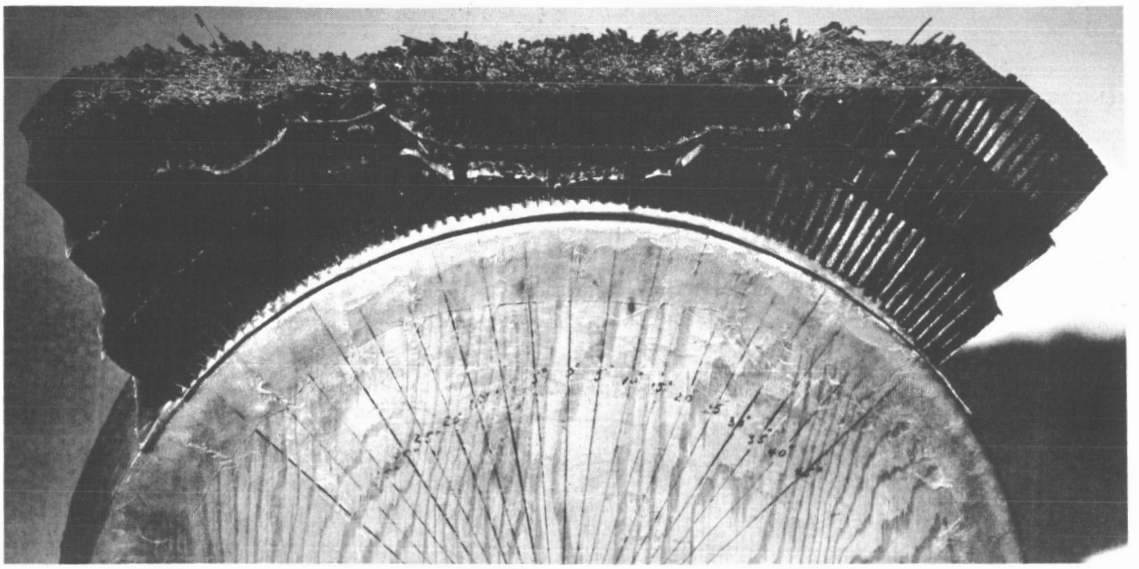

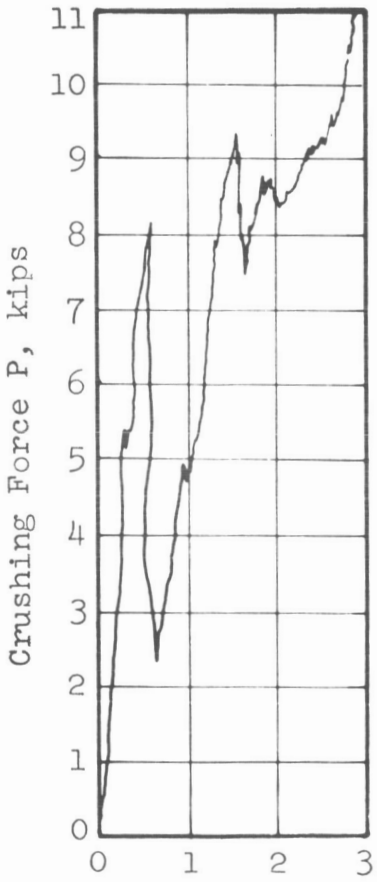

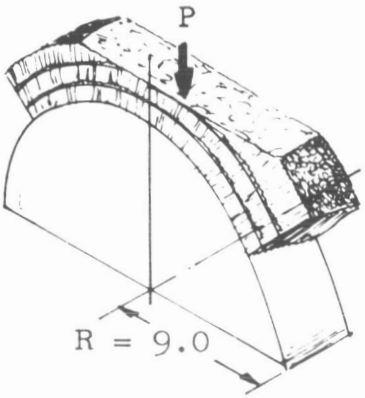

Material:

3 Curved Layers of Nylon Phenolic
1/4 Cell Size 4.2 lb/cu.ft Honeycomb
2 Ply 181 Fabric, Epoxy Resin Laminations

NOTE:

Maximum Force Was Limited By The
12,500 lb. Capacity of the Test Machine.

Figure 24. Load Displacement Graph For A Continuous Curved Three Layer Nylon Phenolic Honeycomb Element.

faces, on a vertex, or on one of the edges. Load deformation characteristics for impacting on an edge were simulated by joining two 3/16 cell size nylon phenolic honeycomb elements as shown in figure 25 to form an edge with 20° slope for each of the faces as in the icosahedron configuration. The interpretation of test results provides anisotropy coefficients for these edges. Limitations to the capacity of the test machine prevented determining the solid height for edge impact as shown in figure 25.

The initial interest in the practical fabrication of the continuous layered honeycomb approach for a spherical landing system resulted in the materials producer producing three layers of double contoured 3/16 cell size nylon phenolic honeycomb. These double contoured elements were bonded together with two ply fiberglas laminations placed between layers as shown in figure 26. The total thickness of the completed sandwich assembly measured 1.05 inches. The 6 inch internal spherical radius placed a severe restriction on forming material in this cell size thick section. The spherical sandwich test element load displacement graph shown in figure 26 is limited by the 12 500 pound capacity of the test machine otherwise the solid height of the three layers could have been determined. The curve shows some slight dip as the deformation approaches each of the lamination spacers, but the dip is not as severe as those obtained in figure 22 three layer element tests.

Composites. - A primary objective of the previous program was to evaluate honeycomb and composite materials as well as frangible tubes which exhibited RF transparency and which had a specific energy absorption capability of 10 000 foot pound per pound or higher. Preliminary tests on 1/4 cell nylon phenolic honeycomb indicated that this cell size would not meet the specific energy objective until it was filled with 4 pound per cubic foot of polyurethane foam. Since considerable improvement in the specific energy absorption capability of honeycomb was obtained by testing the smaller, 3/16 cell size material, further testing of polyurethane foam filled honeycomb was not carried out. It was also

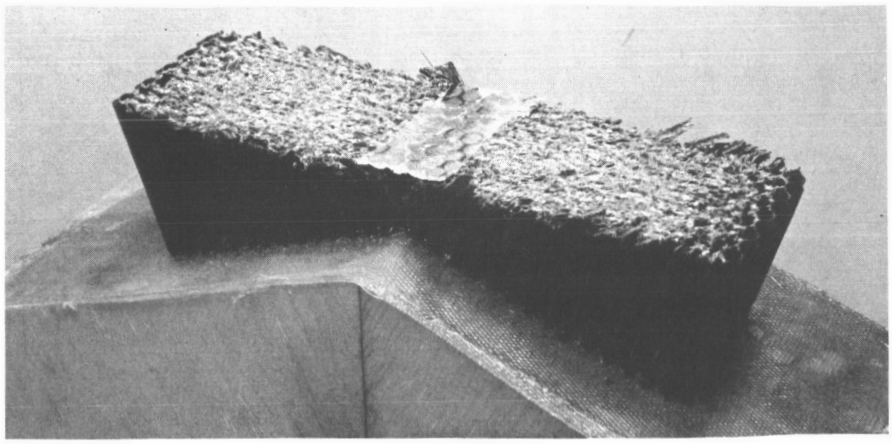

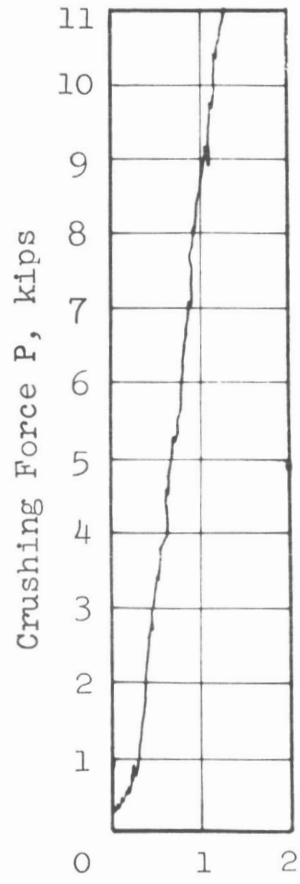

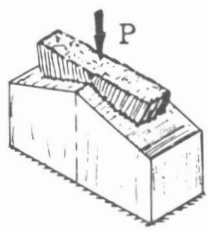

3/16 Cell Nylon Phenolic Honeycomb
8.0 lb/cu.ft Density

NOTE: Maximum Force was limited by the 12,500 lb capacity of the test machine.

Figure 25. Load Displacement Graph For Two Corner Elements of Nylon Phenolic Honeycomb Crushed At 20 Degrees To the Honeycomb Cell Axes.

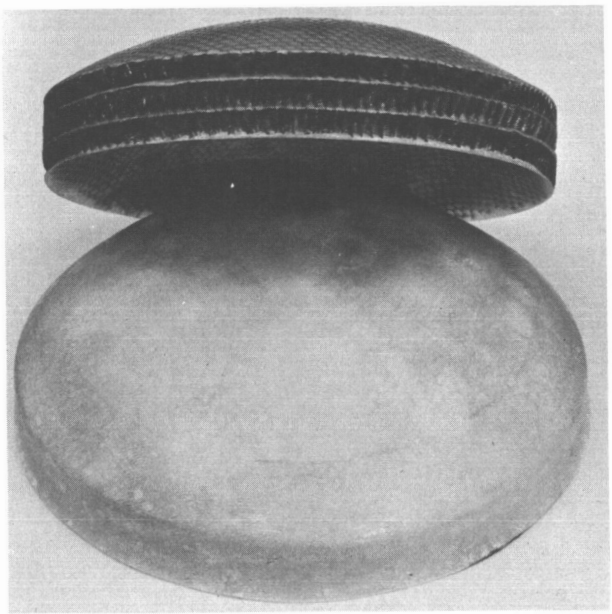

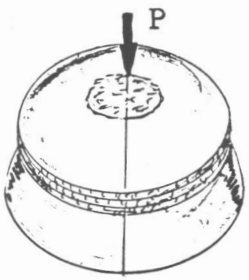

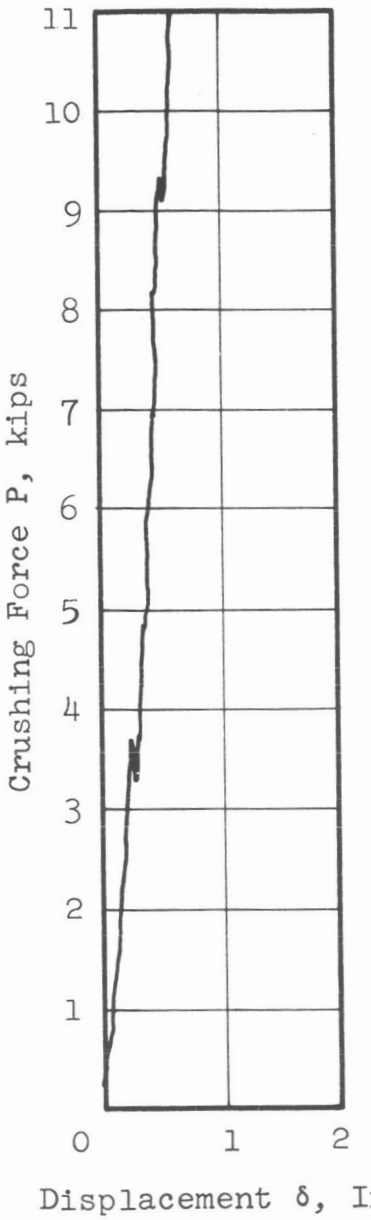

Material:

3 Doubly Curved Layers of 3/16 Cell
Nylon Phenolic Honeycomb, 6.0 lb/cu.ft Density
2 Ply 181 Fabric, Epoxy Resin Laminations
Between Layers. Total Thickness 1.05 inches

NOTE:

Maximum force was limited by the 12,500 lb capacity of the test machine.

Figure 26. Load Displacement Graph For A Three Layer Spherical Segment of Nylon Phenolic Honeycomb.

determined that design information from other literature on foam filled RF transparent honeycomb was not available, therefore, some element testing for this program was required.

Cell Size Evaluation. - Figure B-4 of Appendix B provides a direct comparison of the crushing force capability of specific triangular section composite elements consisting of 1/4 cell size nylon phenolic and 3/16 cell size heat resistant phenolic honeycomb filled with polyurethane foam. The 1/4 cell size elements weighed 4.2 pounds per cubic foot unfilled and 10.96 pounds per cubic foot filled with polyurethane foam. The 3/16 cell size honeycomb weighed 6.7 pounds per cubic foot unfilled and 10.75 pounds per cubic foot filled with polyurethane foam. The direct comparison of the crushing force between these two elements of almost equal weight as shown in figure B-4 shows the 1/4 cell size crushed at 4000 pounds and the 3/16 cell size crushed at above 6000 pounds average force.

Stacked Layers Evaluation. - A stacked layer design approach for a composite landing system requires consideration for using a single composite layer as either the outer or inner layer of the landing system. Previous layered element tests showed the crushing of the layers to progress from the outer surface inward. An evaluation of three layered elements was made with one foam filled honeycomb layer as the outside member, and another specimen with the inside member of the three layers of foam filled honeycomb. Figure 27 shows that the position of the foam filled honeycomb layers influences the load deformation pattern but the total energy absorbed is only slightly higher with the foam filled honeycomb on the outside.

Anisotropy. - Anisotropy tests of composite materials elements were not conducted during the previous program or in this program and design information on this subject was not found in the literature. Preliminary anisotropy design data for polyurethane foam filled Nylon Phenolic honeycomb for several composite densities was supplied by Mr. Fisher[7], and this data is presented in figure 28.

Material: 2 Layers of Nylon Phenolic Honeycomb
1/4 in. Cell Size, 4.2 lb/cu.ft
1 Layer of Polurethane Foam Filled Honeycomb
1/4 in. Cell Size, N.P. H.C./Foam 6.79 lb/cu.ft
Lamination: 2 Ply 181 Fabric, Epoxy Resin

Average Stress, F_{cc}:	320 psi	323 psi
Useable Stroke:	84.8%	87%
Specific Energy, E_{sp}:	4708 ft-lb/lb	4888 ft-lb/lb

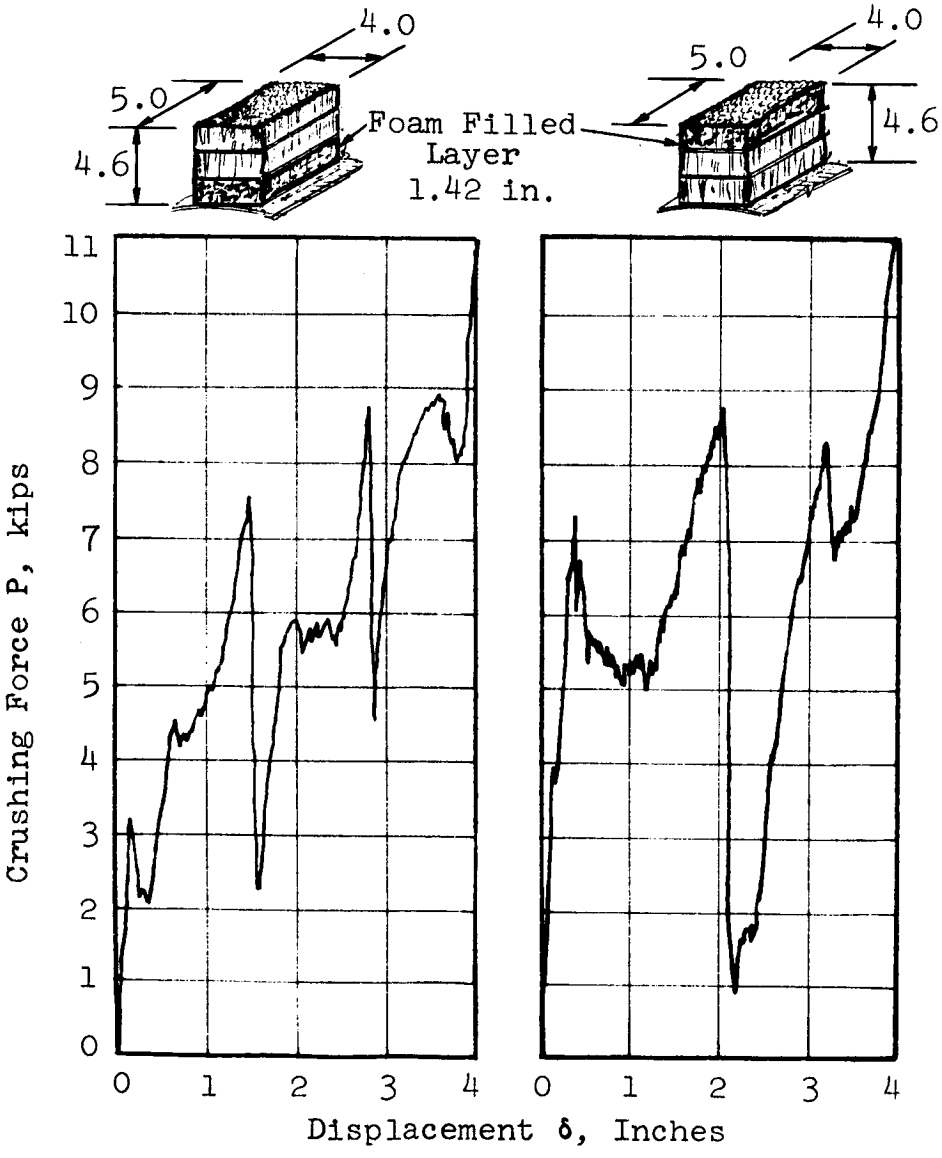

Figure 27. Load Displacement Graph For Nylon Phenolic Honeycomb and Polyurethane Foam Filled Layered Elements Of Nylon Phenolic Honeycomb.

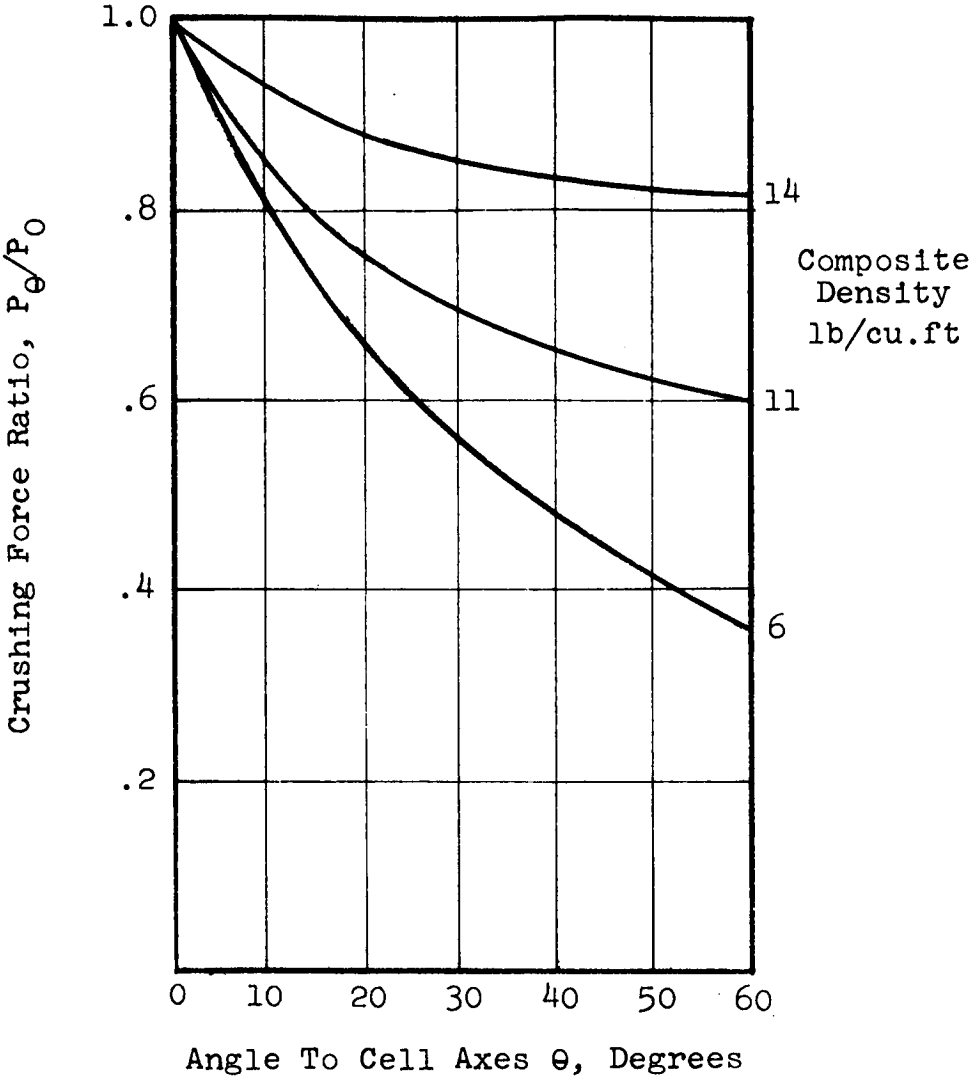

Figure 28. Variation of Crushing Force With Angle To the Honeycomb Cell Axes For Polyurethane Foam Filled Nylon Phenolic Honeycomb Composite of Various Densities.

Foam filled 3/16 cell size heat resistant phenolic honeycomb was found to weigh 10.75 pounds per square foot, which means that the middle of the three density curves in figure 28 is of most design interest for this program.

DETAIL DESIGN AND ANALYSIS

Landing System Configuration Selection. - The design parameters which are used in this section to evaluate and select a landing system for each of the honeycomb, composite, and frangible tube element types are as follows:

1. The landing system shall be fabricated in two hemispherical sections.
2. The internal diameter of the spherical inner surface of the landing system shall be 18 inches.
3. The maximum impacting force shall be limited to 50 000 pounds based on a maximum specified 1000g limitation for a total vehicle weight of 50 pounds.
4. The minimum omnidirectional impact absorbing energy capability shall be 15 527.9 foot pounds or 186 335 inch pounds for a specified resultant impact velocity of 141.5 feet per second and a total vehicle weight of 50 pounds.
5. The maximum weight limit of the landing system shall be 20 pounds.

Preliminary design configurations of candidate omnidirectional energy absorbing landing systems have previously been presented in figures 6 and 7 for spherical and polyhedron shapes respectively. The discussion on these candidate systems has been limited to a description of geometric arrangements, fabrication considerations, and methods of providing lightweight configurations. This section considers the parametric comparison of each basic spherical and polyhedron landing system shape in relationship to its maximum crushing force, energy absorption capability, and landing system weight. A common thickness of 6 inches for the landing system, and the 3/16 cell size 6.7 pound per cubic foot HRP honeycomb with

a 700 psi crushing strength has been used in the development of the crushing force and energy absorption curves for each shape. The weight curves present shell and joint weight variation with landing system thickness. These parametric comparisons were used to select and define honeycomb, composite, and frangible tube element landing systems for the program.

Sphere. - The developed crushing force and energy absorbed is presented for a spherical landing system in figure 29 for three types of anisotropy coefficients. It is immediately apparent that the 50 000 pound force limit is exceeded in all three curves before two inches of stroke, and the energy absorbing capability exceeds minimum requirements before four inches of stroke. The isentropic curve represents an ideal landing system using a material which crushes in a square shaped load deformation manner, and does not have a reduction in efficiency due to angularity to load. The linear anisotropy variation curve corresponds to the tested aluminum honeycomb elements and to the curve presented in figure 20. This linear curve is also considered in this evaluation to approximate the composite shape for 11 pounds per cubic foot density material as presented in figure 28.

The anisotropy curve which is shown to vary exponentially is considered to be representative of the anisotropy test results conducted on single and multiple layers of nylon phenolic honeycomb elements.

Figure 30 presents the variation of landing system core weight with thickness for various core densities. The weight of inner and outer spherical shells and the girth joint weight variation with landing system thickness is presented in figure 31. Figure 31 shows that the weight of inner and outer shells and girth band are 6 pounds for a 6 inch thick system which allows 14 pounds for the core material weight to stay within a 20 pound landing system weight.

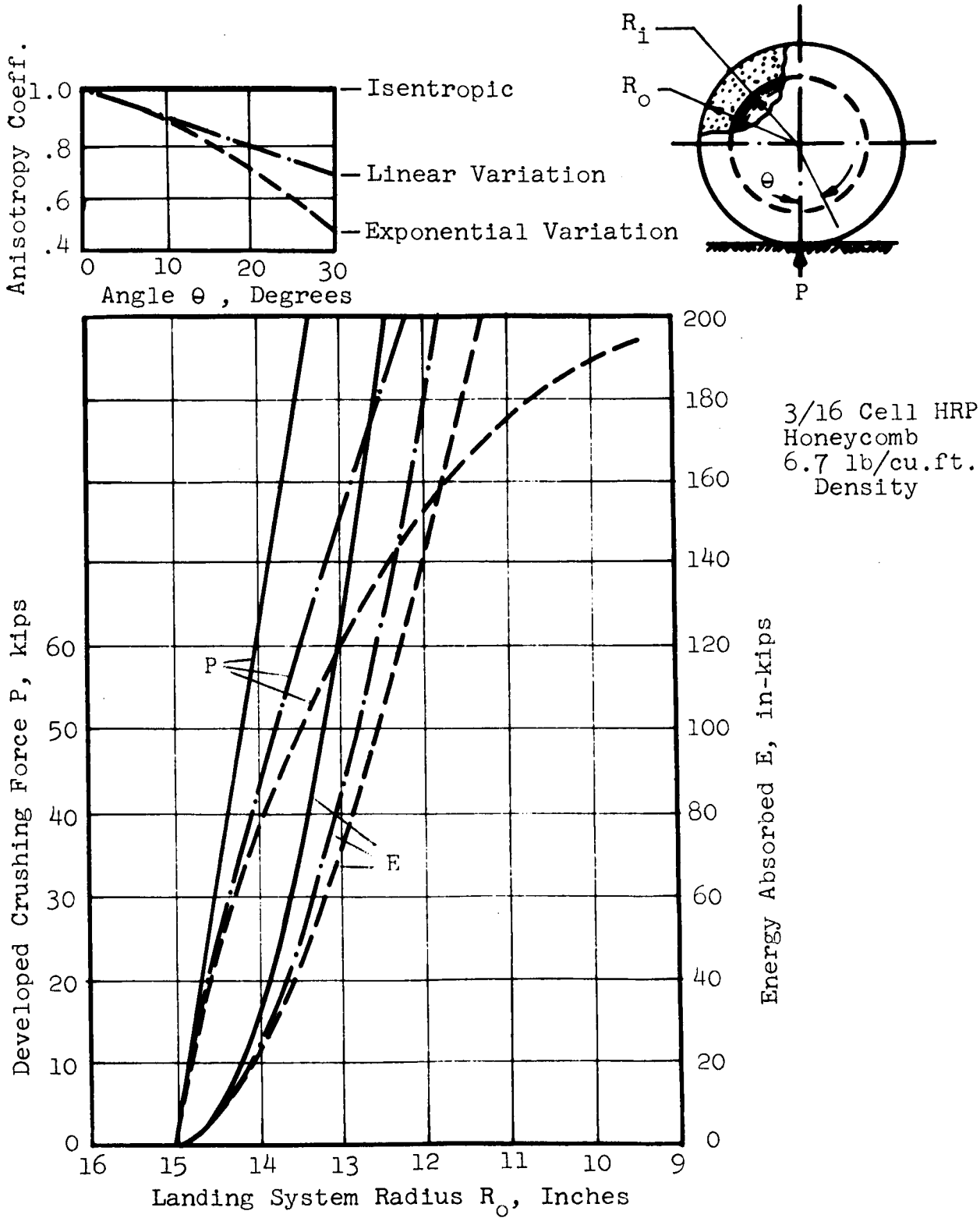

Figure 29. Spherical Landing System Direct Impact Force and Energy Absorption Characteristics.

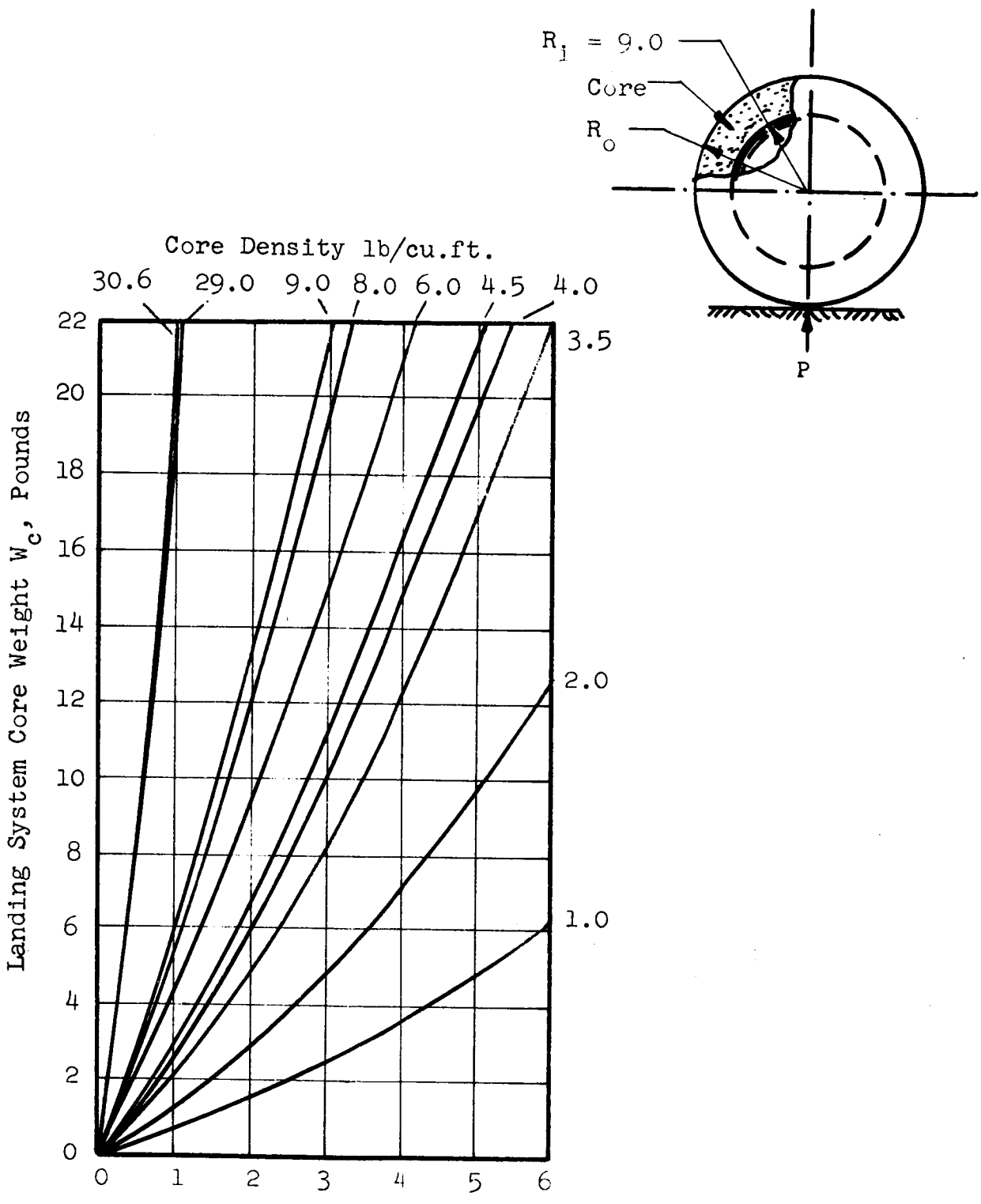

Figure 30. Variation of A Spherical Landing System Core Weight With Outer Shell Inscribed Radius.

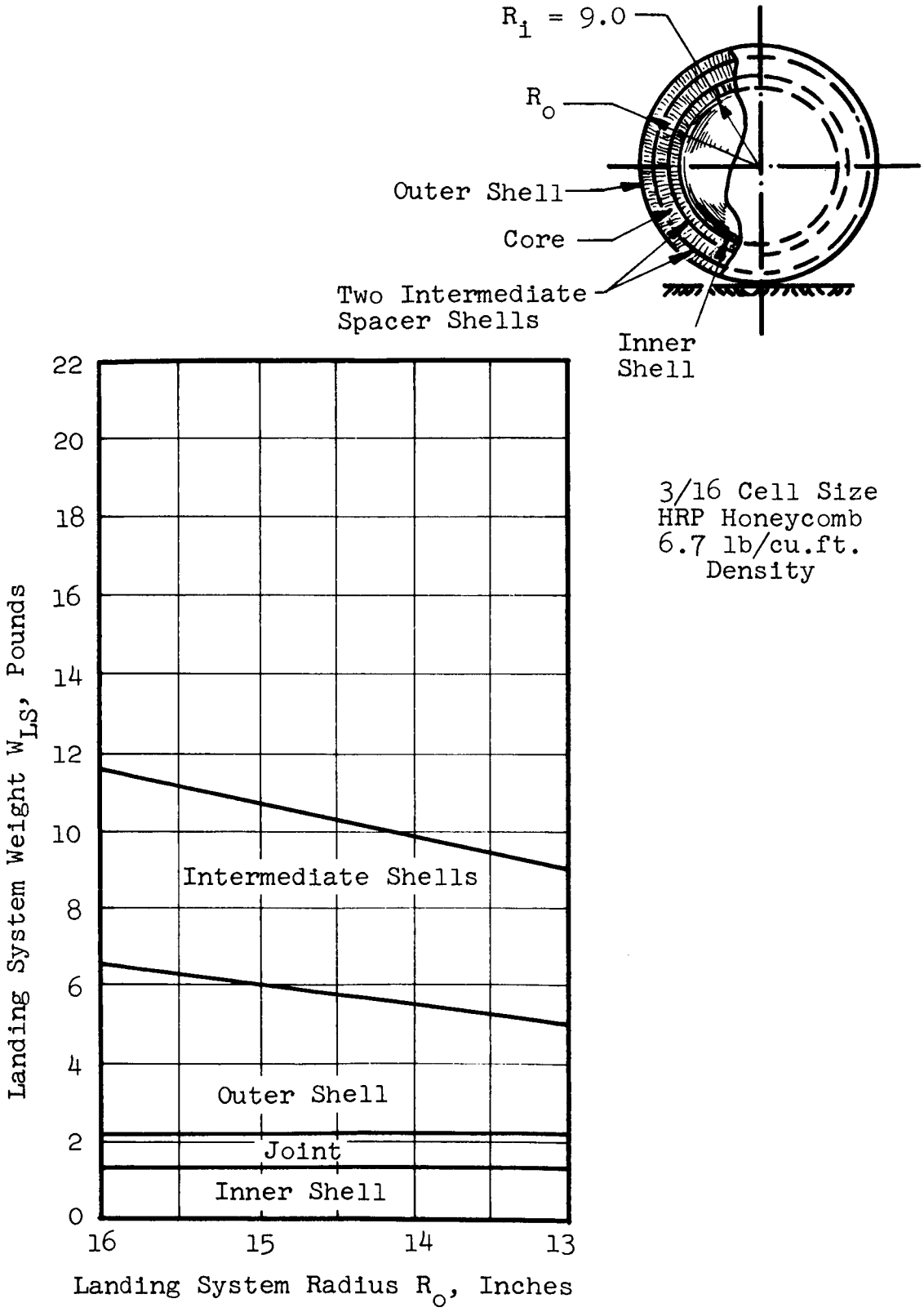

Figure 31. Variation of Spherical Landing System Weight With Outer Shell Inscribed Radius.

Dodecahedron. - The developed crushing force and energy absorbed is presented for the dodecahedron polyhedron shape in figure 32 based on the anistropy coefficient that varies exponentially. It is shown that impacting on a face provides a very high impacting force which drops off linearly with stroke because the impacted element is in the shape of a frustrum of a pyramid. Impacting on an edge or on a vertex provides more stroke than six inches hence the curves commence off the graph. The selection of the 700 psi crushing strength material for plotting these curves has caused these parametric curves to exceed the scale boundaries as presented.

The weight variation of the inner and outer shells, and the girth band joint, including foam material between the square cut core elements and the inner shell, is shown in figure 33. Also shown in figure 33 are methods of varying the weight of the dodecahedron configuration by using square sided elements, figure 33b, by using only rectangular strips of bordering elements, figure 33c, and by further lightening the square sided elements through the use of lightening holes as in figure 33d.

Icosahedron. - The developed crushing force and energy absorbed is presented for the icosahedron polyhedron shape in figure 34 based on the anisotropy coefficient that varies exponentially. It is shown that impacting on the face produces crushing forces that are beyond the boundaries of this figure. Impacting on an edge or a vertex provides more stroke than six inches hence these force curves start off the graph. The selection of the 700 psi crushing strength material for plotting these curves has caused the curves to exceed the boundaries of the graph.

The weight variation of the inner and outer shells and the girth band joint, including the foam material between the square cut core elements and the inner shell, is shown in figure 35. The methods of weight variation illustrated in figure 33 for the dodecahedron are also applicable to this polyhedron shape.

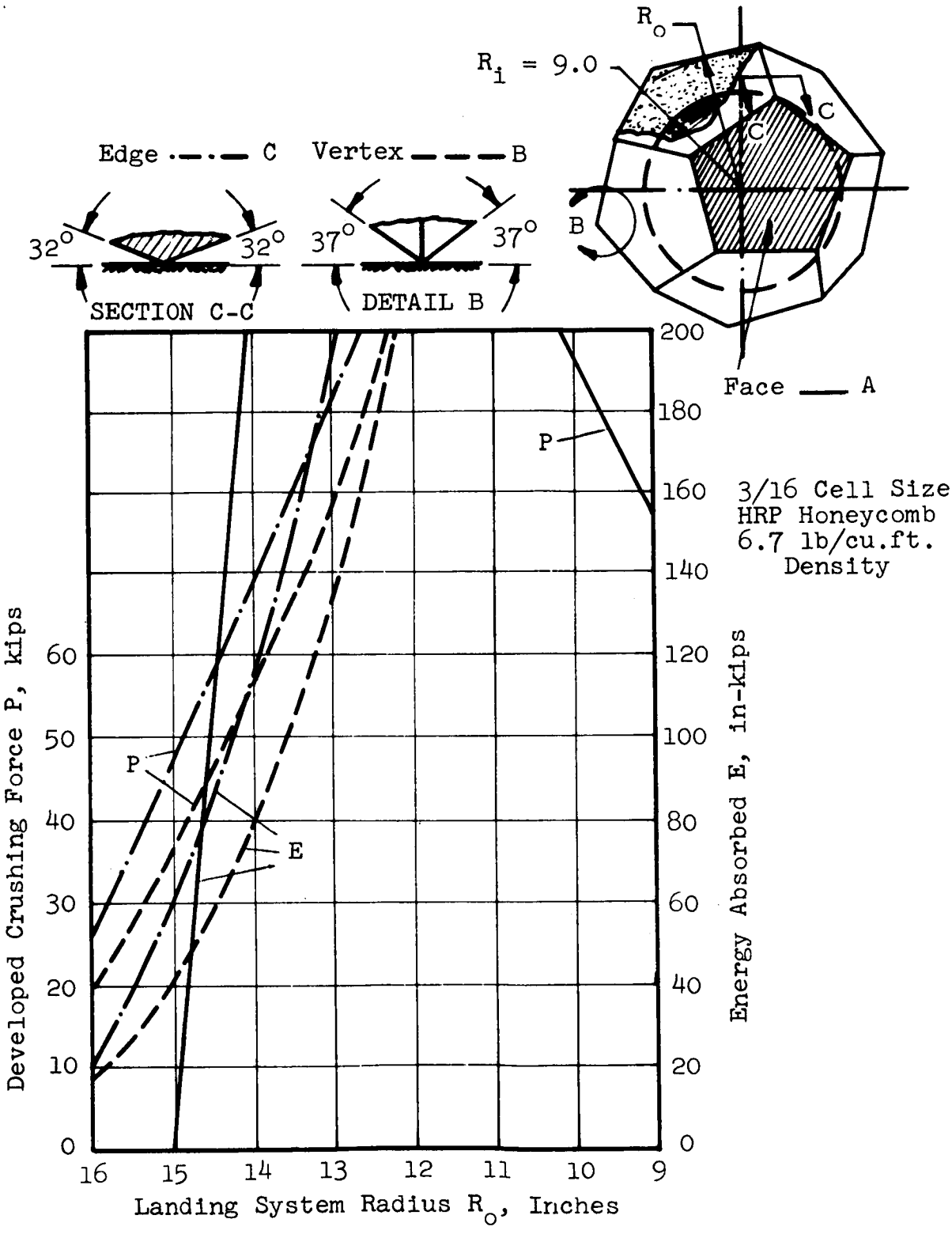

Figure 32. Dodecahedron Landing System Direct Impact Force and Energy Absorption Characteristics.

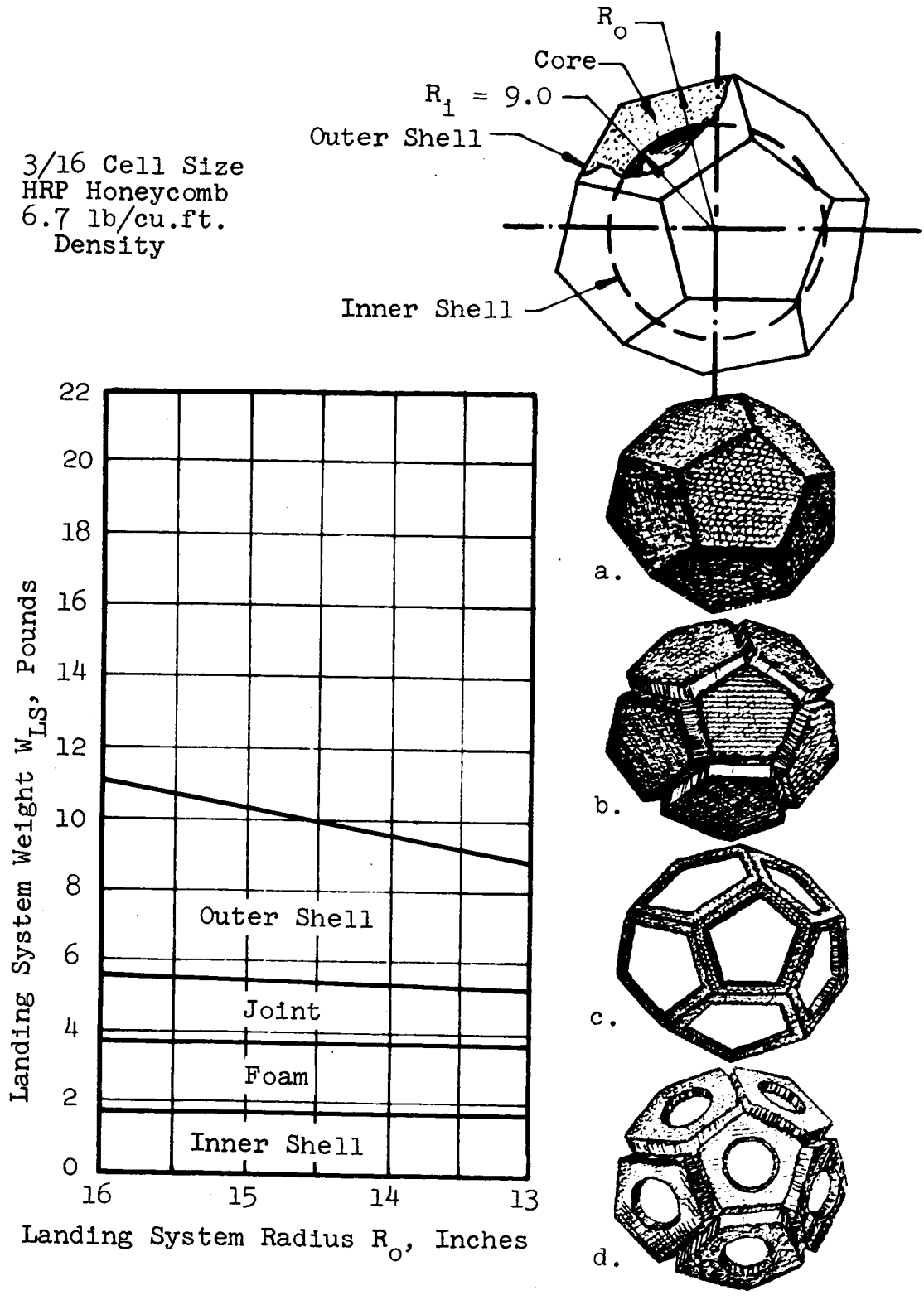

Figure 33. Variation of Dodecahedron Landing System Weight With Outer Shell Inscribed Radius.

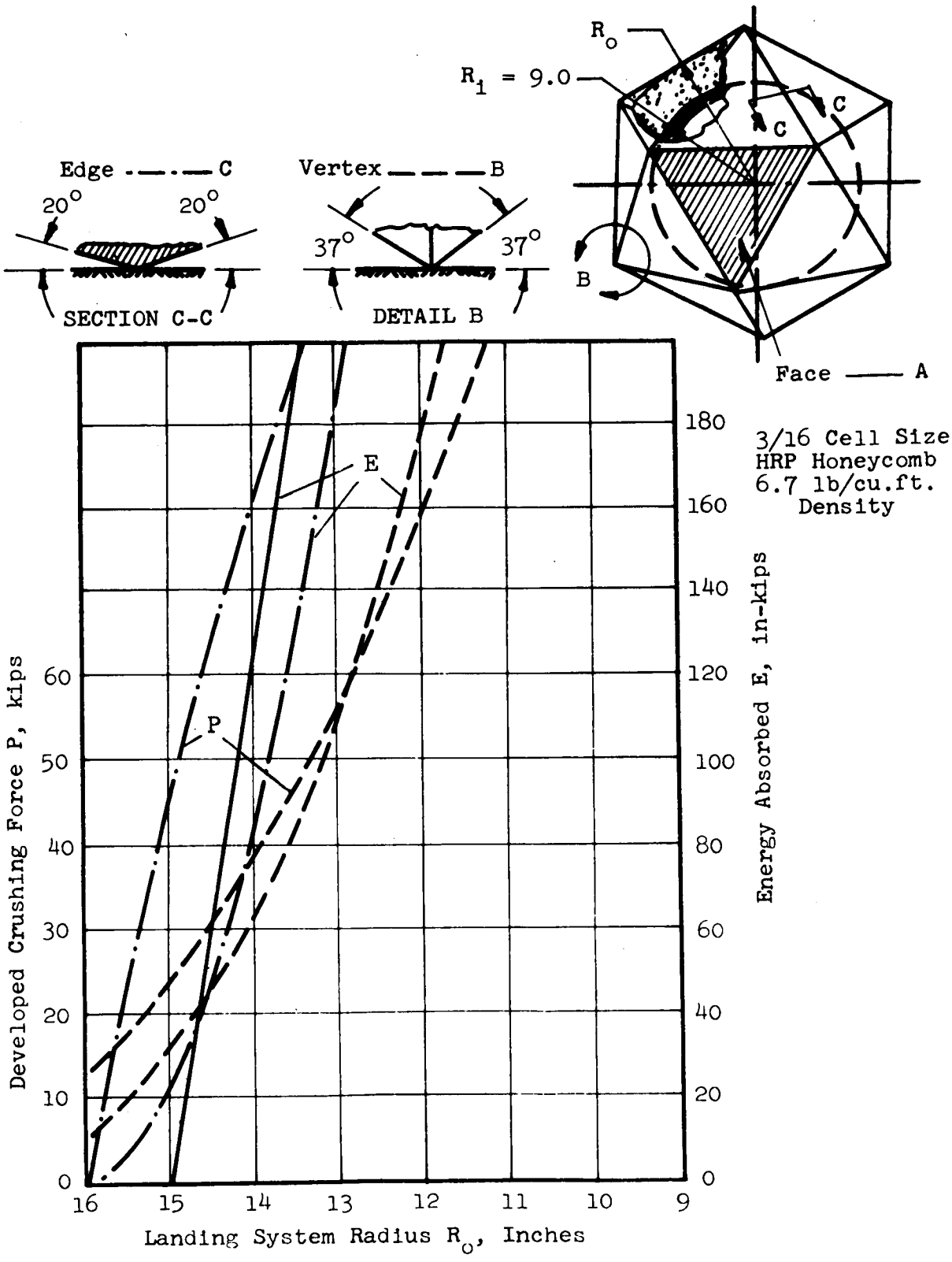

Figure 34. Icosahedron Landing System Direct Impact Force and Energy Absorption Characteristics.

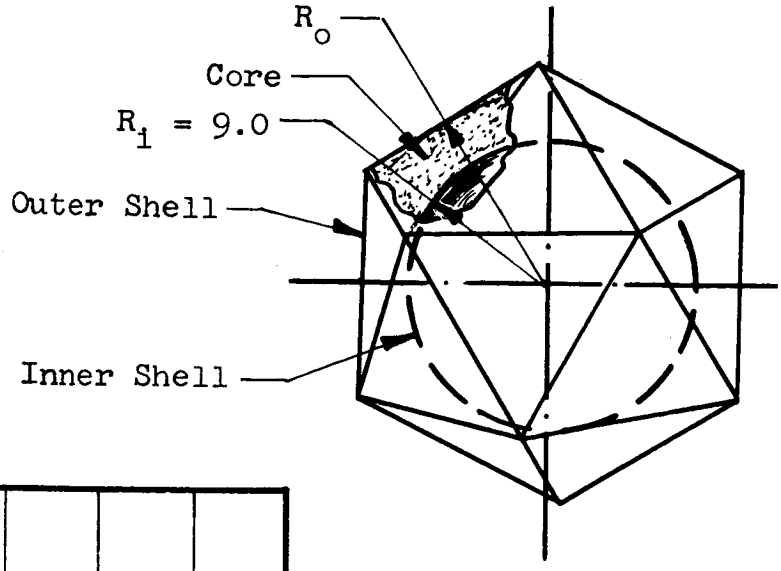

3/16 Cell Size
HRP Honeycomb
6.7 lb/cu.ft.
Density

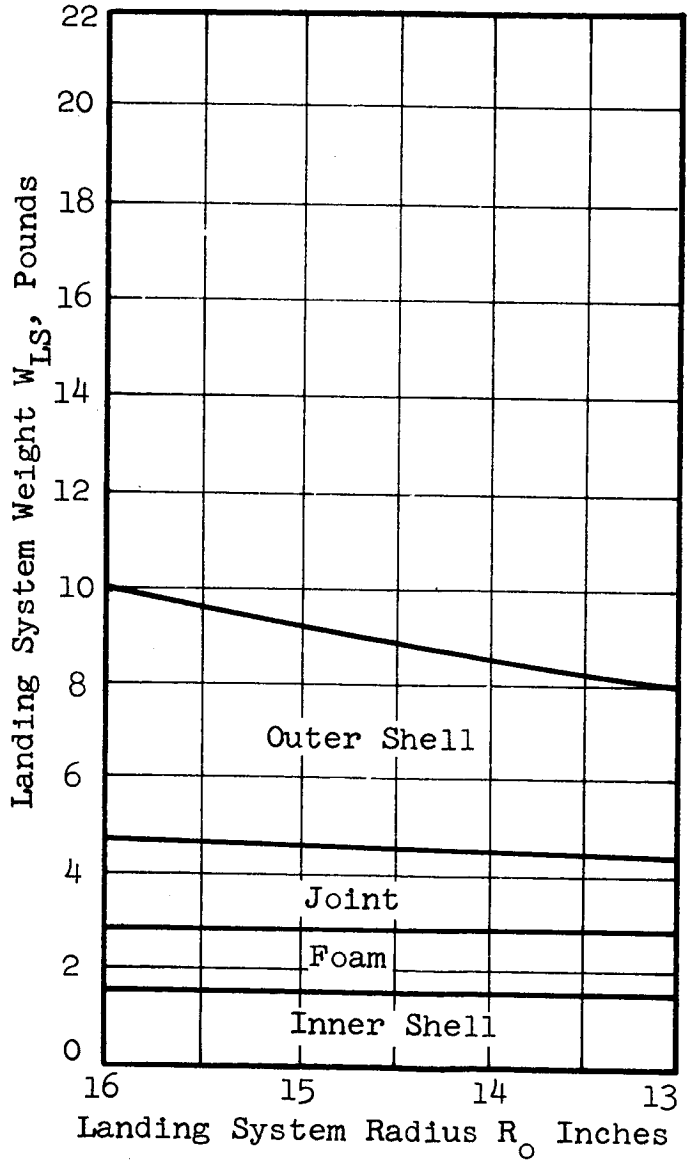

Figure 35. Variation of Icosahedron Landing System Weight and Outer Shell Inscribed Radius.

Truncated Dodecahedron. - The developed crushing force and energy absorbed is presented for the truncated dodecahedron polyhedron shape in figure 36 based on the anisotropy coefficient that varies exponentially. This irregular polyhedron shape presents two faces for impacting, the large hexagonal face, and the smaller pentagonal face. The use of the 700 psi crushing strength for plotting these curves has resulted in the smaller face showing a developed crushing force close to the 50 000 pound limit, but as the stroke increases the load also increases because the bordering faces add increasing crushing area with stroke. The larger hexagonal face exhibits the same load deformation characteristic as the pentagonal face as shown in the figure.

The weight variation of the inner and outer shells, the girth band joint, and the foam material poured between the square cut ends of the core elements and the spherically contoured inner shell is shown in figure 37 plotted against outer shell radius. Methods of weight reduction illustrated in figure 33 as square cut blocks, lightening holes on faces and other methods for the dodecahedron are also applicable to this shape. Figure 7f presents a lightweight configuration for the truncated icosahedron which should be easy to fabricate.

System Comparisons. - Figures 29 through 37 presented comparisons of developed crushing force, energy absorbed, and landing system weight for spherical and polyhedra shapes. The assumptions which were used in the development of these graphical comparisons were as follows:

1. Direct impact of the landing system
2. 30 inch inscribed diameter which results in a minimum landing system thickness of 6 inches
3. 700 psi crushing strength and 6.7 pound per cubic foot density assumed for the core material which corresponds to the efficient heat resistant phenolic honeycomb material

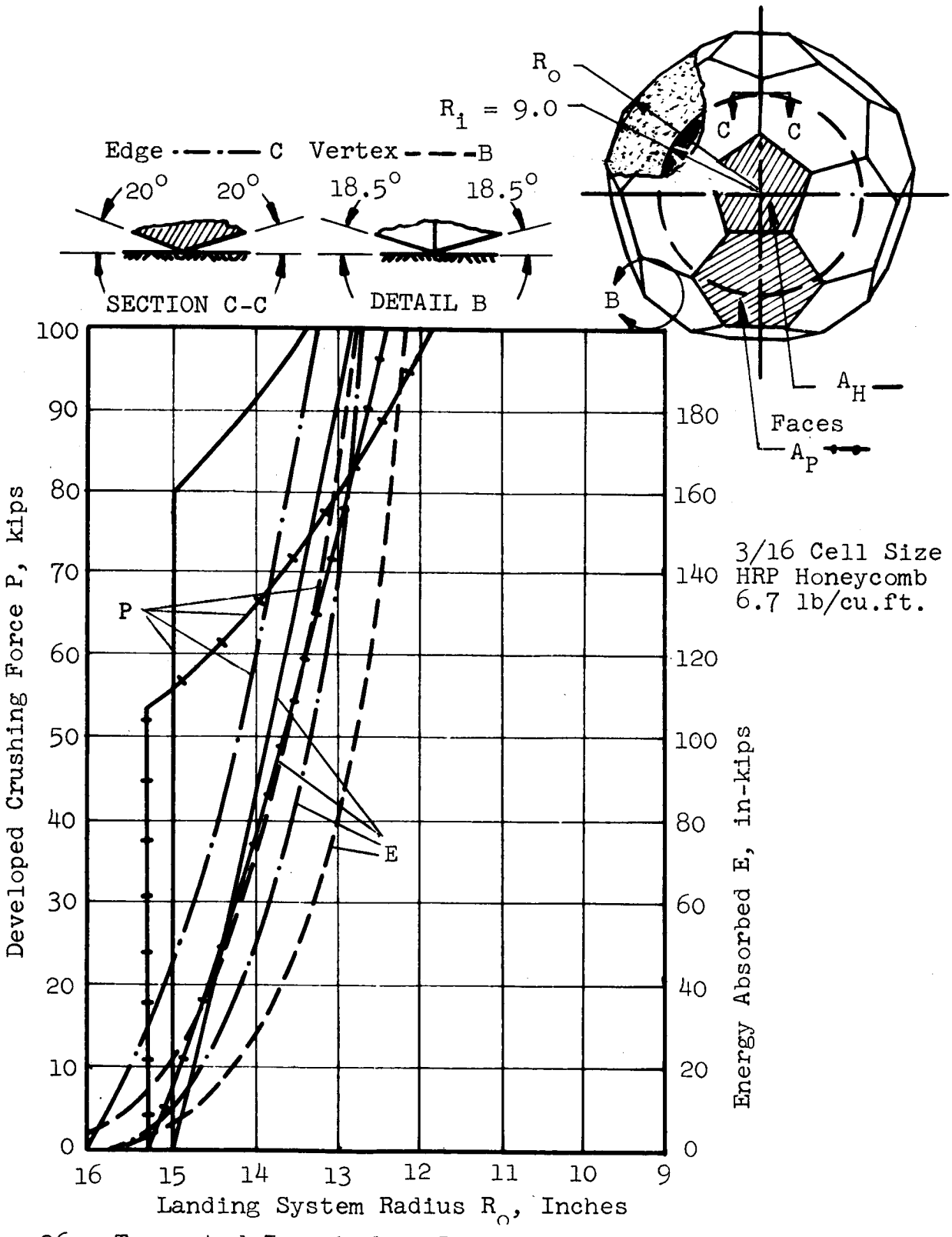

Figure 36. Truncated Icosahedron Landing System Direct Impact Force And Energy Absorption Characteristics.

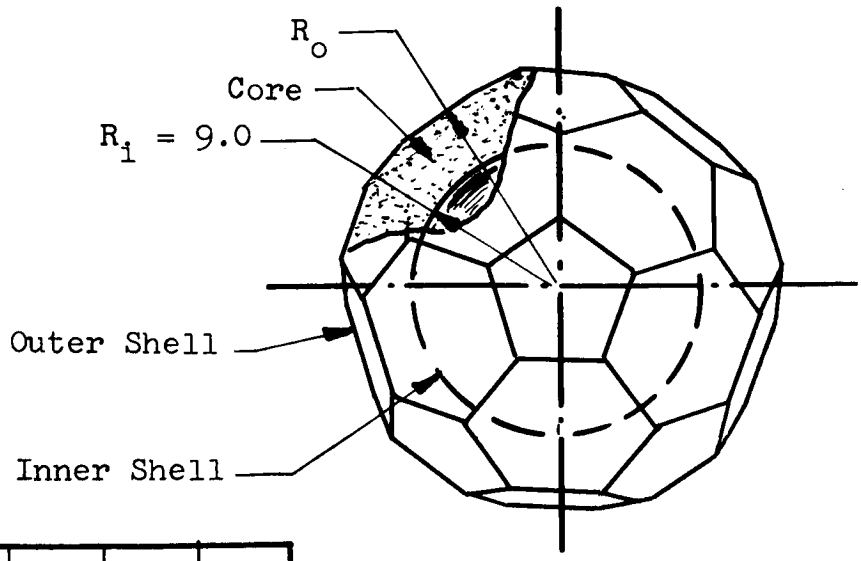

3/16 Cell Size
HRP Honeycomb
6.7 lb/cu.ft.
Density

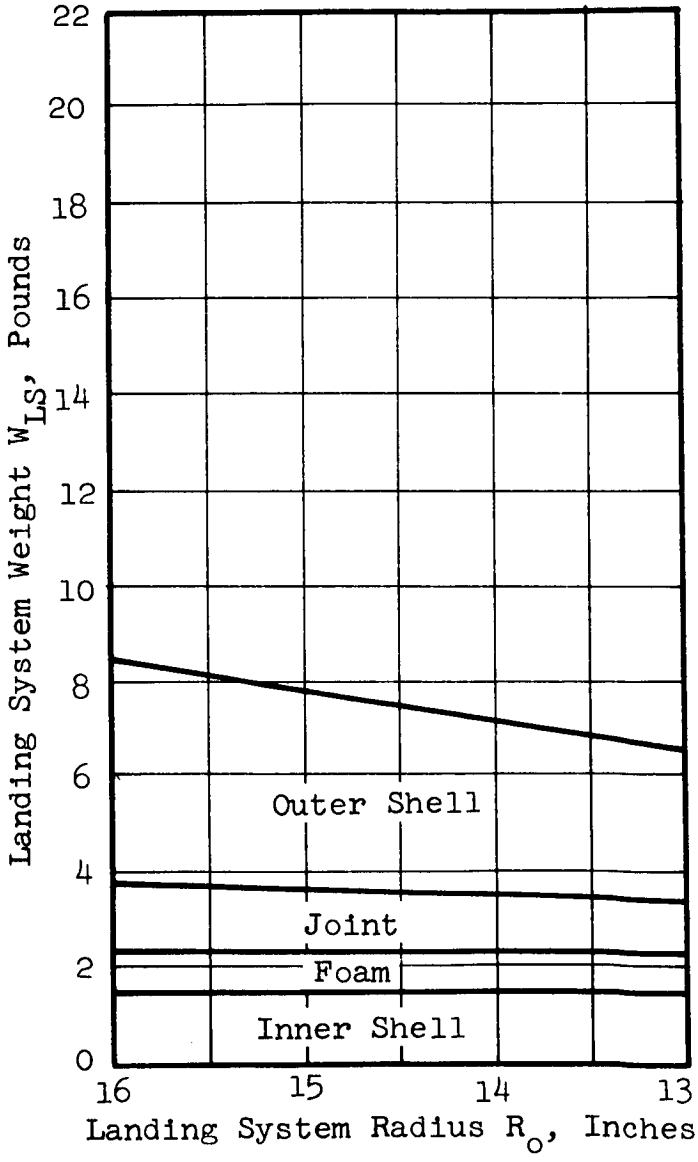

Figure 37. Variation of Truncated Icosahedron Landing System Weight With Outer Shell Inscribed Radius.

4. A stroke of 80 percent of core thickness or 4.8 inches for the 6 inch thick spherical shape and flat face impacts

5. Anisotropy characteristics based on the "exponental" curve shown in figure 29, except that the "linear" and "isentropic" curves also are plotted for the spherical shape.

The use of a 700 psi crushing strength for parametric comparison calculations, and of scale limits which range only just beyond specified limit values for developed crushing force and energy absorbed resulted in plots of extremely high forces and energy absorbed for a short stroke. These values for the 80 percent stroke, 4.8 inches, have been tabulated for comparison purposes in Table V. This table also presents crushing force and energy absorbed in percent of required limits. Developed crushing force exceeds the 50 000 pound limit in each case except for vertex impact of the icosahedron. Both the icosahedron and the dodecahedron shapes fail to achieve the required energy absorbed for vertex impact with values which are 35 and 69 percent respectively of specified limits. A material of very high crushing strength would be required at the vertices of these shapes to achieve the required energy absorbed.

Weight comparisons of the candidate landing systems for 6.7 pound per cubic foot core material are presented in Table VI. The shells and girth band joint weights were read from the parametric weight curves for each shape at the 6 inch thickness point. The weight of these landing systems based on the 6 inch thickness and the 6.7 pound per cubic foot core material density is shown from 224 percent to 336.5 percent of the required 20 pound limit, with the lowest value for the sphere. The weight increases as the shape departs further from the spherical shape. Table VI also compares the average core density required to stay within the 20 pound weight limit. The 6 inch thickness shell and girth band weights remain the same, and the required low average core densities for each shape are tabulated. These densities are much lower than available efficient core materials.

TABLE V. COMPARISON OF ENERGY ABSORPTION FOR 30 INCH INSCRIBED DIAMETER LANDING SYSTEM SHAPES (6 INCH THICKNESS) 700 PSI CRUSHING STRESS

Landing System Shape		Developed Crushing Force		Impact Energy Absorbed	
		kips	% Lim.	in-kips	% Req.
Sphere	Isentropic*	260	520	630	378
	Linear*	160	320	420	252
	Exponential*	94	188	310	186
Truncated	Icosahedron				
	- Face (Pentagonal)	130	260	400	240
	Face (Hexagonal)	150	300	500	300
	- Edge	140	280	350	210
	- Vertex	130	260	300	180
Icosahedron					
	- Face	119	238	630	378
	- Edge	138	276	400	240
	- Vertex	40	80	66	35
Dodecahedron					
	- Face	220	440	770	462
	- Edge	93	186	200	120
	- Vertex	68	136	115	69

* Material anistropy variation with angle to load.

TABLE VI. COMPARISON OF WEIGHTS FOR 30 INCH INSCRIBED DIAMETER LANDING SYSTEM SHAPES (6 INCH THICKNESS)

Landing System Shape	Average Core Density	SYSTEM WEIGHTS					
		Core		Shell & Joints		Total	
	lb/cu ft	lb	% Lim.	lb	% Lim.	lb	% Lim.
Sphere	6.7	38.8	194.0	6.0	30.0	44.8	224.0
	2.4	14.0	70.0	6.0	30.0	20.0	100
Truncated Icosahedron	6.7	48.7	243.0	7.8	39.0	56.5	282.0
	1.7	12.2	61.0	7.8	39.0	20.0	100
Icosahedron	6.7	51.9	259.0	9.3	46.5	61.2	305.5
	1.4	10.7	53.5	9.3	46.5	20.0	100
Dodecahedron	6.7	57.0	285.0	10.3	51.5	67.3	336.5
	0.8	9.7	48.5	10.3	51.5	20.0	100

If the developed crushing force and energy absorbed are reduced in proportion to the core density reduction required by the 20 pound weight limit, the spherical shape which had crushing force and energy absorbed values of 188 and 186 percent, respectively, above limits meets the 100 percent limits. The truncated icosahedron shape also can be reduced down to within the required crushing force and energy absorption limits by using reduced density ratios. Segmented elements arranged in the manner shown in figure 7f could be the practical design approach.

System Selection. - The primary objective of this program is the development of three types of landing systems of honeycomb, composite, and frangible tube elements. The dodecahedron and icosahedron shapes did not meet vertex impact energy requirements and were extremely heavy, therefore they were eliminated. The sphere and truncated icosahedron shaped landing systems using frangible tube type elements can be compared as concepts shown in figure 6c and 7d respectively. The spherical shaped configuration is feasible and consists of evenly spaced radial tubes with dies in quantities and sizes which are within the ranges of tubes tested. The truncated icosahedron shape configuration was dependent on the development of efficient large diameter tubes to be used on the pentagonal faces. This development was not achieved, therefore, the truncated icosahedron shape was eliminated and the spherical shaped segmented element design approach was selected for each of the three honeycomb, composite, and frangible tube types. The three selected spherical types with identical shells and girth bands are presented in figure 38. Each of 80 elements of the honeycomb, composite, and frangible tube types are located in an evenly spaced pattern in accordance with the triangular division of a spherical surface as shown in figure 4b. This type of design approach for the spherical shaped landing system had two particular advantages over other configurations, a method of rapid fabrication of 80 elements of the same basic triangular shape could be developed, and the assembled elements on the sphere provided a natural hemispherical parting surface between elements.

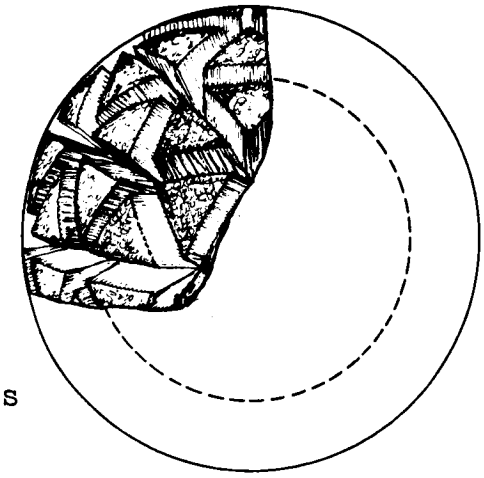

a. Honeycomb Elements

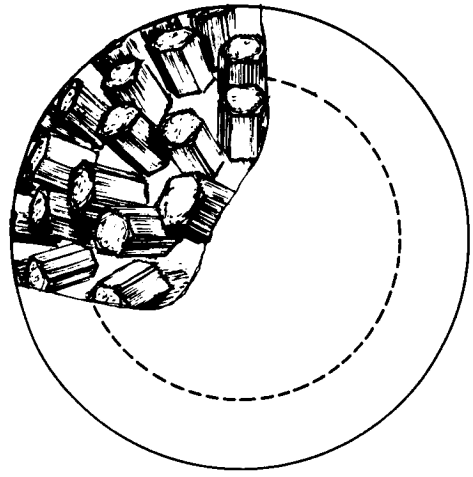

b. Composite Elements

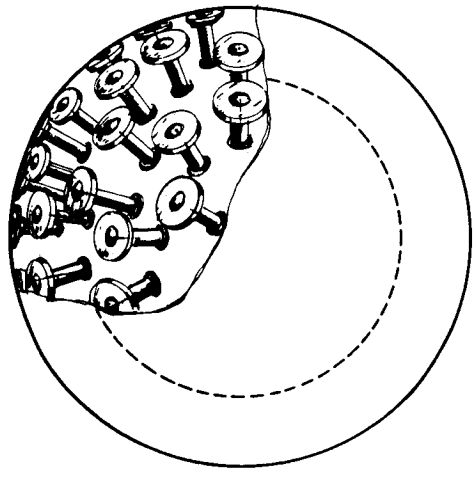

c. Frangible Tube Elements

Figure 38. Selected Spherical Landing System Configurations.

Development of Spherical Test Sectors. - A detail analysis of the landing system weight requirements for each of the three types of systems is presented in Appendix A. The calculated allowable weight limits for an 80 element core are tabulated in Table AIV. The results of this weight analysis are graphically presented in figure 39 as three systems which have identical inner and outer shells and girth band. The frangible tube landing system is shown to be below the weight limit of 20 pounds even for a 32 inch spherical diameter. Later it was necessary to consider the addition of honeycomb elements to this frangible tube design to provide retention for the franging dies and shear stability for the tube elements.

An analysis presented in Appendix B provided the detail element geometry properties which were used in the design and fabrication of representative landing system honeycomb and composite elements. Figure B-2 and B-3 of Appendix B present measured weight and crushing force characteristics for triangular and hexagonal section honeycomb elements fabricated and tested in two cell sizes. Figure B-4 presents a similar test program for triangular composite honeycomb elements in two cell sizes but with similar composite densities. A detail weight breakdown is also presented in Appendix B for the tube and die elements based on measured weights. It was determined that for 6 inch long elements, 80 tubes and dies weighed 12.15 pounds consisting of 5.97 pounds and 6.17 pounds for the tubes and dies respectively. This weight comparison of tubes and dies is an indication of the significant advancement which was made in this program to succeed in making the dies light enough to keep the frangible tube concept competitive.

Detailed analysis of the three types of landing systems to determine the developed crushing force and energy absorbed by each of the systems was conducted. The analysis details are tabulated in Appendix C and summarized in the following table.

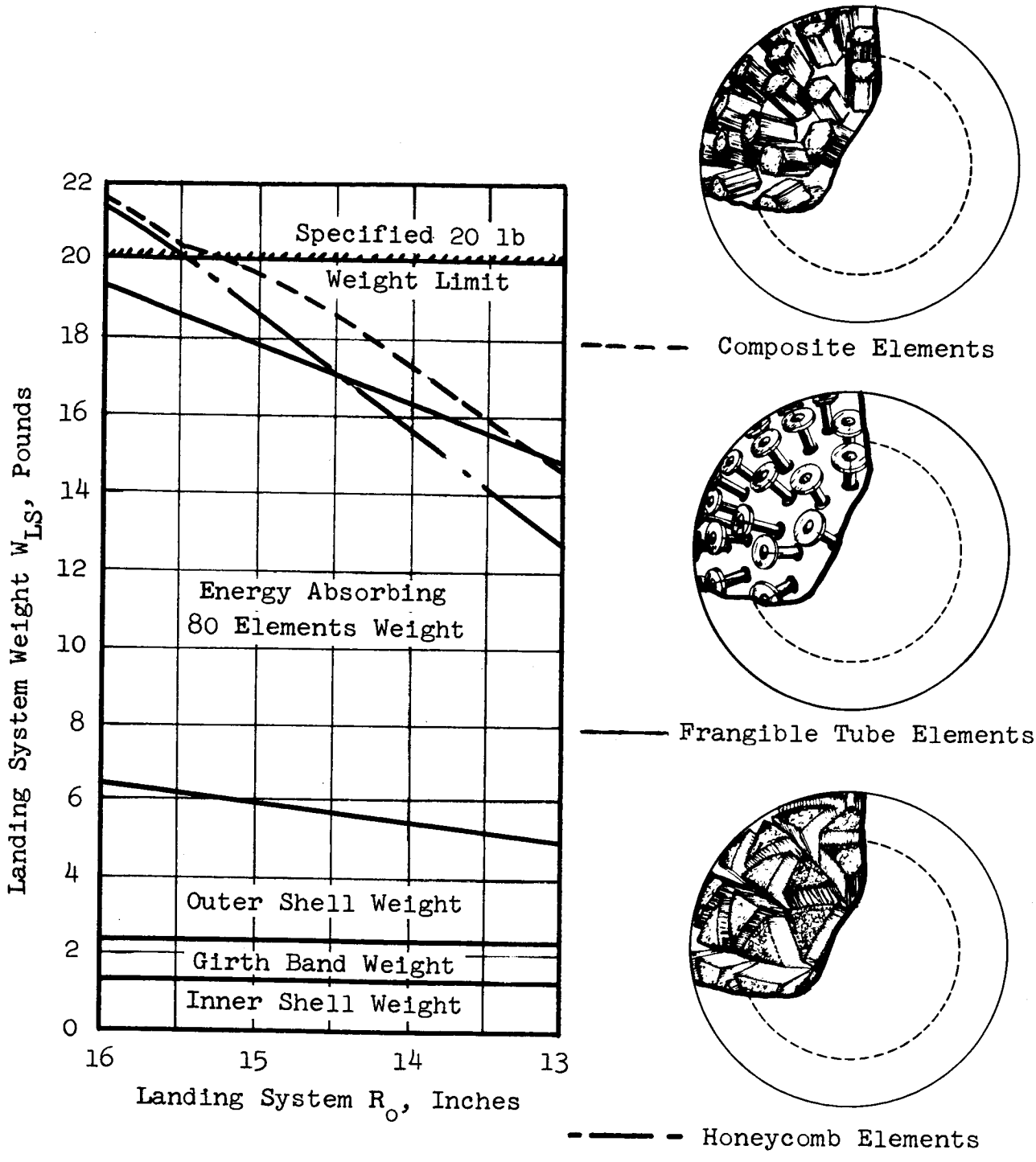

Figure 39. Variation of Three Configurations of Spherical Landing System Weights With Outer Shell Circumscribed Radius.

Diam. in.	Thick-ness in	Weights Limit	Weights Actual in.	G's Limit	G's Actual	Energy Absorbed Required in-lb	Energy Absorbed Actual in-lb	%
HC 31	6.5	20.0	19.97	1000	950	186,335	194,000	104
CO 31	6.5	20.0	20.22	1000	935	186,335	190,000	102
FT 31	6.5	20.0	18.75	1000	763	186,335	153,000	82
HC 30	6.0	20.0	18.72	1000	950	186,335	177,000	95
CO 30	6.0	20.0	19.69	1000	987	186,335	175,000	94
FT 30	6.0	20.0	17.81	1000	763	186,335	136,200	74

The parametric curves which provide the developed crushing force and energy absorbed data are presented as figures 40, 41, and 42 for honeycomb, composite, and frangible tube types respectively. The analytical effort indicated that for each of the three types of systems a similar 31.0 inch diamter, or a 6.5 inch landing system thickness was optimum. The table above indicates that the G limitation is the most critical limitation for the honeycomb (HC) and composite (CO) element systems. The frangible tube type of element does not achieve the required energy absorption, but this was corrected in detail design of the elements by the addition of a hexagonal section of honeycomb through which the frangible tube was threaded. Figure 29 presented the "exponential" anistropy curve which was used in the development of figures 41 and 42. Since a very minimum of effort was expended on the development of reliable anistropy curves a high level of confidence could not be placed on parametric plots which used this data. Table VI showed that the "exponential" versus the "linear" anisotropy curve data for the spherical shape provided results which were 186 and 252 percent respectively over the energy absorption requirements. The "linear" curve which corresponds to the aluminum honeycomb data may actually be a closer curve to non-metallic honeycomb properties, then the test results of the segments would be 35 percent higher than those predicted using the "exponential" shaped curve.

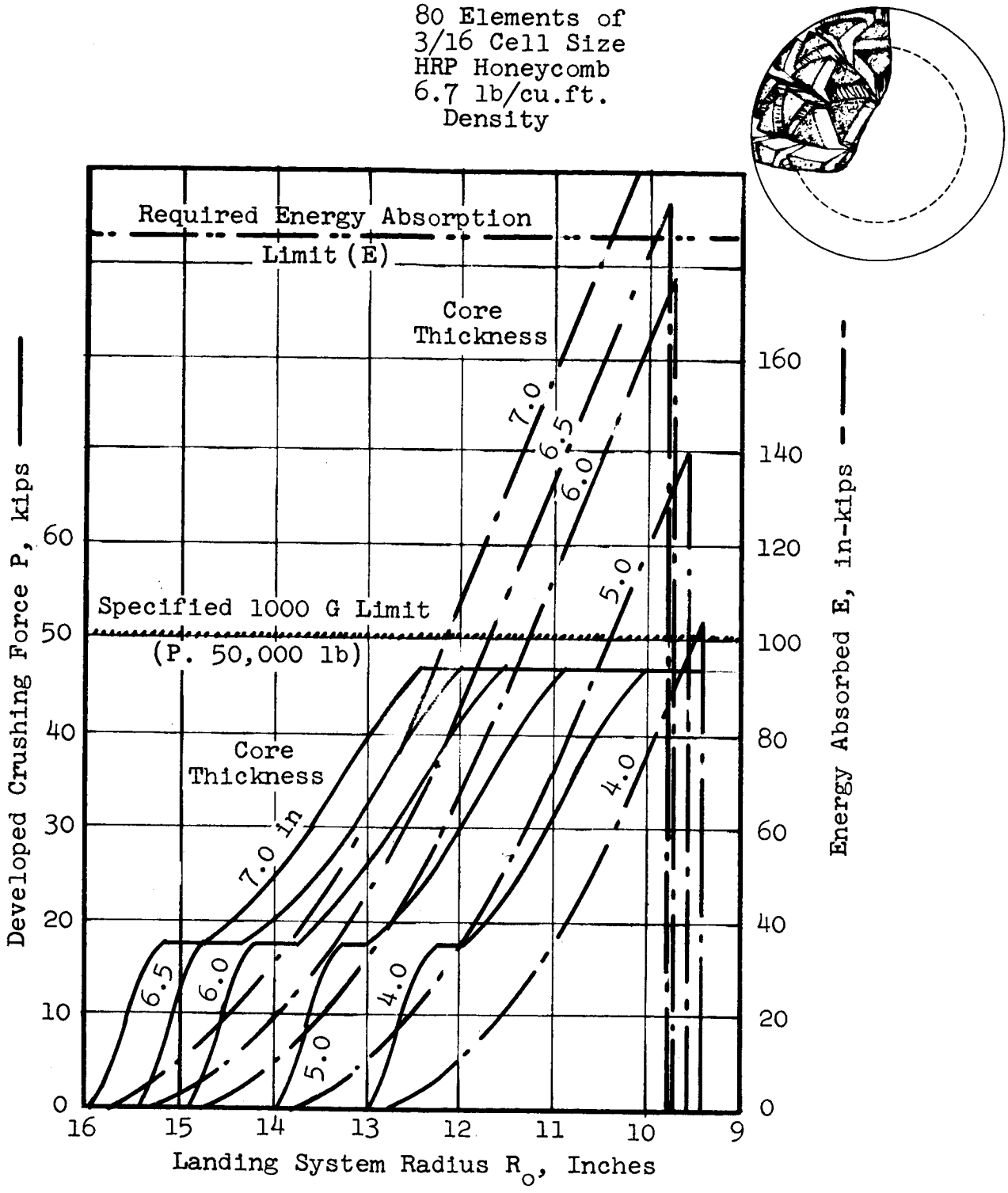

Figure 40. 80 Honeycomb Element Spherical Landing System Direct Impact Force and Energy Absorption Characteristics.

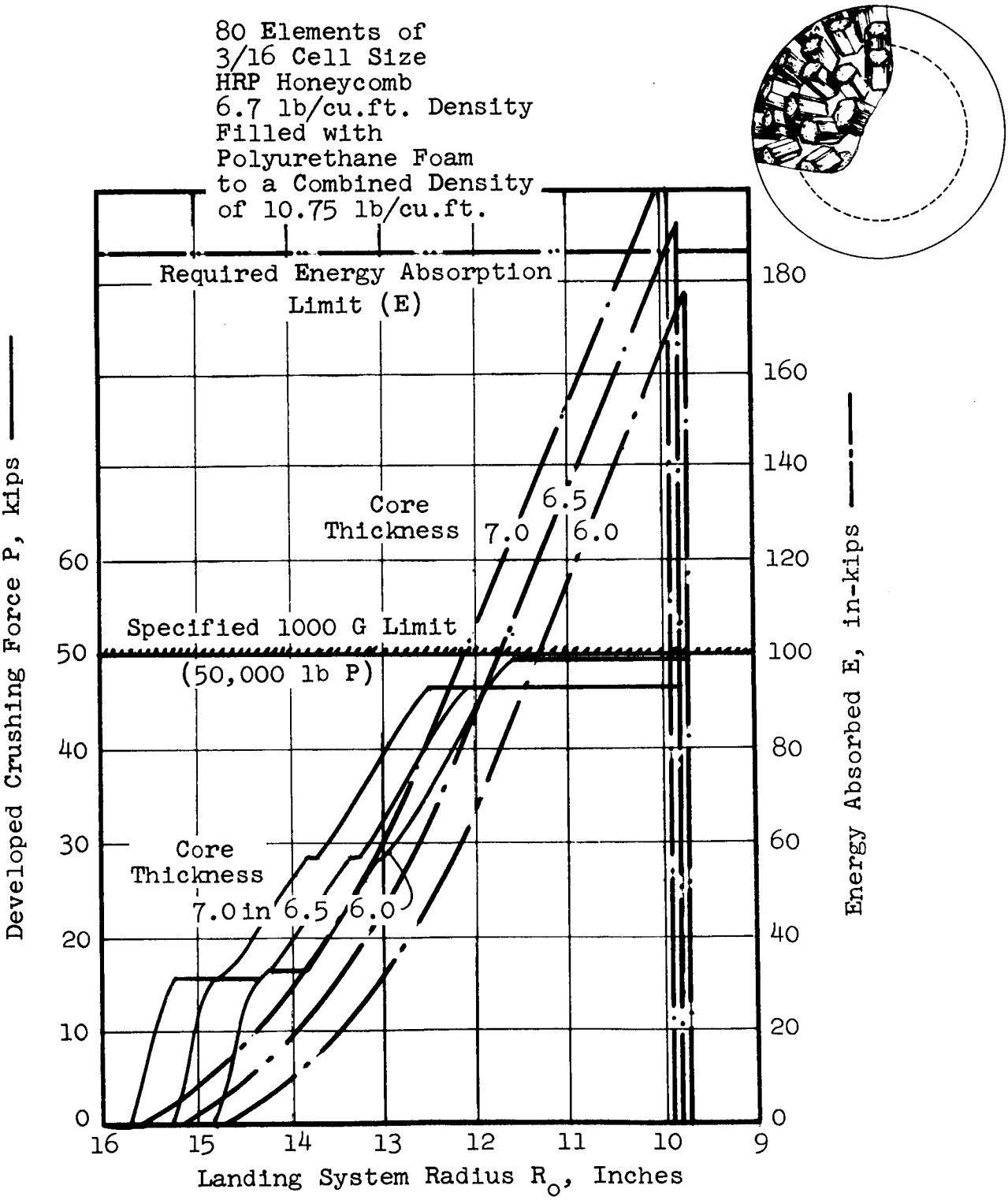

Figure 41. 80 Composite Element Spherical Landing System Direct Impact Force and Energy Absorption Characteristics.

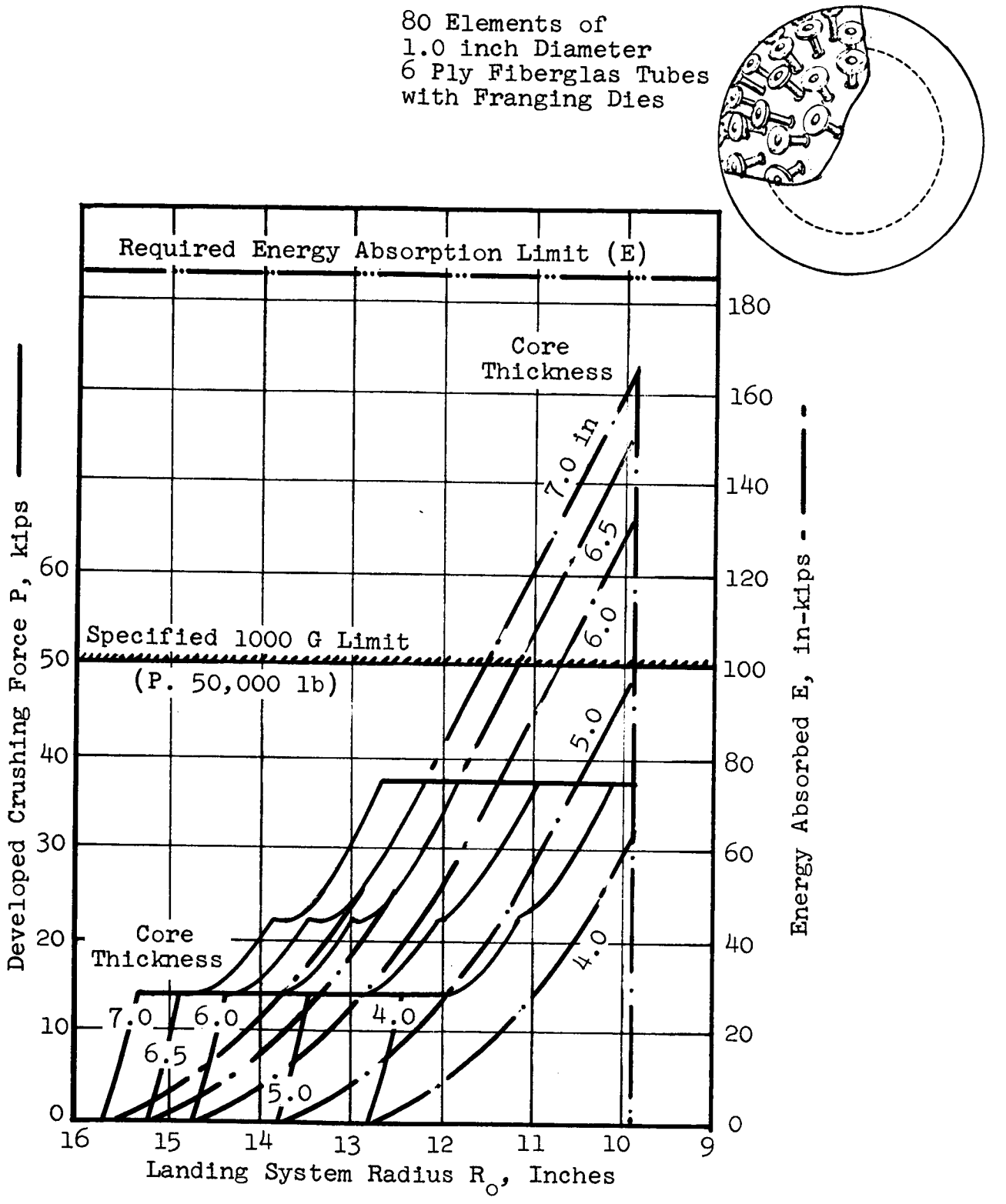

Figure 42. 80 Frangible Tube Element Spherical Landing System Direct Impact Force and Energy Absorption Characteristics.

Honeycomb Elements Test Segment Design. - The design for the three static test segments which represented the honeycomb type of landing system is presented in Sketch SK 78054. Advanced planning for the delivery of honeycomb block material for both the honeycomb and composite types was based on preliminary calculations which indicated that 6 inch deep blocks should be obtained. The longest spherically contoured elements which would be fabricated from a block of this depth are less than 6 inches long. All segment specimens were designed to weigh the same with weight controlled by element length and cross-sectional area. A range of honeycomb element lengths and corresponding element cross-sections was established which would provide a series of force and energy tests that would be interpreted to establish the required landing system thickness for design. Elements were fabricated in 5.0, 4.5 and 4.0 inch lengths with sections which varied from full triangles to hexagonal, for weight control, in accordance with the geometry data of Appendix B, figure B-1. The curves for the honeycomb type shown in figure 40 include element lengths of the sizes described. The 6.5 inch thickness load-deformation shape corresponds to that of the shorter elements, therefore it was considered that 5.0, 4.5, and 4.0 inch long elements would provide an accurate shape of the required landing system design curve as well as establishing the required landing system thickness.

Composite Elements Test Segment Design. - The design for the static test segments which were to be fabricated with composite elements is presented in SK 78054. The same procedure as has been described for the honeycomb segments was followed to establish three element lengths of 5.0, 4.5, and 4.0 inches for each of the three segements to be tested. Since the density of the composite material was 10.75 pounds per cubic foot, and that of the honeycomb elements was 6.7 pounds per cubic foot, the composite elements had a much smaller cross-sectional area for equal element length and weight.

Frangible Tube Elements Test Segment Design. - The design for the static test segments which were fabricated with frangible tube and honeycomb elements is presented in SK 78055, and the design for the matched die molded lightweight plastic dies is presented in SK 78057. The procedure described for the selection of the honeycomb segment element lengths was also applied to these three segments so that the test results of the three types of elements in 5.0, 4.5, and 4.0 inch lengths would be directly comparable. Parametrically developed crushing force and energy absorbed curves for these three element lengths are included in figure 42. These parametric curves did not include the use of honeycomb as a tube support since initial fabrication effort to make drilled honeycomb elements always resulted in split tubes. Franging dies were installed on each end of the tube to provide better tube alignment when franging commenced, and to ensure franging action continuing if one die was jammed or damaged in initial landing impact on unknown terrain.

Spherical Test Vehicle Design. - The design criteria which was used in the detail design and analysis of the spherical test vehicle was as follows:

1. Design to be based on two hemispherical shells for each in the installation of the test instrumentation.
2. An 18 inch external diameter shall be used.
3. The strength of the test vehicle shell shall be such that it resists permanent deformation after the application of loads 100 percent greater than the design impact loads for the landing system.
4. The test vehicle shall weigh 25 pounds maximum.

Test Vehicle Weight Analysis. - Figures 43 and 44 present parametric weight graphs which were used in establishing the detail design approach. Three candidate design concepts were considered for the test vehicle. The first concept was to fabricate a

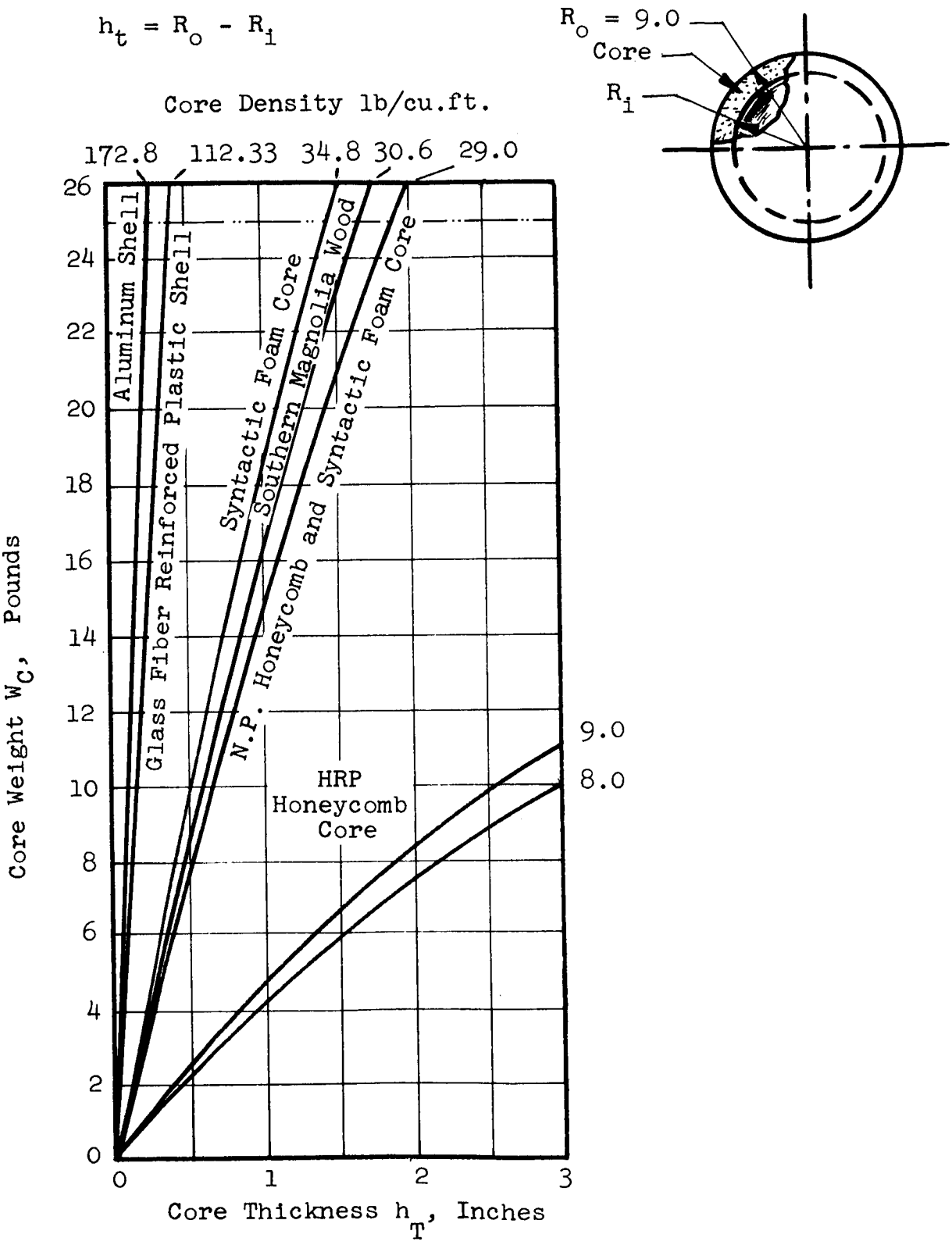

Figure 43. Variation of A Spherical Test Vehicle Core Weight With Core Thickness and Density.

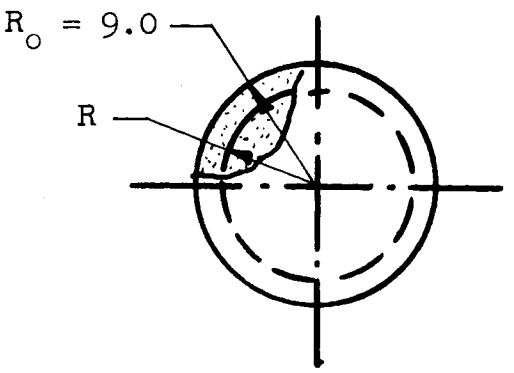

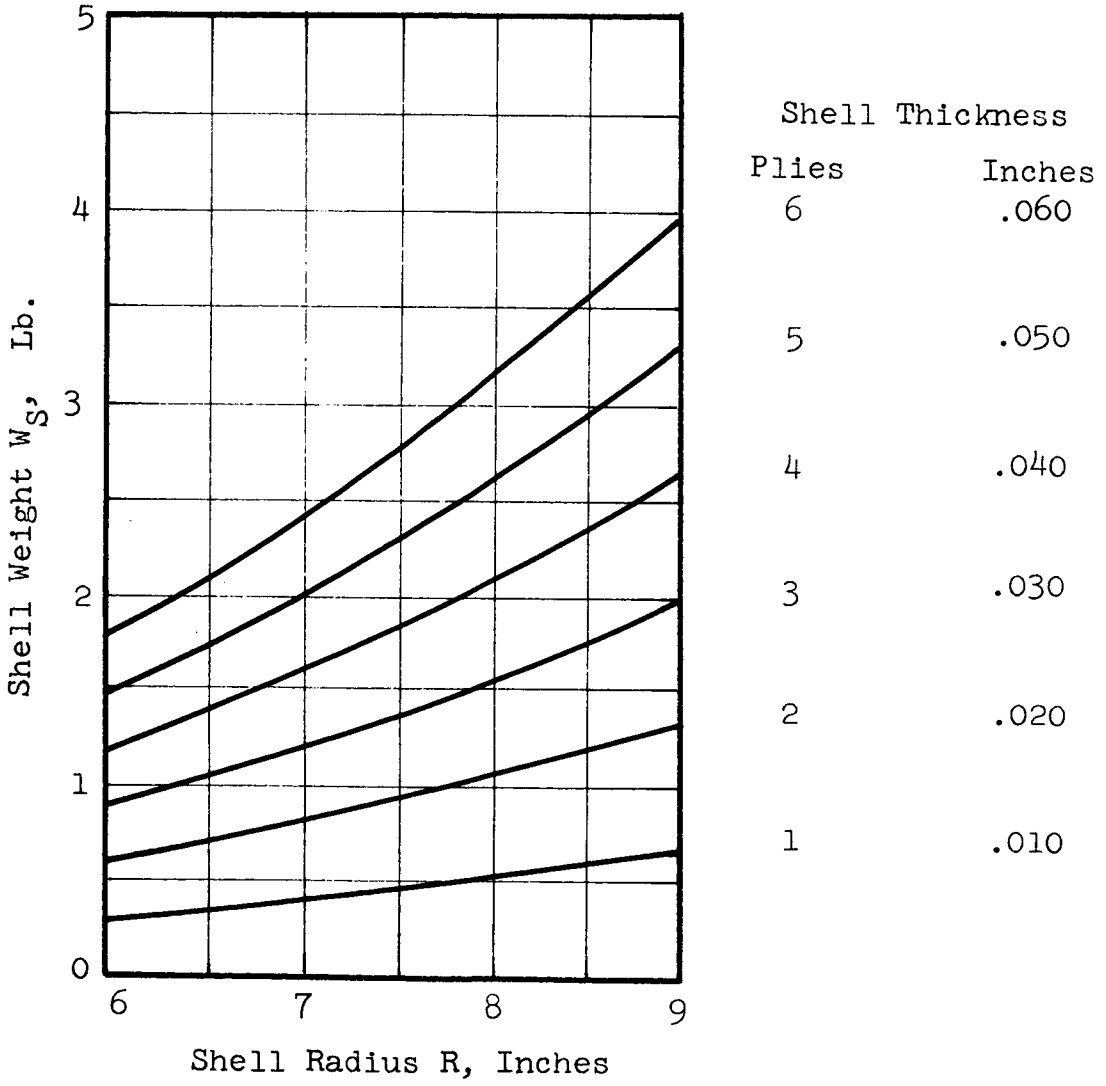

Figure 44. Variation of Spherical Test Vehicle Glass Fiber Reinforced Plastic Shell Weight With Shell Radius and Number of Plies.

honeycomb core which completely filled the shell and surrounds the payload instrumentation. The core elements radiated from the center of the shell as a series of 20 triangular based, pyramid elements with sides touching each large base end contoured to the 18 inch outer diameter. The spherical shaped honeycomb core would have been wrapped in a multiple outer skin to complete the fabrication. This concept was eliminated because a core material which was of adequate crushing strength to meet the 100 percent overload design requirement would be too heavy. A second design concept was to form a thick fiberglas shell which could resist the buckling impact and other stresses from the surrounding landing system. The payload instrumentation would be retained in inverted "cake" pan containers at the hemispherical joint. Figure 43 compares weight limiting fiberglas and aluminum shell thicknesses. It is indicated that the shell weight limitation restricts the thicknesses of the shell to .25 and .3 inches for the aluminum and fiberglas shells respectively at 20 pounds upper limit. These thicknesses were inadequate to resist local snap buckling of the shell on impact therefore, the second concept was eliminated. Figure 43 also provides a weight comparison of southern magnolia wood, syntactic foam, and nylon phenolic honeycomb with a syntactic foam versus thickness. These could form the core of a sandwich shell concept which was the third design concept considered. Figure 44 was used to determine the weight contribution of various inner and outer sandwich skin plies of fiberglas laminations when the design based on a sandwich shell concept was evaluated. The calculations for a sandwich type shell weight are presented in Appendix D. It was determined that the most practical design approach was that triangular shaped nylon phenolic honeycomb elements could be cut to thickness, crushed to spherical contour, assembled in a female mold and filled with foam. The outer skin would have been installed before the elements were assembled. Other approaches using syntactic foam without honeycomb made the sandwich shell core too thin and the fabrication process to provide a uniform core thickness would be complex.

Test Vehicle Stress and Strength Analysis. - The detail layout of the sandwich shell test vehicle is shown in Sketch SK 78056. Appendix D provides a stress and strength analysis of the selected nylon phenolic syntactic foam sandwich shell for the critical conditions of collapse buckling and local crushing. The sandwich shell was tested for local crushing strength as reported in element tests in figure D-1. The highest loading condition was provided by the frangible tube die element pressing against the shell. A plastic die was actually used in the test to load levels which were more than twice the landing system design impact levels with results indicating no permanent set.

FABRICATION

Test Segments. - A total of nine static test segments, three each of honeycomb, composite, and frangible tube element type were fabricated in accordance with Sketch SK78054 for honeycomb and composite, and Sketch SK78055 for frangible tubes. A further description of each of these segments is as follows:

a) Spherical test segment landing system with 20 elements 3/16-inch cell, 6.7 lb/cu.ft. HRP honeycomb.

   1. triangular section elements 4-inches long
   2. hexagonal section elements 4.5 inches long
   3. hexagonal section elements 5-inches long.

b) Spherical test segment landing system with 20 elements 3/16-inch cell, 6.7 lb/cu.ft. HRP honeycomb foam filled to weigh 9 lb/cu.ft. (polyurethane foam)

   1. hexagonal section composite elements 4-inches long
   2. hexagonal section composite elements 4.5-inches long
   3. hexagonal section composite elements 5-inches long.

c) Spherical test segment landing system with 20 elements of 6-ply, one-inch diameter tubes, 1/10-inch die radius plastic molded dies, and hexagonal section 3/16-inch cell, 6.7 lb/cu.ft. HRP honeycomb.

   1. hexagonal section honeycomb and tube 4-inches long
   2. hexagonal section honeycomb and tube 4.5-inches long
   3. hexagonal section honeycomb and tube 5-inches long.

Honeycomb Elements. - The honeycomb element consists of a basic constant cross-section of equilateral triangular shape cut from the honeycomb block. For one segment the triangular shape is used as cut, but for the longer elements weight control is achieved by cutting away the corners of the triangle to form a hexagonal section. Since each segment has 20 elements and there are three honeycomb segments to fabricate, a total of 60 elements were fabricated. A rapid method of cutting the equilateral triangular section from the honeycomb block was required. The conventional method for cutting fiberglas honeycomb is by using a band saw or in hand operations a bread knife is recommended by the materials producer. Figure 45 shows a rapid method of cutting the triangular elements by using a sheet metal formed "cookie cutter" and pressing the elements out with force from the test machine. The fabricated elements were of consistent high quality with smooth straight sides. The cutting action shown in figure 45 has just stamped out two elements at a time, succeeding stampings after the block has been relocated will produce four elements at a time.

The triangular elements are trimmed to hexagonal shape for different lengths using the edger also shown in figure 45. A wide chisel type cutter is used to slice the corners away guided by the boundary of the wooden fixture holding the element.

The block was pre-cut to the standard 6.65 inch width and depth required for the particular segment prior to the initial cutting of the triangular elements from the honeycomb block. Figure 45 shows that a 5 inch finished element is cut from a 5.25 inch block. Figure 46 shows the method used to produce a 5 inch long element which has a 9.0 inch radius concave hemispherical inner end contour and a 14 inch radius convex hemispherical outer end contour. The element is shown fitted in the 5.0 inch length triangular shaped wooden retaining fixture, which also has hemispherical contoured ends, with extra element length projecting beyond each end. An aluminum convex die of 9.0 inch hemispherical radius is placed

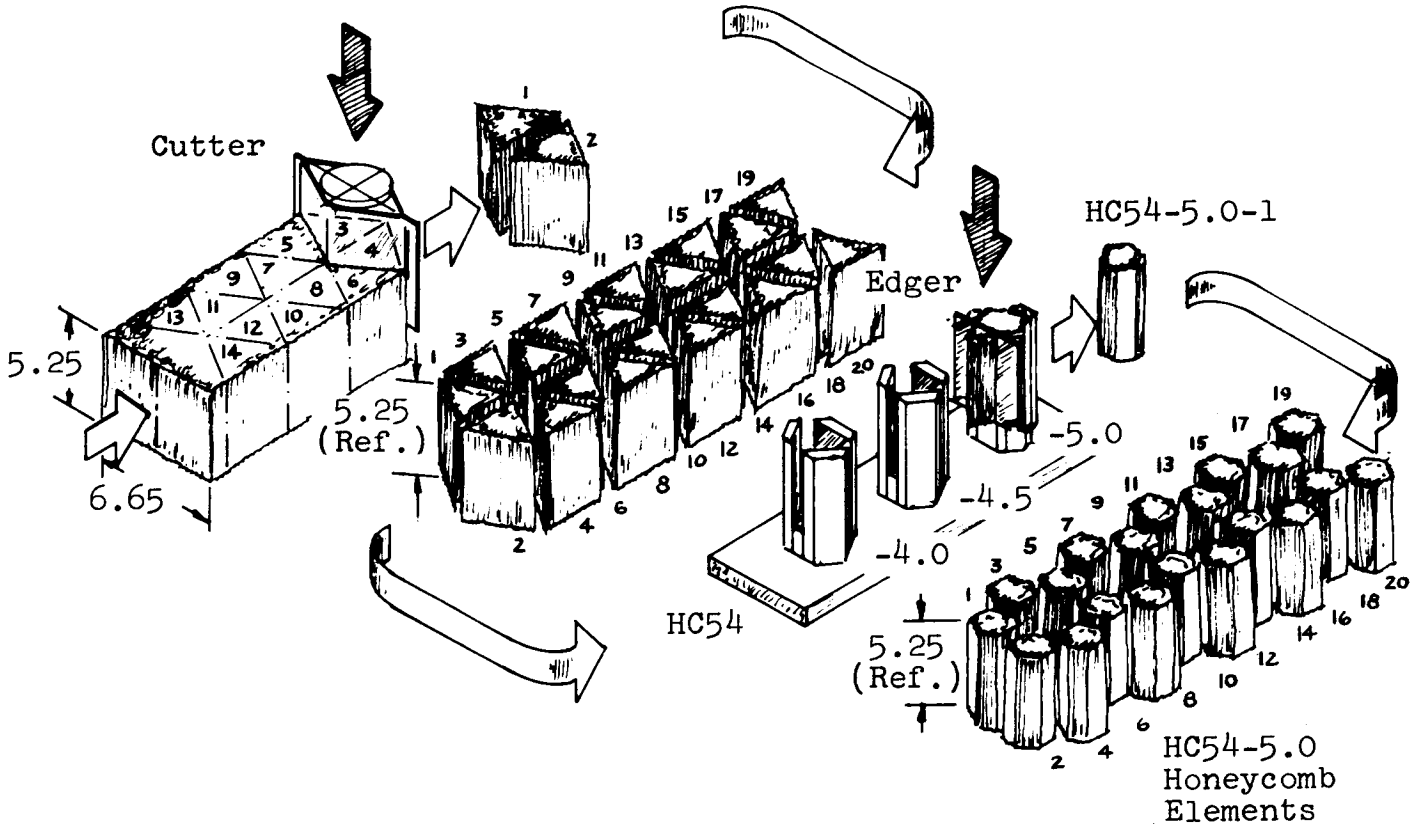

Figure 45. Method of Fabricating Honeycomb and Composite Energy Absorbing Structural Elements

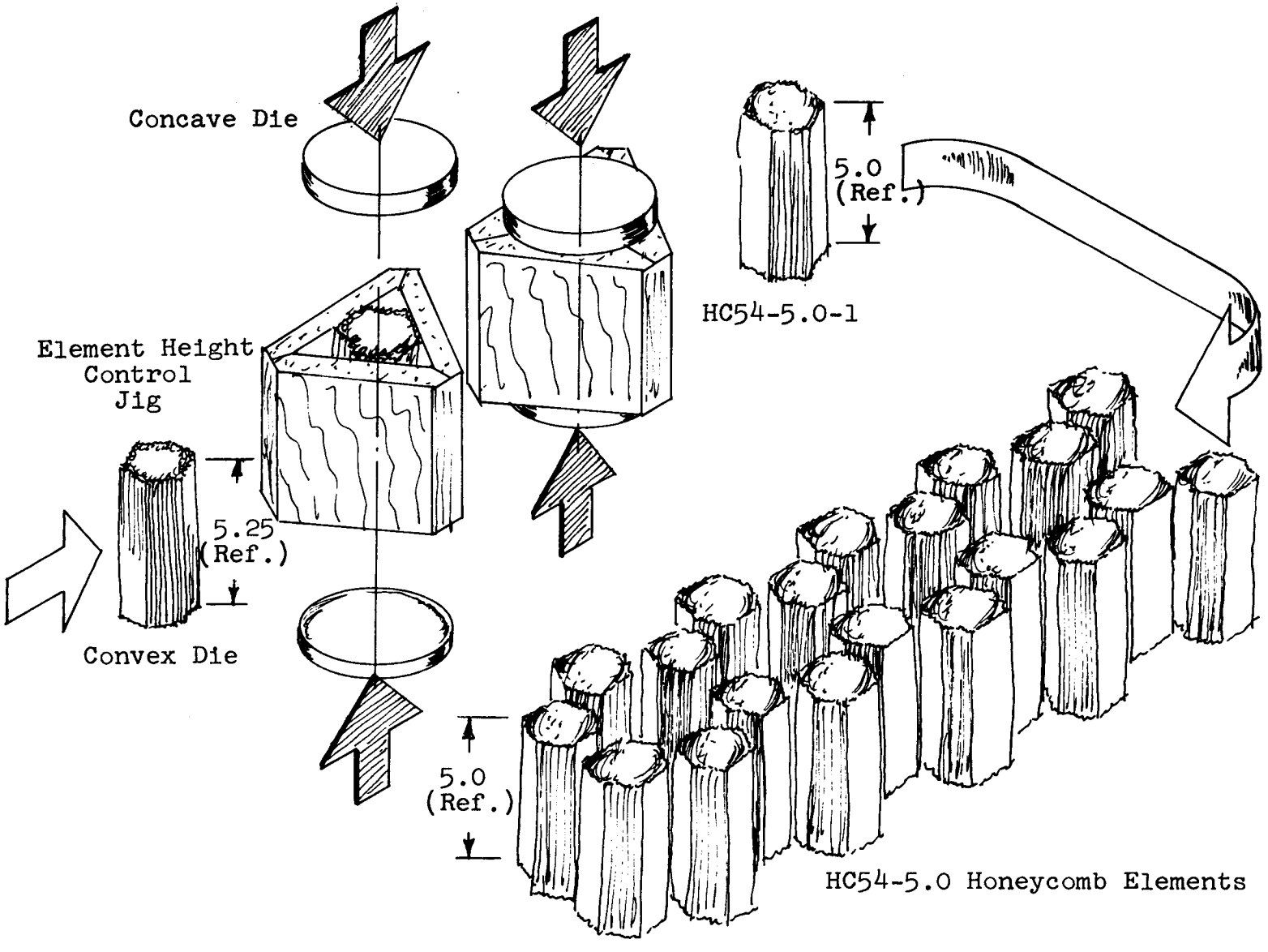

Figure 46. Method of Providing Contoured Ends and Height Control For Honeycomb and Composite Energy Absorbing Structural Elements.

below this fixture, and an aluminum concave die of 14 inch hemispherical radius is placed above the fixture. The triangular fixture containing the element is placed in the test machine with the aluminum discs on each end. Each projecting end of the element is contour crushed by the discs under the application of a steady compression load which rises sharply when the discs contact the ends of the fixture. This rapid rise in load is an indication that the element has been crushed to length, hence the load is then reduced to zero and the assembly is moved from the test machine. The crushed ends of the contoured element are blown clean while it is still in the fixture, and the ends are smoothed with sandpaper before the finished element is pushed from the fixture. The crushing load level provides a check on the crushing force capability of each element when it is contour-formed in this rapid manner.

Composite Elements. - The identical procedure which has been performed for the fabrication of honeycomb elements is followed in the fabrication of composite elements using the same size honeycomb blocks filled with foam. A particular problem in the fabrication of composite elements is in foam filling the 3/16 cell size heat resistant phenolic honeycomb blocks. The ability to fill blocks in this small cell size to a block depth of 6 inches and to achieve uniformity in the distribution of the foam represents an advancement in the state-of-the-art of composite construction of this type. The procedure for foaming the block consists of fabricating a plywood box without an upper side, that just surrounds the block. A 2 pound polyurethane foam is poured into the empty box in a quantity which would freely form a block of foam of one and a half times the box depth. The honeycomb block is immediately pressed into the foam in the box so that the foam starts to fill the cells and escape through them from the upper side of the box. The foam generates considerable pressure as it is forced upward through the cells of the block. The block is held against the foam pressure by two weighted channel strips which are rested on the top of the block parallel to the long sides. The overhanging ends of the channels

have weights attached. A polyurethane foam mixture for producing a 2 pound density foam is used to fill the 3/16 cell size 6.7 pound per cubic foot honeycomb. When the foam fills the cells, the composite material weighs 10.75 pounds per cubic foot.

Frangible Tube Elements. - The frangible tube element consists of a machine wrapped 1.0 inch diameter tube which is assembled through a central hole in a hexagonal cross section of 3/16 cell size honeycomb, and is capped at each end with plastic franging dies. The frangible tubes were fabricated as a separate operation using the machine wrapping procedure with 181 glass fabric and an epoxy resin system. The plastic dies were fabricated as a separate operation also in the matched die molding machine procedure described in the materials section. The hexagonal cross-section honeycomb is fabricated in the same manner as illustrated in figure 45, then drilled and counterbored for the tube and dies respectively as shown in figure 47. The drilling operation at first was difficult because the honeycomb element had a tendency to split apart. Counterboring for the dies presented no particular problem, and permitted the assembly of dies which are flush with the end of the honeycomb, and which retained the franging tube.

Test Segment Assembly. - After twenty energy absorbing elements for each of the three types of landing systems have been fabricated for the total of nine test segments, the six step segment assembly sequence shown in figure 48 is followed. The test fixture for the segments is also used for segment assembly, therefore, this fixture is fabricated before preparation for segment assembly begins. A single ply of 181 glass fabric and an epoxy resin system is draped and stretched over the dome shape of the test fixture to form the inner skin of the segment. Three plies of the same material in the form of an inverted frustrum of a conical shell form the edge skins for the segment and are attached to the inner skin by lapping the skin material. A pattern for the twenty segments, which is identical for each of the three types of landing systems, is marked on the surface of the inner skin. This pattern corresponds to dividing

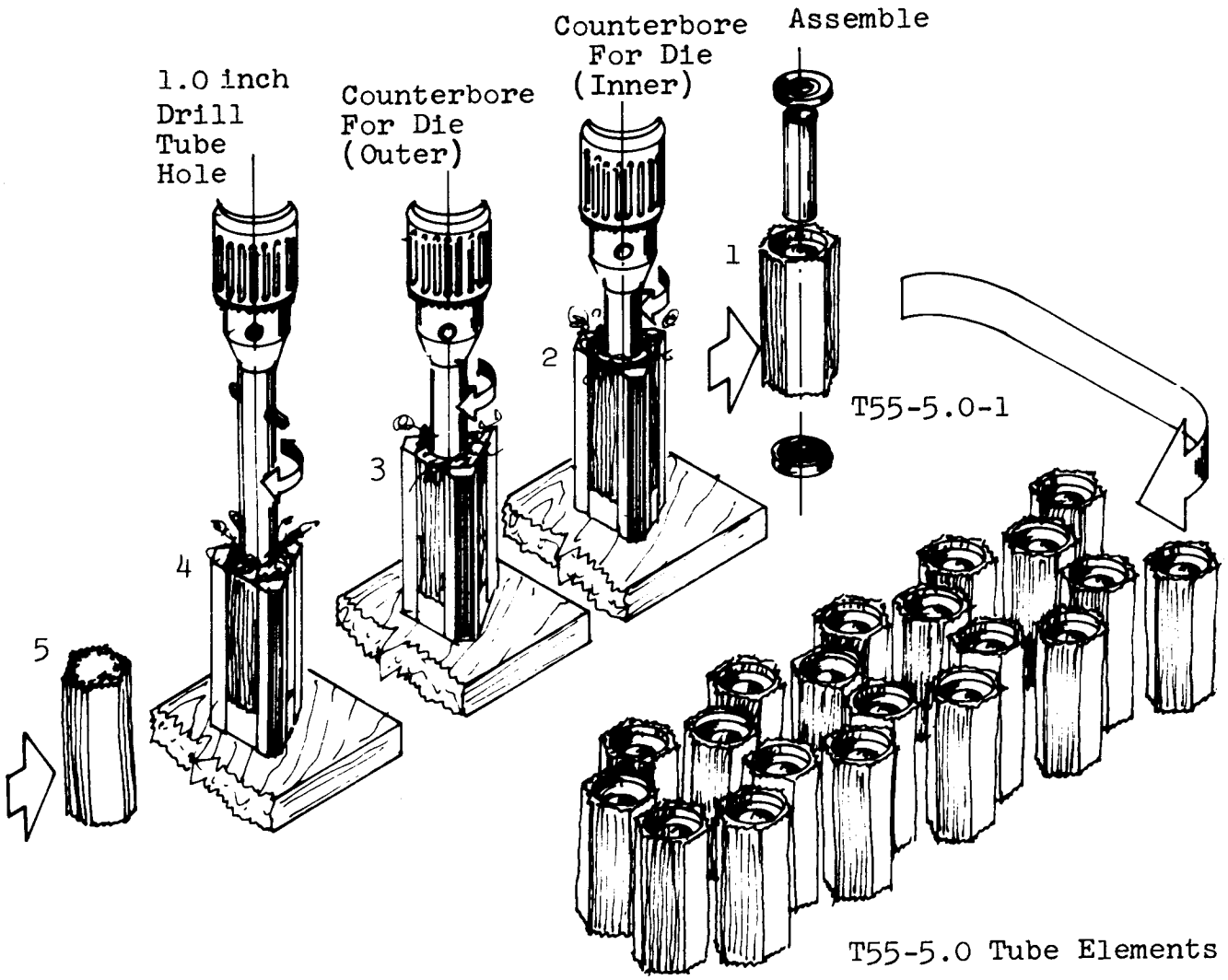

Figure 47. Method of Fabrication and Assembly of Frangible Tube With Honeycomb Energy Absorbing Structural Elements.

Step 1. Fabricate Wooden Mold and Test Fixture

Step 2. Layup Inner Shell Skin Ply

Step 3. Layup Segment Elements

Step 4. Bond 20 Crushable Elements

Step 5. Layup Outer Shell Skin Plies

Step 6. Oven Cure Assembly and Remove From Mold

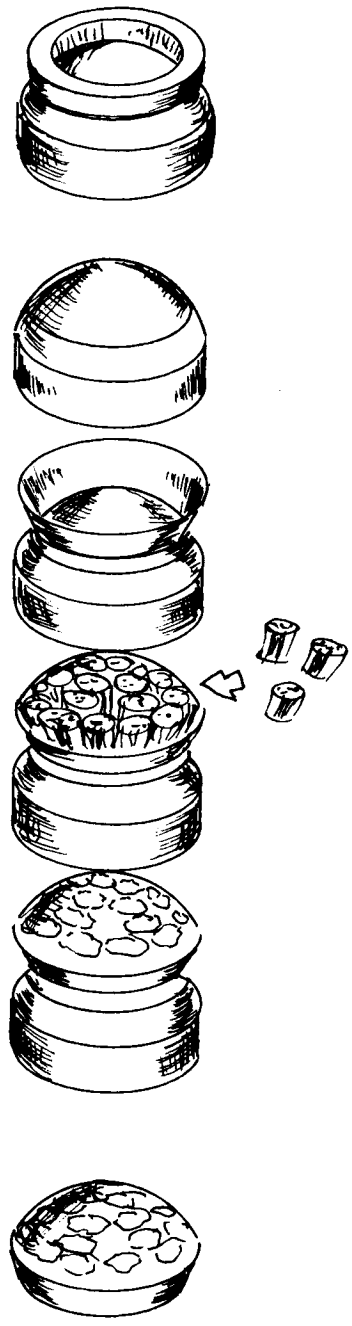

Figure 48. Fabrication Sequence For Test Segments Using An 18 Inch Spherical Shaped Mold and Test Fixture.

the spherical surface into triangular faces as was illustrated in figure 4. The assembly of the elements to the marked pattern results in an inner circle of five elements about the axis of the test fixture, five additional elements installed back to back to the first five in a large intermediate circle, and an outer circle of ten elements which butt against the segment edge skin. The assembly of elements on the inner skin which is mounted on the test fixture, is installed in the oven and cured. When the cured assembly is cooled, an outer skin of 181 glass fabric and epoxy resin is draped over the outer ends of the elements and drawn over the edge skin to form a lap joint. The assembly is again oven cured, and the finished segment is then removed from the mold and finish trimmed.

Figure 49 shows typical fabricated test segments for each of the three types of landing systems.

Test Vehicle System. - A procedure for fabrication of the spherical test vehicle is shown in figure 50. The procedure is similar to the fabrication of the test segments, since triangular elements are fabricated first then the hemispherical test vehicle components are fabricated in a wooden mold.

Honeycomb Core Elements. - The outer diameter of the test vehicle corresponds to the 18 inch inner diameter of the test segments; consequently, a total of eighty triangular honeycomb core elements of the same dimensions and corresponding to the pattern shown in figure 4 make up the basic core material of the test vehicle. These eighty elements are stamped from a short thickness of 1/4 cell size nylon phenolic honeycomb in the same manner and using the same tool as shown in figure 45 for the landing system elements. The completed thickness of sandwich test vehicle including inner and outer skins is 1.19 inches as shown in Sketch SK 78058. The triangular elements are crushed to core thickness and to spherical inner and outer end contour in the same manner as shown in figure 46 except for the use of a triangular core thickness-fixture and inner radius aluminum disc that matches core inner spherical radius.

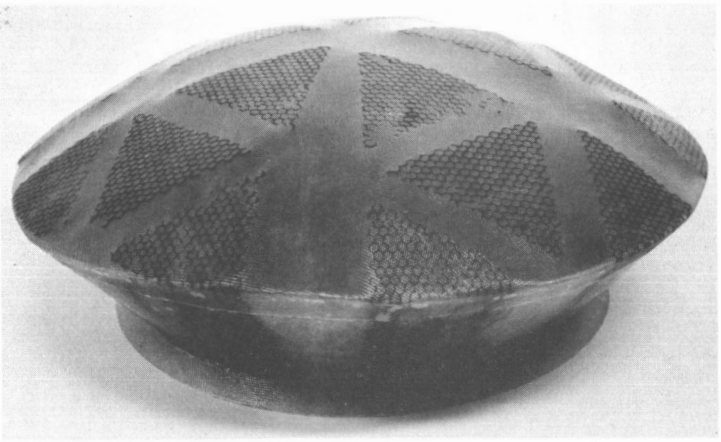

a. Honeycomb Elements

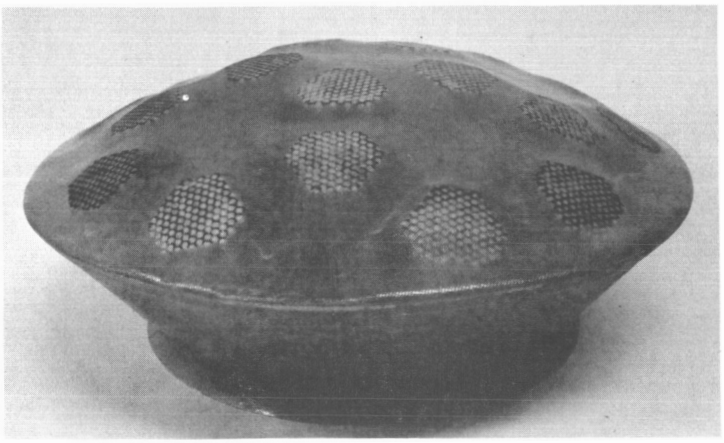

b. Composite Elements

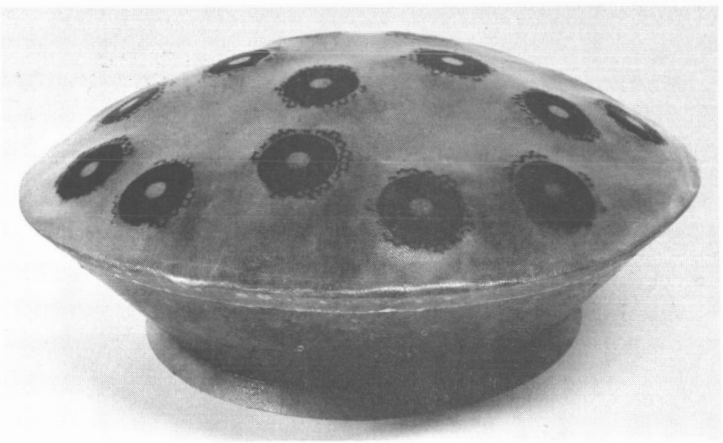

c. Frangible Tube Elements

Figure 49. Typical Fabricated Honeycomb, Composite, and Frangible Tube Test Segments.

Step 1. Fabricate Wooden Female Hemispherical Mold

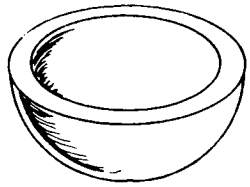

Step 2. Layup Outer Skin Plies In Mold

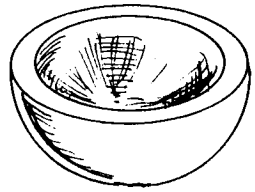

Step 3. Fabricate Triangular Honeycomb Core Elements and Bond In Place To Outer Skin

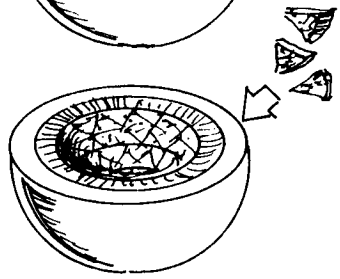

Step 4. Fill Honeycomb Core With Syntactic Foam

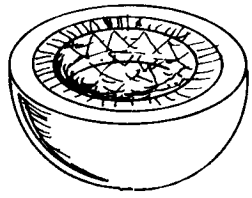

Step 5. Layup Inner Skin Plies Over Core

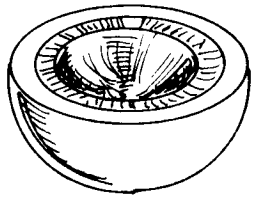

Step 6. Oven Cure Assembly and Remove From Mold

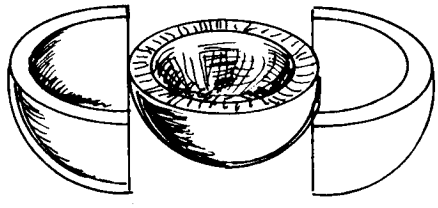

Step 7. Machine Mating Surfaces of Hemisphere

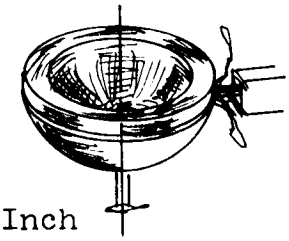

Figure 50. Fabrication Sequence For The 18 Inch Outer Diameter Sandwich Shell Hemisphere For The Test Vehicle.

Test Vehicle Assembly. - The sandwich shell hemispheres of the test vehicle are fabricated in the seven steps shown in figure 50. A female wooden mold which has a hemispherical radius of 9 inches is fabricated as two wooden segments. Three plies of 181 glass fabric and an epoxy resin system are draped in the mold and smoothed to the outer skin contour. The fabricated triangular honeycomb elements are bonded to the outer skin in accordance with a marked pattern that matches the figure 4 illustration for 40 elements per hemisphere. An epoxy syntactic foam mixture is prepared in accordance with the same procedure described in the previous program for 1/8 inch glass macro-balloons suspended in a one part epoxy based matrix. The additional step which was taken in this program was to screen the macro-balloons to use only sizes which would pass through a 1/8 inch screen, otherwise the odd sizes would stick in the honeycomb cells. The matrix was pasted into the honeycomb core elements until each of the core cells was filled and a smooth interior surface was presented. This assembly procedure is a hand operation which requires skill to ensure that no voids occur in the fabrication of the composite core. Three inner plies of 181 glass fabric and epoxy resin are draped over the composite core and all voids are worked out of the material by hand and trowel methods.

The hemispherical assembly is oven cured while in the mold, then the cooled assembly is removed from the mold by splitting it in two halves. The fabricated hemisphere is mounted in a lathe, and the mating surfaces and band ring grove are machined to sketch SK 78056 final dimensions. The fabricated test vehicle is shown in figure 51 disassembled.

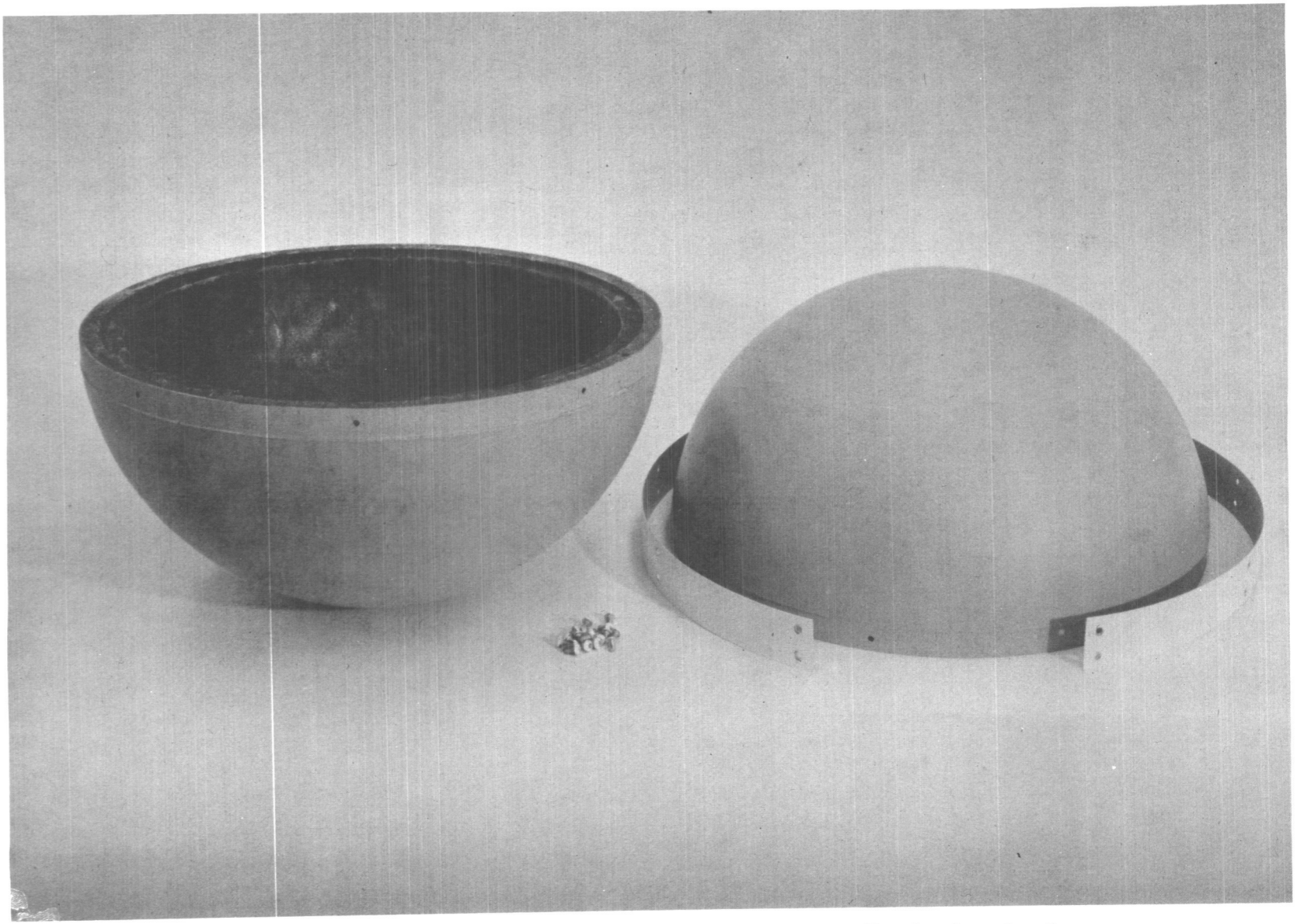

Figure 51. Disassembled Test Vehicle Showing Hemispherical Sandwich Shell Components And Joining Girth Band.

SEGMENT TESTS

Test Specimens. - A total of nine spherical test segments, three each of honeycomb, composite, and frangible tube element types were fabricated for static testing. The test specimens were identified by energy absorption element types and by thickness of the energy absorbing system as follows:

5.0 Inch Thickness

Honeycomb	HC54-5.0
Composite	CO54-5.0
Frangible Tube	T 55-5.0

4.5 Inch Thickness

Honeycomb	HC54-4.5
Composite	CO54-4.5
Frangible Tube	T 55-4.5

4.0 Inch Thickness

Honeycomb	HC54-4.0
Composite	CO54-4.0
Frangible Tube	T 55-4.0

Test Setup. - The test segments were tested in a universal testing machine of 120 000 pound capacity. The machine was equipped with a Baldwin Model EXT-6137 ram deflectometer which measures travel over 10.0 inches of gage length. The machine was equipped with an X-Y recorder for graphically recording load-deformation characteristics of the specimens. The machine was also equipped with a load pacer device, a load cycling mechanism, and a constant head travel control for loading rates which could be varied from 0 to 20 inches per minute.

Test Procedure. - Test segments were mounted on the test fixture and retained by a collar in the manner shown in figure 52.

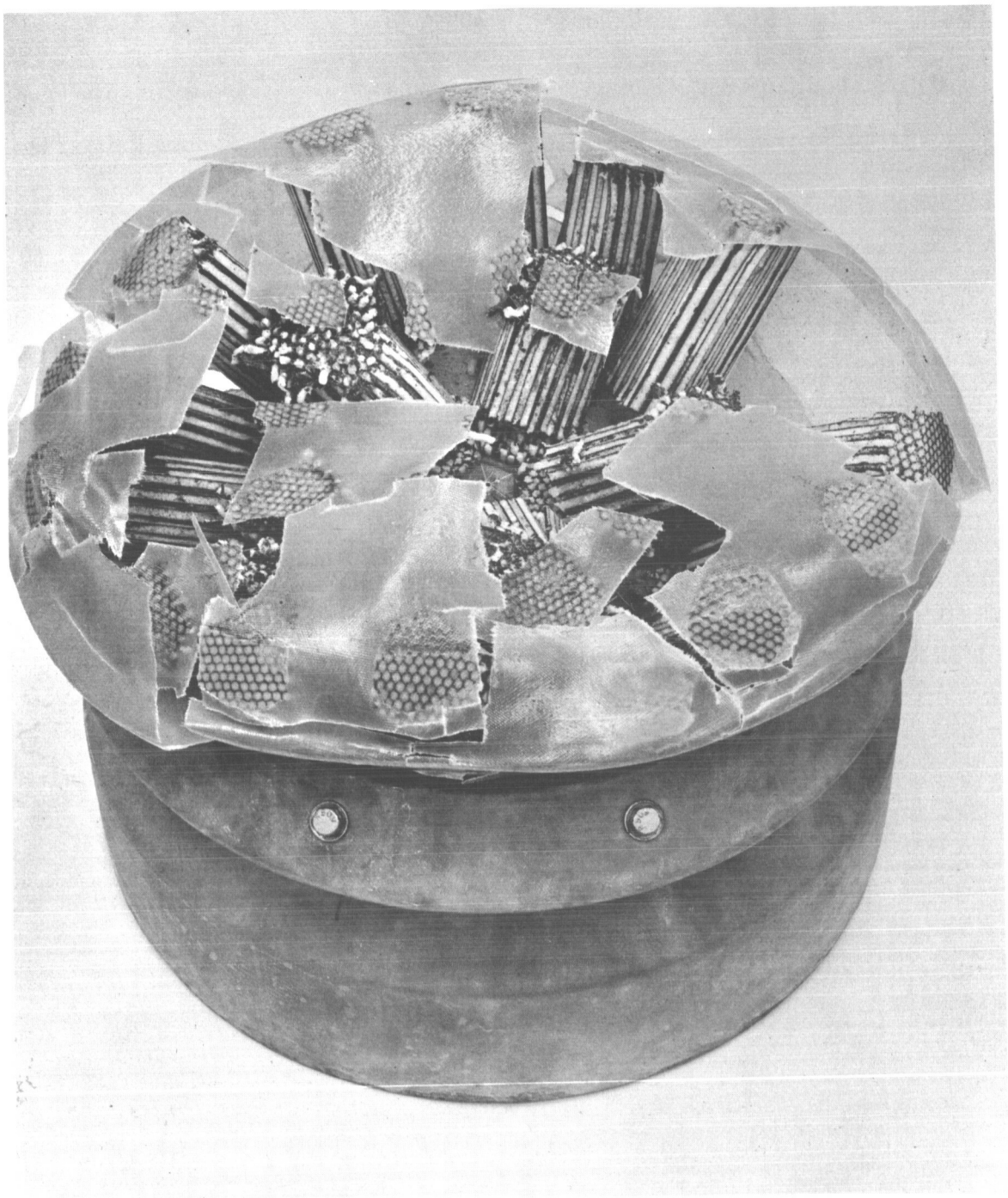

Figure 52. Typical Test Setup of Test Segment In Test Fixture Shown After Test.

The mounted specimen and fixture assembly was inverted when it was installed in the test machine. The supporting plate on which the spherical surface of the test segment rested was a square aluminum plate 1 inch thick, which was larger than the diameter of the largest specimen.

The moving head of the test machine was carefully lowered until it contacted the aluminum base plate on the test fixture. When it was determined that the specimen was symmetrically installed in the test machine a compressive loading rate of 1 inch per minute was applied. This compressive load was applied along the rotational axis of the spherical test segment. The 5 inch specimens were tested first, and were stopped after a stroke of 4 inches. The initial load-deformation pattern for each of the honeycomb, composite, and frangible tube segments was higher than calculated up to 2 inches of stroke. Beyond 2 inches of stroke the load dropped off rapidly in each case. The crushed specimens showed that the first circle of five elements had collapsed. It was decided that the 4.5 inch and the 4.0 inch thick specimens would have more resistance to this collapsing tendency because the elements were shorter and had increasingly larger cross-sections in proportion to reduced thickness. Test results on the 4.5 inch and 4.0 inch specimens which were tested in that order still showed a rapid reduction in load after 2 inches of stroke.

Analysis of Test Results. - The three types of failed specimens are shown in figure 53 and load deformation recordings for the 4.5 inch thick typical specimens are presented in figure 54. These test results are shown in comparison with calculated load-deformation curves. The significant difference between the specimens with elements of different length and cross section was in the load peaks. The shortest specimens, which had the elements with the greatest cross-section, had the highest load peaks for each of the three element types.

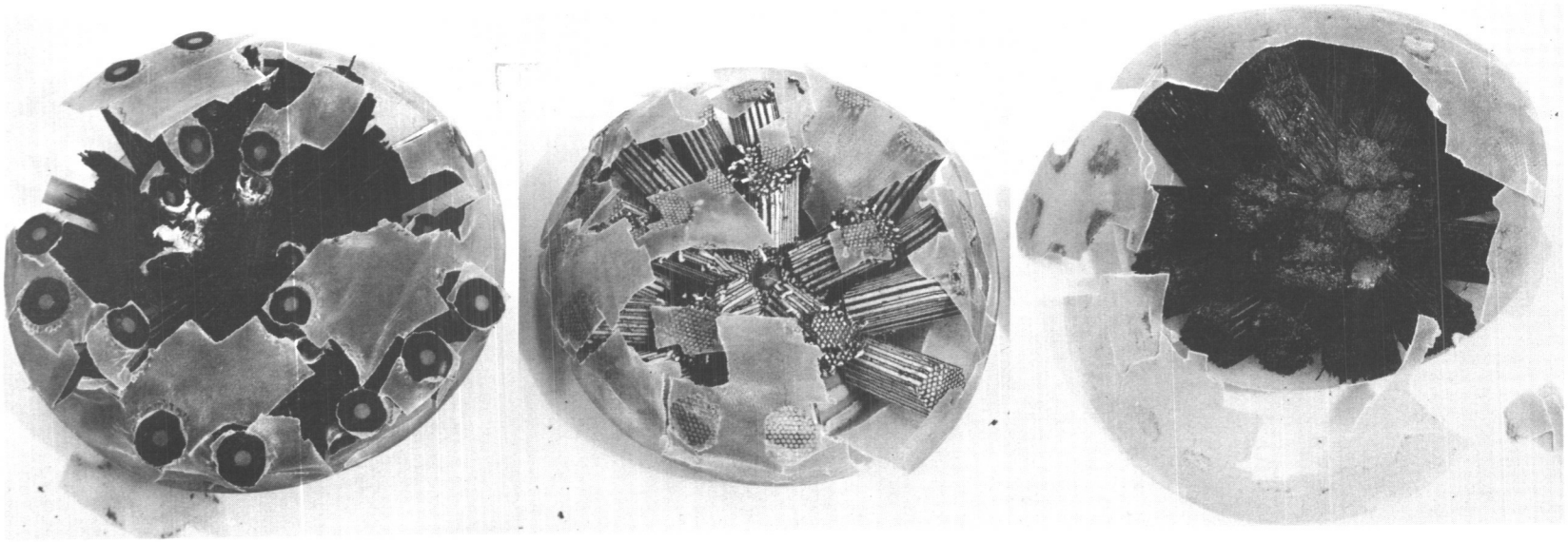

a. Frangible Tube Segments

b. Composite Segments

c. Honeycomb Segments

Figure 53. Typical Condition of The Honeycomb, Composite, and Frangible Tube Test Segments After Static Test.

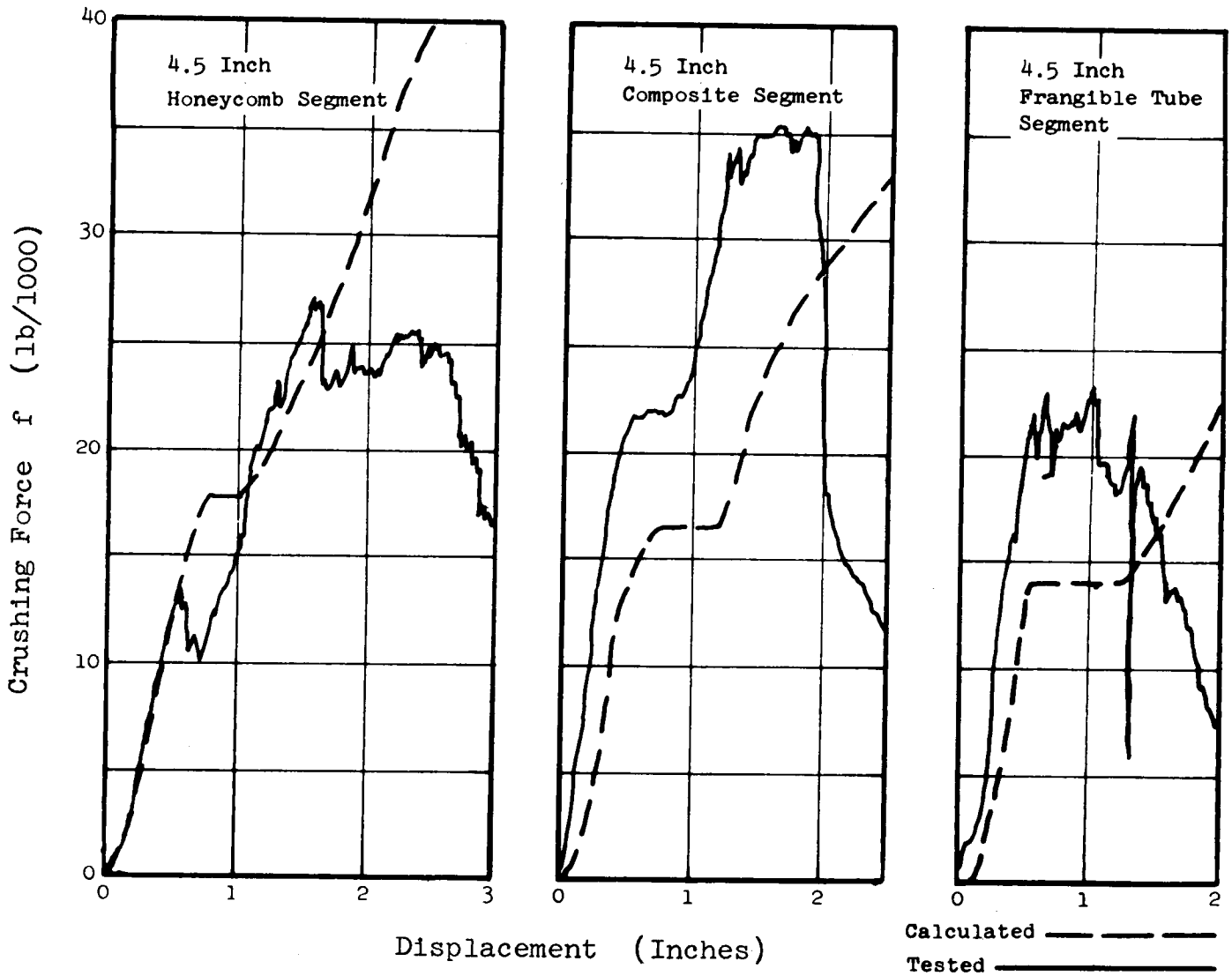

Figure 54. Load Versus Displacement Test Comparisons With Calculations For 4.5 Inch Thick Honeycomb, Composite and Frangible Tube Segments.

The composite element segment was found to provide the highest energy absorption, which was significantly higher than the calculated values for the first 2 inches of stroke. As shown in figure 54, the area under the test curve represents 24 percent of the required energy absorption for the first two inches compared with the calculated 17 percent over the same stroke. Failure of the specimens beyond 2 inches of stroke is attributed to collapse of the elements which could be caused by failure of one or more of the following element supports:

1. Tension failure in the skin
2. Element shear failure at skin attachment
3. Element base support failure

The obvious conclusion seems to be that the skin failed, however, a more detailed evaluation will be presented to show that the failure mode varied according to the type of element system.

Element Loading Sequence. - There are 20 elements in each of the spherical test segment specimens, arranged in three circular rows about the axis of rotation of the segment. The first circle has 5 elements inclined at 13 degrees to the loading axis, the second circle has 5 elements inclined at 26 degrees to the loading axis, and the third circle has 10 segments inclined at 35 degrees to the loading axis.

The first circle of 5 elements which are inclined at 13 degrees to the load axis provide all of the initial axial loading of the test segment. The loading first increases linearly then levels off at 0.8 inches of stroke. A radial component of the axial loading is induced by each angled element at the skin attach point in the ratio of 44 pounds for each 1000 pounds of first circle of elements axial loading.

The second circle of 5 elements which are inclined at 26 degrees to the loading axis, add a linear increase in the total load to the

first circle level loading starting at 1 inch of stroke and leveling off at 2.5 inches. A radial component of axial loading is induced in the skin at each element in the ratio of 102 pounds for each 1000 pounds of second circle of elements axial loading.

The third circle of 10 elements which are inclined at 35 degrees to the load axis, add an upward curving load increase to the total load starting at 1.7 inches of stroke and leveling off at 3.2 inches. A radial component of axial loading is induced in the skin at each element in the ratio of 70 pounds for each 1000 pounds of third circle of elements axial loading.

Honeycomb Segment Failure Analysis. - The actual test curve for each of the three honeycomb element lengths follows the calculated linear loading increase of the first circle of 5 elements up to a stroke of 0.7 inches then a 5000 pound dip in the curve occurs. The loading curve recovers from this dip and increases to higher than the load level at the point when it dipped when it reaches the 1 inch stroke point. Beyond the point at which the second circle of 5 elements start to add load the curve increases linearly as expected up to a peak of 30 000, 26 000 and 22 000 pounds for the 4, 4.5 and 5 inch segments respectively. These peaks all occur at 1.6 inches of stroke which is just before the third circle of elements would commence to add load. The load leveled off beyond the peaking point for each segment out to a 2 inch stroke or beyond, then dropped off. If the tension load in a radial strip of 2 inch wide skin is calculated at each significant loading level representing the tension tie of the skin to the element, then at the first drop in the load which was close to 15 000 pounds, a 660 pound load is induced. At the highest peak loading of 30 000 pounds the first and second circle loadings induce 660 pounds plus a 1530 pounds respectively, or a total of 2190 pounds load is induced in the 2 inch wide strip of skin at each element. If a 40 000 psi tensile strength for a single ply skin of 181 fabric and epoxy resin is considered, a 2 inch strip would fail at 800 pounds maximum. It

can not be said therefore, that skin failure induced collapse of the elements. Examination of the failed honeycomb segments shows detachment of the element from the outer skin. This condition of detachment can be caused by inadequate bond area to carry the shear load, and crushing of the honeycomb at the attachment point. It can be concluded therefore that most of the support for the honeycomb elements came from attachment to the base, and failure was caused by shear failure in the elements as shown in figure 53.

Composite Segment Failure Analysis. - The test curves for each of the three composite element lengths followed the calculated pattern of loading for the first inch, except the crushing load level was higher in each case. The contribution of the second circle of elements seemed to commence at 1 inch of stroke instead of the predicted 1.2 inches for composite elements, and the rate of loading buildup was steeper then calculated. The shortest element lengths of 4 inches achieved the highest peak load of 40 000 pounds, and the intermediate, 4.5 inch element lengths as shown in figure 54 peaked at 35 000 pounds. If these axial loading peaks are converted to radial loading components at each element as was done in the discussion on honeycomb element failure analysis still higher loads would have been induced in the skin which would have caused early skin failure and collapse of the elements. It can therefore be concluded that the composite elements were supported by the base, had better beam strength and had better bond attachment to the skin. The illustrations in figure 53 show crushed elements firmly attached to the skin.

Frangible Tube Segment Failure Analysis. - The test curves for the three frangible tube segments tested also followed the general pattern calculated for load-deformation. Higher loading values were attained than were calculated and can be attributed to greater support from the honeycomb part of the elements than was allowed. Each of the three segments peaked at 22 000 pounds during the loading phase of the first circle of 5 elements. This high load level

should have failed the single ply skin in tension but element collapse did not occur during the 1.0 inch stroke portion of the loading pattern. It can be concluded that the frangible tube elements had good shear attachment between the die and the skin but low base bending support because the friction contact of the inner die provided no moment capability for the element. The illustrations in figure 53 show that the elements collapsed by breaking free from the base in contrast to the shear failure of the honeycomb elements.

CONCLUSIONS

The development, design, and fabrication of three landing systems of honeycomb, composite, and frangible tube element types was not accomplished because the spherical test segments developed an instability failure under static test.

The design, and fabrication of a spherical test vehicle was accomplished, and the fabricated vehicle weighed 20 pounds. Static tests of specimens of the composite shell demonstrated an adequate strength to resist permanent deformation when subjected to critical local loads from the frangible tube and die elements which were more than 100 percent greater than the design impact loads of the landing system.

Lightweight tube franging dies which permitted the frangible tube type of landing system to be competitive on a weight basis with honeycomb, and composite elements were successfully developed. The matched die molded dies were fabricated using chopped glass fiber reinforcement in a phenolic resin system. Compressive strengths of 28 000 psi were demonstrated with no permanent set. Die weights were one sixth the weight of steel dies.

Anisotropy design data which was required for the design of the three types of landing systems was generated by conducting limited tests on frangible tubes and single and multiple layer nylon phenolic honeycomb elements. This data represents the first available literature on these two element types on anisotropy properties.

RECOMMENDATIONS

The static testing of the spherical test segments indicated that for the composite and frangible tube elements the load-deformation test curves were considerably more efficient up to the 2 inch stroke when instability of the elements caused them to collapse radially. The composite element spherical test segment with 4.5 inch element lengths absorbed 24 percent of the required energy absorption for the first 2 inches of stroke compared to a calculated 17 percent. These elements could be stabilized by two design modifications:

a. The base of each element could be braced by small honeycomb wedge elements with the core axis horizontal.

b. The greater efficiency of the elements than predicted would reduce the estimated required element length from 6.5 inches to 6.0 inches if they could be stabilized. These 6 inch elements could be further divided into 2 inch lengths and the landing system assembled in layers. The outer layer would be glass fiber reinforced plastic laminations, but the intermediate layers would be of high directional strength, light weight, flexible, 143 fabric straps as cross bracing between each group of five elements.

Although dynamic testing was originally planned the landing systems were to be developed in this program from the successful static testing of spherical segments only. Since dynamic impact, especially with high horizontal velocities, was specified as design criteria, the development of reliable landing systems based on direct load static testing of segments only could not be assured. It is therefore recommended that a program of increased scope which includes dynamic loading and horizontal velocity components should be conducted.

APPENDIX A

LANDING SYSTEM WEIGHT ANALYSIS

Landing system weight is composed of the weights of the inner shell, girth band joint and energy absorbing elements. Total landing system weight can be expressed as:

$$W_{LS} = W_{IS} + W_{OS} + W_J + W_{80E} \qquad \text{(A-1)}$$

where

W_{IS} = weight of inner shell skin

W_{OS} = weight of outer shell skin

W_J = weight of girth band joint

W_{80E} = weight of energy absorbing elements

Inner Shell Weight (W_{IS}). - The external diameter of the inner shell is specified to be eighteen (18) inches. Plies are added to this shell diameter to make a fiberglas (.065 lb/cu.in density) shell.

$$\text{Shell Volume} = V_{IS} = \frac{4}{3}\pi(R_0^3 - R_I^3)$$

$$\text{Shell Weight} = W_{IS} = V_{IS}\rho_p = .065 \times \frac{4}{3} \times \pi \times (R_0^3 - R_I^3)$$

$$W_{IS} = .272271\ (R_0^3 - R_I^3) \qquad \text{(A-2)}$$

where R_0 and R_I are outer and inner radii of the shell respectively in inches. Inner shell weights are tabulated in Table A1.

TABLE AI. VARIATION OF INNER SHELL WEIGHT WITH NUMBER OF PLIES

No. of Plies	R_0 in.	R_I in.	$(R_0^3 - R_I^3)$ in^3	W_{IS} lb
1	9.01	9.00	2.4327	.66235
2	9.02	9.00		1.32618

Outer Shell Weight (W_{OS}). - The outer shell consists of two plies (.020 thick) which represent the difference between the outer

radius (R_{O_O}) and inner radius (R_{I_O}) respectively of the outer shell. The outer shell radii vary with the thickness (h) of the impact absorbing material which is added to the inner shell. The weight equation for this fiberglas laminate is identical to the inner shell equation (A-2) and is used. Outer shell weights are tabulated in Table AII.

TABLE AII. VARIATION OF OUTER SHELL WEIGHT WITH THICKNESS OF THE IMPACT ABSORBING MATERIAL

h in.	R_{O_O} in.	R_{I_O} in.	$(R^3_{O_O} - R^3_{I_O})$ in^3	W_{OS} lb
4.0	13.03	13.01	10.1712	2.7693
4.5	13.53	13.51	10.9674	2.9861
5.0	14.03	14.01	11.7936	3.21106
5.8	14.83	14.81	13.17796	3.5880
6.0	15.03	15.01	13.53602	3.68545
6.5	15.53	15.51	14.4522	3.9349
7.0	16.03	16.01	15.3984	4.1929

Girth Band Joint Weight. - A separate analysis has shown that the girth band for landing systems of larger diameters would not exceed .8 pound. In this weight analysis a value of 1.0 pound for all thicknesses of landing systems has been used.

Energy Absorbing Elements Weight (W_{80E}). - The maximum allowable weight of the landing system to stay within the fifty (50 pound) total weight limit is:

$$W_{LS} \leq 20.0 \text{ lb}$$

The allowable weight for the energy absorbing system components of the landing system is

$$W_{80E} = W_{LS} - W_{OS} - W_{IS} - W_J \qquad \text{(A-3)}$$

substituting the known landing system, two ply inner shell, and girth band weights then:

$$W_{80E} = 20.0 - 1.3262 - 1.000 - W_{OS} = 17.6738 - W_{OS} \qquad (A-4)$$

This equation is used to establish limiting element weights as presented in Table AIII.

TABLE AIII. VARIATION OF ALLOWABLE IMPACT ABSORBING MATERIAL WEIGHT WITH THICKNESS BETWEEN SHELLS

h in.	W_{OS} lb	W_{80E} lb $(17.6738-W_{OS})$	W_E* lb $W_{80E/80}$	W_{80E}** HC Above h=5.8	W_E HC Above h=5.8
4.0	2.7693	14.9045	.186306	-	-
4.5	2.9861	14.68770	.18359	-	-
5.0	3.21106	14.46274	.18078	-	-
5.8	3.5880	14.08580	.17607	-	-
6.0	3.6854			13.3243	.16655
6.5	3.9349			13.07487	.16343
7.0	4.1929			12.81687	.16021

* The surface of the sphere is divided up into 80 elements and therefore W_E represents the weight of one element.

** Added weight of 80 honeycomb element space plies gives
$= 17.6738 - W_{OS}$ - WT of spacer/plies

$W_{80E} = 17.6738 - W_{OS} - .66403 = 17.01427 - W_{OS}$

The allowable weight for the energy absorbing elements which are presented in Table AIII are further identified as honeycomb and composite or frangible tube elements in Table AIV. The difference is caused by the need for adding space plies to honeycomb and composite elements when lengths are above 5.8 inches in order to assemble the longer specimen and this reduces the allowable weight in the longer lengths.

Appendix A

TABLE AIV. ALLOWABLE WEIGHT OF 80 ENERGY ABSORBING HONEYCOMB, COMPOSITE OR FRANGIBLE TUBE ELEMENTS

Thickness (Element Length h in.	Allowable Honeycomb Or Composite 80 Element Weight lb.	Allowable Frangible Tube 80 Or 122 Element Weight lb.
5.0	14.46274	14.46274
6.0	13.3243	13.98835
6.5	13.07487	13.73890
7.0	12.81687	13.48090

APPENDIX B

LANDING SYSTEM ELEMENTS ANALYSIS

Element Section Properties. - The surface area of the outer surface of the inner shell (R_o = 9.02 in) is:

$$A_{IS} = 4\pi R^2 = 4 \times \pi \times \overline{9.02}^2 = 1022.40 \text{ in}^2 \qquad \text{(B-1)}$$

this area is to be entirely covered by the cross-sectional areas of eighty (80) basic elements therefore the area of one element is:

$$A_E = A_{IS}/80 = 12.7800 \text{ in}^2$$

The section shape of this basic element is an equilateral triangle, and its dimensions are

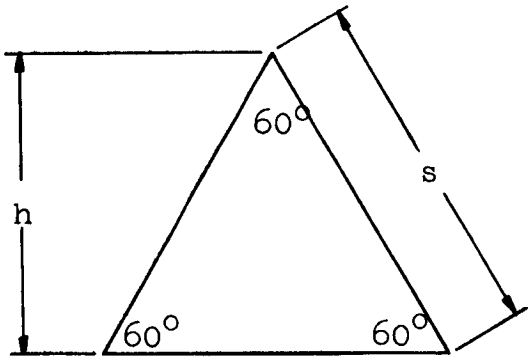

$$h = 2 \sin 60^\circ$$

$$A_E = \frac{sh}{2} = \frac{s^2}{2} = \sin 60$$

then

$$s = \left(\frac{2A_E}{\sin 60}\right)^{\frac{1}{2}} = 1.51967 \sqrt{A_E}$$

$$s = 5.43269 \text{ inches.}$$

Actual dimensions of sides of 3.84 inches for the triangle are used to allow room for debris after crushing and to ensure full stroke capability of the element. The basic element is therefore a triangular constant cross-section prism of height equal to the energy absorbing thickness. Variations in weight are obtained by cutting corners in the six jig fixtures as identified in figure B-1. and the geometry equations are as follows:

$$A_E = \frac{3.84h}{2} = \frac{\overline{3.84}^2}{2} \sin 60 = 3.84 \times 3.3255 \times \frac{1}{2} = \underline{6.385_m}^{-2}$$

$$A_C = \tfrac{1}{2} h_c s_c = \tfrac{1}{2} h_c \times 2h_c \tan 30^\circ = h_c^2 \tan 30^\circ = .57735\ h_c^2$$

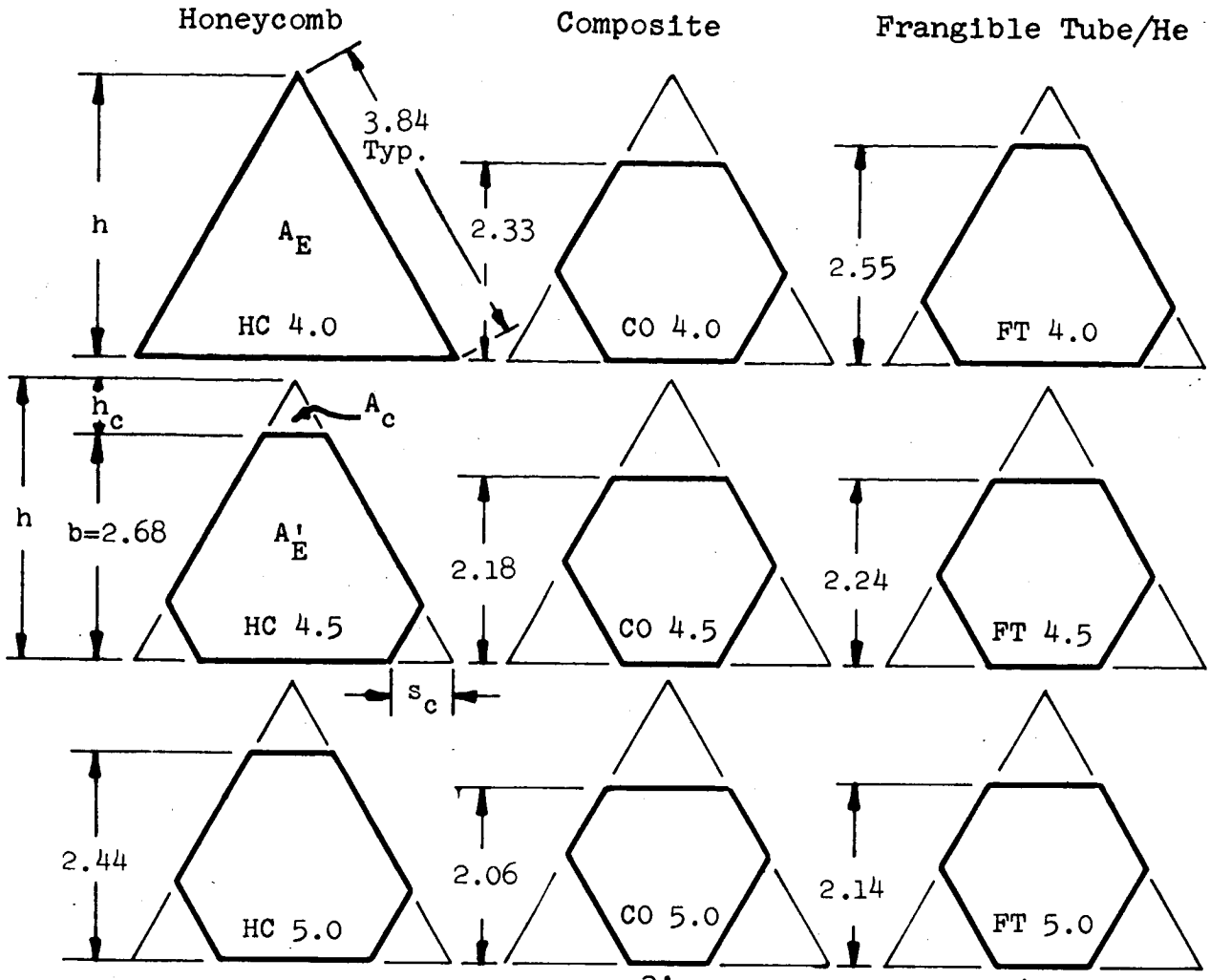

	b in	h_c in	$3A_c$ in^2	A'_E in^2	A'_{E_3}/A_E
HC 4.0	-	-	-	6.38496	1.0000
HC 4.5	2.68	.64551	.72171	5.66325	.88692
HC 5.0	2.44	.88551	1.35813	5.02683	.78725
CO 4.0	2.33	.99551	1.71653	4.66843	.73112
CO 4.5	2.18	1.14551	2.27277	4.11219	.64401
CO 5.0	2.06	1.26551	2.77389	3.61107	.56552
FT 4.0	2.55	.77551	1.04167	5.34329	.83681
FT 4.5	2.24	1.08551	2.04092	4.34404	.68032
FT 5.0	2.14	1.18551	2.43427	3.95069	.61871

Figure B-1. Cross-Section Geometry of Landing Systems Energy Absorbing Elements.

where

$$S_C = 2h_c \tan 30^\circ, \qquad h_c = h - b$$

$$A_E' = A_E - 3A_C = 6.385 - 1.73205\, h_c^2$$

identify

$$h_c = h - b = 3.3255 - b$$

Elements Strength Properties. - Figure 15 of this report summarized all design information on the crushing strength/density characteristics for fiberglas honeycomb materials. This information was used in conjunction with requirements on weight for the landing system to fabricate and test actual triangular and hexagonal section honeycomb and composite elements. The results of these direct loading element crushing tests are presented in figures B-2, B-3 and B-4. In figure B-2 a direct comparison can be made for equal cross-section of 1/2 cell Nylon Phenolic honeycomb, of 4.27 lb/cu.ft. density, and 3/16 cell HRP honeycomb of 6.79 lb/cu.ft. density. Figure 15 showed a slope of a line through test results for 3/16 and 1/4 cell honeycomb which did not pass through the origin but went through 2 lb/cu.ft. density for zero crushing strength. Since the specific energy function of the crushing strength/density ratio, the line from the origin in figure 15 with the steepest slope passes through the 6.79 lb/cu.ft. material and this has been established in element form in figure B-2 with a specific energy of 14,800 ft.lb/lb specific energy for the selected 3/16 cell honeycomb material.

The effect of fabricating hexagonal cross-section elements on the crushing strength is shown for 3/16 cell size material in figure B-3. A slight reduction in specific energy to 13,500 ft.lb/lb is noted.

The development of composite elements was achieved by filling the 1/4 cell and 3/16 cell honeycomb with polyurethane foam material. A direct comparison of the crushing strength and specific energy for

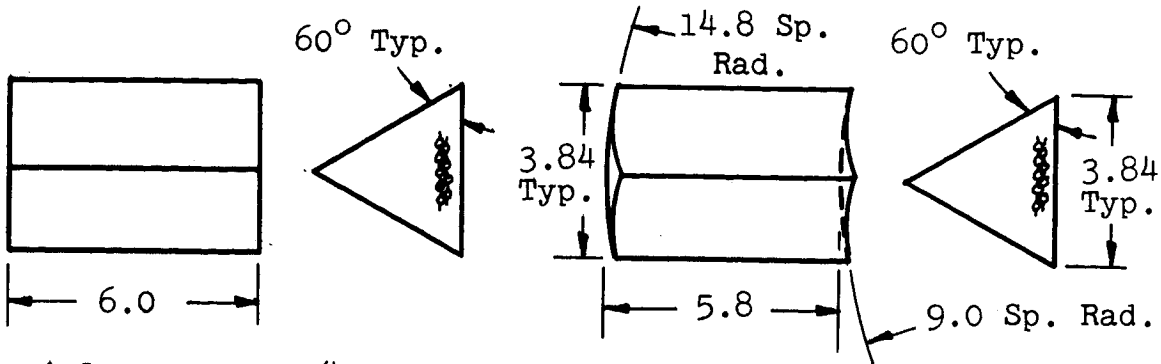

Material:	1/4 Cell N.P.	3/16 Cell H.R.P.
Density:	4.27 lb/cu.ft.	6.79 lb/cu.ft.
Weight:	.0948 lb	.1451 lb
	.0158 lb/in	.02501 lb/in
	1.263 lb/in x 80	2.000 lb/in x 80
Average Force:	1700 lb	4480 lb
Average Stress:	266 psi	700 psi
Specific Energy:	9000 ft-lb/lb	14800 ft-lb/lb

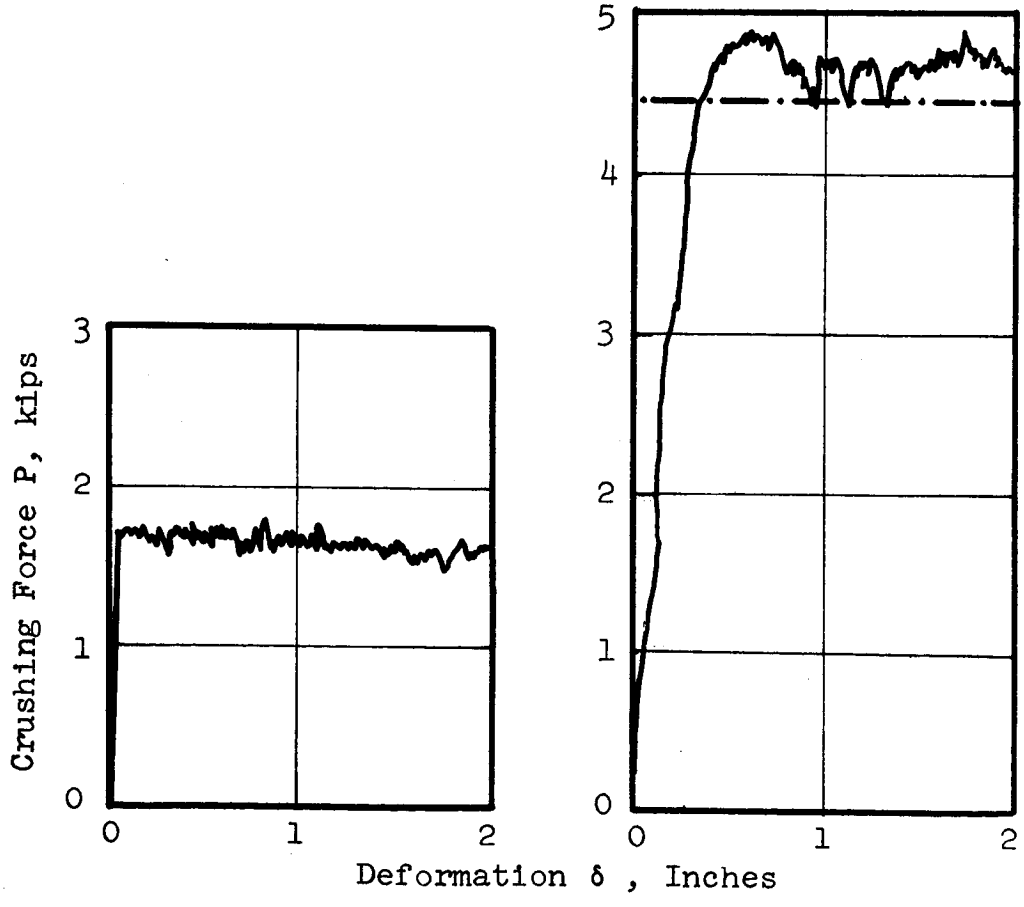

Figure B-2. Triangular Honeycomb Elements Crushing Strength, Weight, and Energy Absorption Efficiency Comparisons.

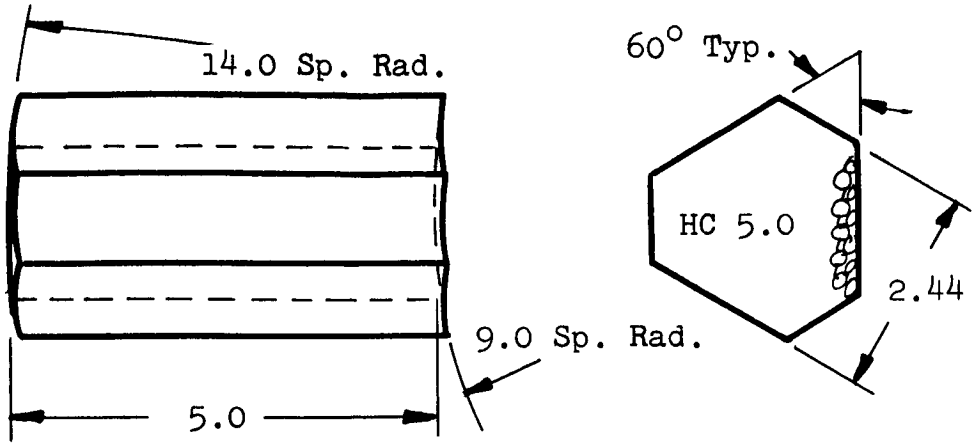

Material:	3/16 Cell H.R.P. Honeycomb
Density:	6.79 lb/cu.ft.
Weight:	.0959 lb
	.0192 lb/in
	1.5344 lb/in x 80
Average Force:	3200 lb
Average Stress:	637 psi
Specific Energy:	13,500 ft-lb/lb

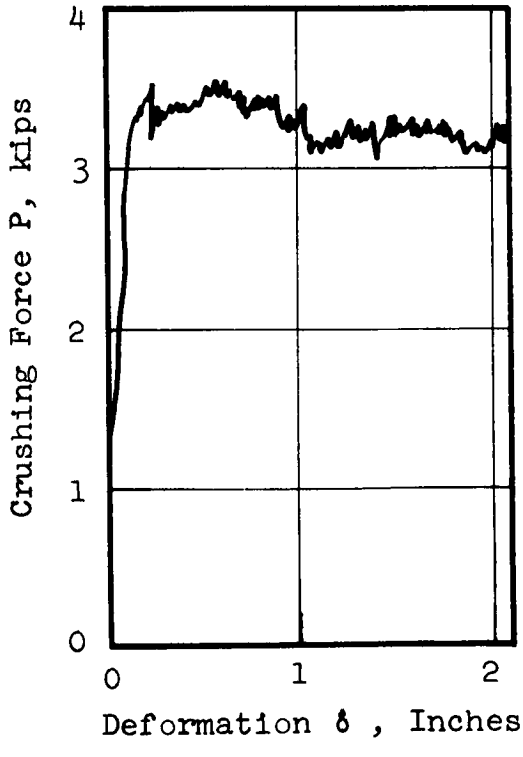

Figure B-3. Hexagonal Honeycomb Elements Crushing Strength, Weight, and Energy Absorption Efficiency.

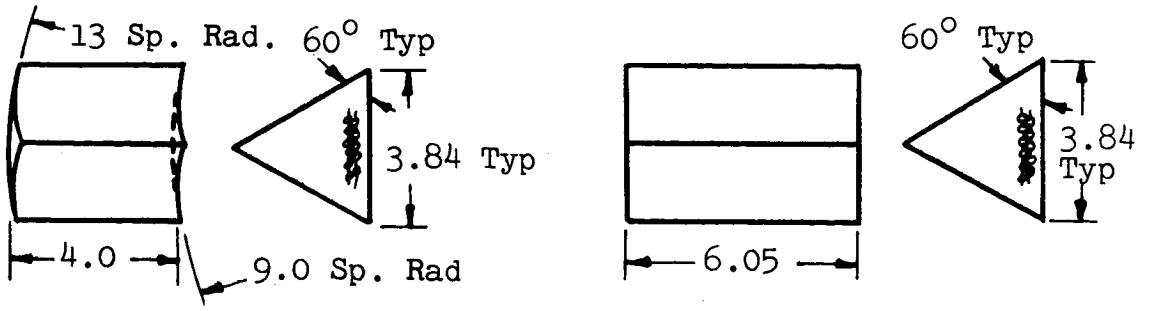

Material:	¼ Cell N.P. Polyurethane Foam Fill	3/16 Cell H.R.P. Fill
Density, lb/cu.ft.:	10.96	10.75
Weight, lb:	.1801	.2403
lb/in:	.0405	.0397
lb/in x 80:	3.242	3.177
Average Force, lb:	4000	6000
Average Stress, psi:	627	940
Specific Energy, ft-lb/lb:	8220	12,560

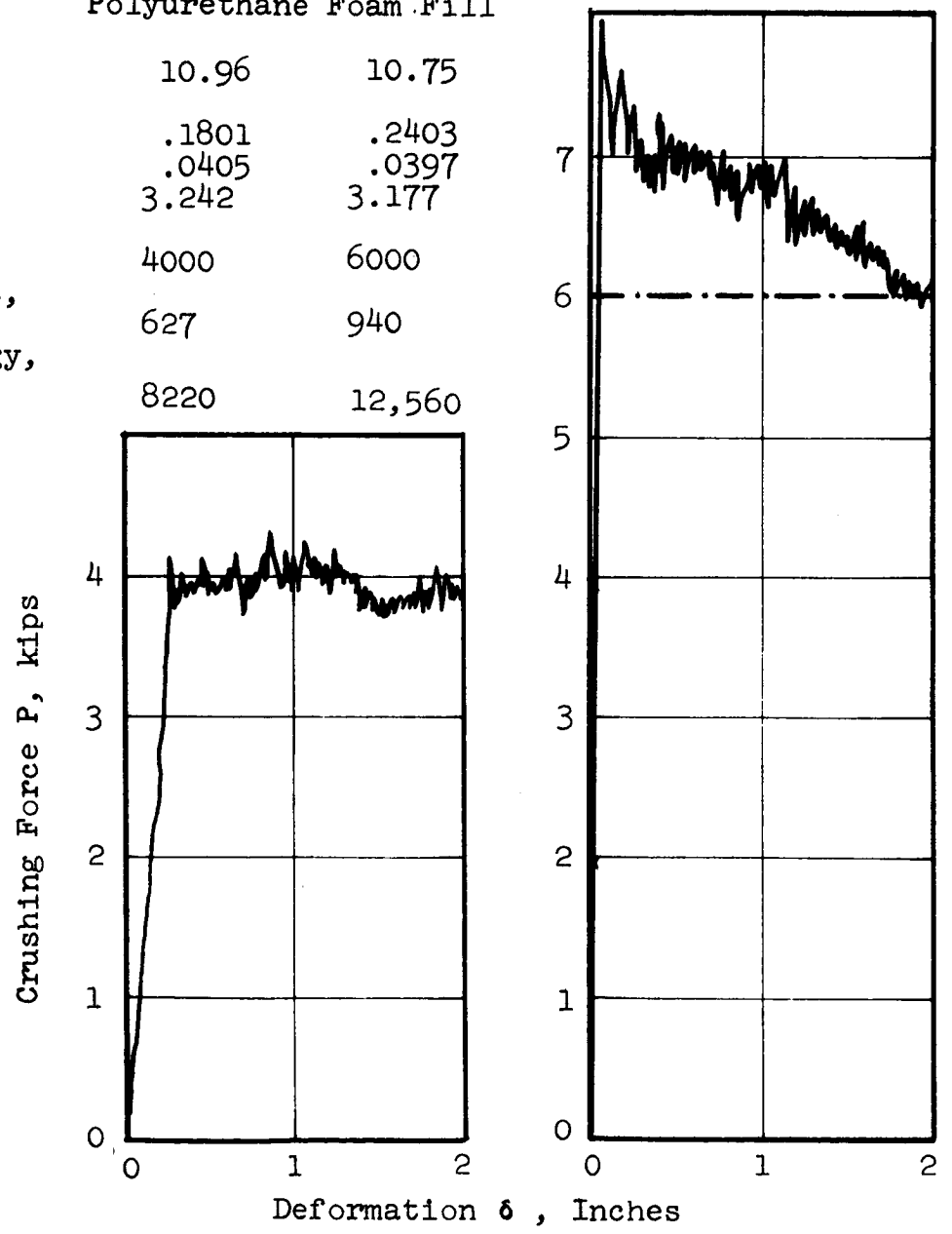

Figure B-4. Triangular Composite Elements Crushing Strength, Weight, and Energy Absorption Efficiency Comparisons.

these two cell sizes can be made in figure B-4. Although the densities of each of these two composite element cell sizes are approximately the same, the 3/16 cell size is significantly more efficient than the 1/4 cell size but less efficient than the honeycomb when unfilled.

The average crushing force values shown in figures B-2, B-3, and B-4 have been used in the design of the honeycomb and composite landing system segments.

Element Actual Weight. - The actual weight of the honeycomb elements and the foam filled honeycomb or composite elements used in detail design of the segments were based on the values shown in figures B-2, B-3, and B-4. These figures show three weights, the actual weight of the element of the length shown, the weight per inch, and the weight per inch x 80 for eighty elements in a landing system.

Detail weight breakdowns based on actual weight for the frangible tube elements are as follows:

Die

	Weight	
	Grams	Pounds
10 Dies	169.5	.3737
1 Die		.0374
80 Dies		2.9896
160 Dies		5.9792

6 Ply Tubes

	Weight		
	Grams	Pounds	lb/in
10 Tubes	271.4	.5983	
1 Tube		.0598	.01286
80 Tubes		4.7864	

Appendix B

Honeycomb Element

Weight

	Grams	Pounds
10 Elements	217.3	.47906
1 Element		.0479

lb-6.0 in. long

Weight of 80 Tubes	5.9792
Weight of 160 Dies	6.1728
	12.1520 lb.

APPENDIX C

LANDING SYSTEM DETAIL ANALYSIS

Honeycomb Elements Weight Analysis. - The 3/16 cell HRP fiberglas honeycomb material (6.79 lb.cu.ft actual weight) weights 2.000 lb. per inch when fabricated in the triangular elements as listed in figure B-2 for 80 elements. The actual weight/allowable weight comparison for varying stroke is as follows:

Landing System Diameter in	Thickness h in	Allowable Weight lb	Actual Weight lb	Weight Difference lb	Landing System Weight lb
28	5.0	14.46274	10.360	- 4.42674	15.5733
30	6.0	13.3243	12.0432	- 1.28110	18.7189
31	6.5	13.07487	13.0468	- .02807	19.97193
32	7.0	12.81687	14.0504	+ 1.23353	21.23353

Honeycomb Elements Energy Absorption Analysis. - A graphical analysis of the energy absorbing capability of 3/16 cell honeycomb elements presented in figures of the text. The crushing strength used in the calculations is 4480 lb based on 700 psi (ref. figure 15 crushing strength/density graph) and on actual tests of the element (figure B-2). The results of the calculations are summarized below:

Landing System Diameter in	Thickness h in	Required Energy Absorption in/lb	Actual Energy Absorption in/lb	Allowable g's	Actual g's	Element Strength lb
28	5.0	186,335.4	141,000	1000	949.6	4480
30	6.0	186,335.4	177,000	1000	949.6	4480
31	6.5	186,335.4	194,000	1000	949.6	4480
32	7.0	186,335.4	209,000	1000	949.6	4480

Composite Elements Weight Analysis. - The 3/16 cell HRP fiberglas honeycomb filled with polyurethane foam (10.75 lb/cu.ft. actual weight) when fabricated as 80 equilateral triangular elements weighs 3.1768 lb/in as listed in figure B-4. Since this weight requires

trimming the corners of the block the following table compares weights and also identifies required and actual weight fraction and the trim jig identity as listed in figure B-1.

Landing System Diameter in	Thickness h in	Actual Weight Triangular Section lb	Allowable Weight lb.	Section Ratio Required A'_E/A_E	Fixture Identity Used	Act. Sec. Ratio A_E/A_E	Act. Wgt. Hexagonal Section	Weight Difference lb	Landing System Weight lb
28	5.0	15.8840	14.46	.91047	CO 4.0	.73112	11.61	- 2.84	17.15
30	6.0	19.0608	13.32	.69904	FT 4.5	.68032	13.01	- .30	19.69
31	6.5	20.649	13.07	.63319	CO 4.5	.64401	13.29	+ .22	20.22
32	7.0	22.2376	12.81	.57636	CO 4.5	.64401	14.32	+ 1.50	21.50

Composite Elements Energy Absorption Analysis. - A graphical analysis of the energy absorbing capabilities of 3/16 cell honeycomb/foam composite elements is presented in figure 41 of the text. The crushing strength used in the calculations is based on a test value of 6000 lbs for the full triangular section and is corrected by the actual section ratio (A'_E/A_E) (See Figure B-4).

Landing System Diameter in	Thickness h in	Required Energy Absorption in lb	Actual Energy Absorption in lb	Allowable g's	Actual g's	Element Crushing Strength
28	5.0	186,335.4	-	1000	-	4386.7
30	6.0		175,000	1000	987	4081.9
31	5.6		190,500	1000	935	3864.6
32	7.0		206,000	1000	935	3864.6

80 Frangible Tube Elements Weight Analysis. - The frangible tube elements consist of a fixed weight item for the dies regardless of stroke determined by actual weights as listed on page 122 and the variable weight of the varying tube length. The actual weight/allowable weight comparison is as follows:

Appendix C

Diameter in	Thickness h in	Allowable Weight lb	Actual 80 Tubes Weight 160 Dies lb	Weight Difference lb	Landing System Weight
28	5.0	14.4627	10.7656	- 3.6971	16.3029
30	6.0	13.9884	11.7949	- 2.1935	17.8065
31	6.5	13.7389	12.3096	- 1.4293	18.5707
32	7.0	13.4809	12.8242	- .6567	19.3433

80 Frangible Tube Elements Energy Absorption Analysis. - A graphical analysis of the energy absorbing capability of 80 frangible tube elements in an omnidirectional spherical arrangement is presented in figure 42 of the text. The franging force used in the analysis is based on the previous program effort for the 6 ply 181 fabric 1.0 inch tube of 3000 lbs franging force.

Diameter in	Thickness h in	Required Energy Absorption in lb	Actual Energy Absorption in lb	Allowable g's	Actual g's
28	5.0	186,335.4	100,000	1000	763
30	6.0	186,335.4	136,200	1000	763
31	6.5	186,335.4	153,000	1000	763
32	7.0	186,335.4	166,500	1000	763

APPENDIX D

CALCULATION OF SPHERICAL TEST VEHICLE WEIGHT

The test vehicle weight is composed of the weights of the inner shell, outer shell syntactic foam/honeycomb core material and girth band joint. Total test vehicle weight can be expressed as:

$$W_{TV} = W_{IS} + W_{OS} + W_J + W_{CC}$$

where

W_{IS} = weight of inner shell skin

W_{OS} = weight of outer shell skin

W_J = weight of girth band joint

W_{CC} = weight of composite core

Inner Shell Weight (W_{IS}). - The external diameter of the test vehicle is specified to be eighteen (18.00) inches, the core thickness has been selected as one (1.00) inch and the inner and outer shells are each constructed of three plies of fiberglas (.030 inch thickness and .065 lb/cu.in density), therefore the inner shell outer radius is 7.97 inches and the shell weight is:

Shell Weight $$W_{IS} = .065 \times \frac{4}{3} \times \pi \times (R_O^3 - R_I^3)$$

$$W_{IS} = .272271 \, (R_O^3 - R_I^3)$$

where R_O and R_I are outer and inner radii of the shell respectively in inches. Then:

No. of Plies	R_O in.	R_I in.	$(R_O^3 - R_I^3)$ in^3	W_{IS} lb.
3	7.97	7.94	5.6954	1.55068

Outer Shell Weight (W_{OS}). - The outer shell consists of three plies (.030 inches thickness) which represents the difference between the outer radius (R_{O_O}) and the inner radius (R_{I_O}) respectively of the outer shell. Then:

Appendix D

No. of Plies	R_O in.	R_I in.	$(R_O^3 - R_I^3)$ in^3	W_{OS} lb.
3	9.00	8.97	7.26573	1.97824

Girth Band Joint Weight (W_J). - The girth band consists of a six ply (.060 inch thickness) laminate of fiberglas of 1.5 inches width which has an outer diameter of eighteen (18.0 inches). The weight of the girth band is:

$$W_J = .065 \times 18.0 \times 1.5 \times .060 = .33080 \text{ lb.}$$

Syntactic Foam/Honeycomb Core Weight (W_{CC}). - The core material consists of 1/4 cell size Nylon Phenolic honeycomb of 4.27 lb/cu.ft. density filled with syntactic foam and 1/8 inch diameter micro balloons to a composite weight of 32 lb/cu.ft. The same weight equation which has been used in shell weight calculations is used with the coefficient corrected for the difference between the fiberglas density (112.32 lb/cu.ft.) and the composite core density. Then:

$$W_{CC} = \frac{32}{112.32} \times .272271 \left(R_{O_I}^3 - R_{I_O}^3\right) = 16.71367 \text{ lb.}$$

Test Vehicle Weight (W_{TV}). -

$$W_{TV} = W_{IS} + W_{OS} + W_J + W_{CC}$$

$$= 1.55068 + 1.97824 + .33080 + 16.71367$$

$$= 20.57339 \text{ lb}$$

Allowable weight for instrumentation packaging allowing the specified 5.0 lb for instruments and a total test vehicle weight of 30.0 lb.

$$\text{Packaging Weight} = 30.0 - 20.57339 - 5.0 = 4.42661 \text{ lb.}$$

Appendix D

TEST VEHICLE DETAIL DESIGN ANALYSIS

Sandwich Shell Strength Analysis. - The sandwich shell experiences external collapse buckling pressures which are actually local points of load application from each of the elements. If these points of load application are assumed to represent a continuous pressure equal to the crushing stress of the element then the shell can be checked for collapse buckling due to this pressure. The Karman-Tsien practical collapse buckling equation for a spherical shell is:

$$P_{CR} = .308\ E\ (t/R)^2$$

where t = shell thickness

R = shell mean radius

let t_f = sandwich shell facing thickness (.030 in.)

h = sandwich shell core thickness (1.0 in.)

then for equal flexural stiffnesses

$$t^3/12 = 1/2\ t_f(t_f + h)^2$$

substituting

$$t^3 = 6 \times .03 \times (1.03)^2 = .196$$

$$t^2 = .335$$

then substituting in the buckling equation:

$$P_{CR} = .308 \times 3.28 \times 10^6 \times .335/8.48^2 = 4{,}700 \text{ psi}$$

where the modulus stresses of elasticity for fiberglas in compression is

$$E = 3.28 \times 10^6 \text{ psi}$$

The crushing stresses and buckling margins for each system are:

Appendix D

	Crushing Stress psi	Buckling Pressure psi	Margin Of Safety
Honeycomb	700	4,700	570%
Composite	940	4,700	400%
Frangible Tube	1608	4,700	192%

The crushing stress of the elements of each system could cause permanent damage or even failure of the core material in local areas under each element. A section of the composite core was fabricated including three ply facing skins and a tube franging die was impressed against the surface simulating the actual franging force. A test value of twice the 3600 lb. franging force was applied and did not represent the limit of strength of the core, then the load was removed and the surface examined for permanent set. The examination indicated no sign of permanent deformation, and the test curve reproduced as figure D-1 showed no sign of permanent set for the die and sandwich section combination. This test was also proof of the die strength because is appeared to still be useable. A tabulation of margins of safety based on this proof test is given in figure D-1 also. The test vehicle total weight is 30 lb. including an allowance of 5.0 lb. for instrumentation, and since the calculated weight for the sandwich shell is 20.57 lb. an allowance of 4.43 lb. for packaging the instrumentation is made. Considering all weight items inside the sandwich shell and the weight of the shell itself, a design condition is reached from the inertia of these weight items which act as an internal pressure tending to burst the shell. A graphical solution of the design condition was made, and the results indicated that a maximum of 57 psi external pressure would be experienced from the inertia of the external landing system acting on the side away from the impact while the impacting side experiences a uniform burst pressure of 150 psi.

MARGINS OF SAFETY FOR TEST VEHICLE

(Core Crushing Permanent Deformation)

Landing System	Element Crushing Stress psi	Test* Compression Stress psi	Margin of Safety
Honeycomb Honeycomb	700	3217	360%
Composite Elements	940	3217	242%
Frangible Tube Elements	1608*	3217	100%

NOTE: No visible evidence of brinelling or permanent set of the test vehicle core material with facing plies attached.

* Based on a die area of 2.2379 in^2.

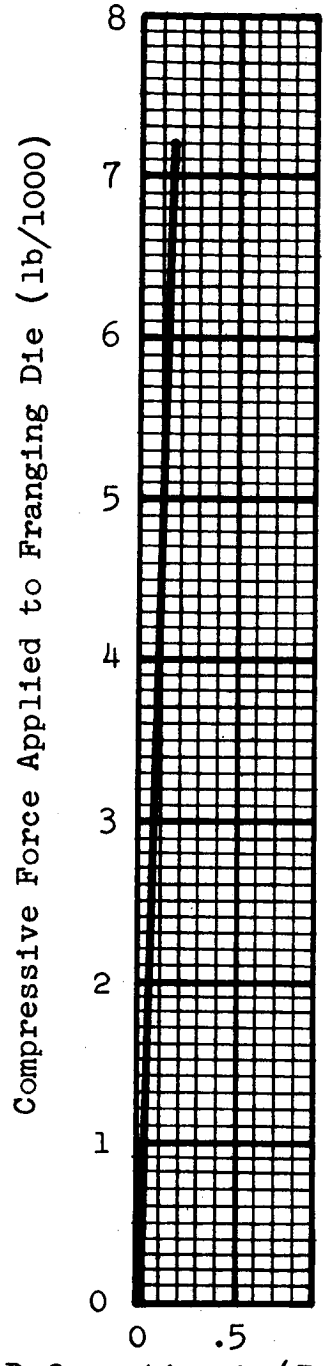

Figure D-1. Compressure Load Deformation Characteristics Of A Plastic Franging Die and Test Vehicle Syntactic Core Material Sandwich Element.

The burst strength of the sandwich shell with three ply fiberglas facings is:

$$P_{TU} = \frac{2 \times F_{TU} \times (2\ t_f)}{R} = 2 \times 35{,}000 \times .06/8.47 = 495 \text{ psi}$$

The margin of safety for this condition is the same for each landing system configuration and is as follows:

$$\text{M.S.} = 495/150 - 1 = 2.2 \text{ or } 220\%.$$

REFERENCES

1. Smith, Ronald H.; Development of A Radio-Frequency Transparent Energy-Absorbing Structural Element. NASA CR-253, July, 1965.

2. McGehee, John R.; A Preliminary Experimental Investigation of An Energy-Absorption Process Employing Frangible Metal Tubing. NASA TN D-1477, October, 1962.

3. Meyers, W. W.; A Radio Frequency Transparent Impact Energy Absorbing Material, AIAA 6th Structures and Materials Conference, Palm Springs, April, 1965.

4. Engelbrecht, T.; Hexcel Corporation Memorandum; Crush Strength of GF Honeycomb Materials. June 23, 1965.

5. Flora, C. L.; Impact Deceleration Systems Applicable To Lunar Landing Vehicles. Report 2324, Radioplane, Division of Northrop Corporation, Van Nuys, California, November 21, 1960.

6. McFarland, R. K.; Hexagonal Cell Structures Under Post-Buckling Axial Load. AIAA Journal, Vol. 1, June 1963.

7. Fisher, L., NASA, Langley; Graph, Anisotropy of Crushable Materials. June 1965

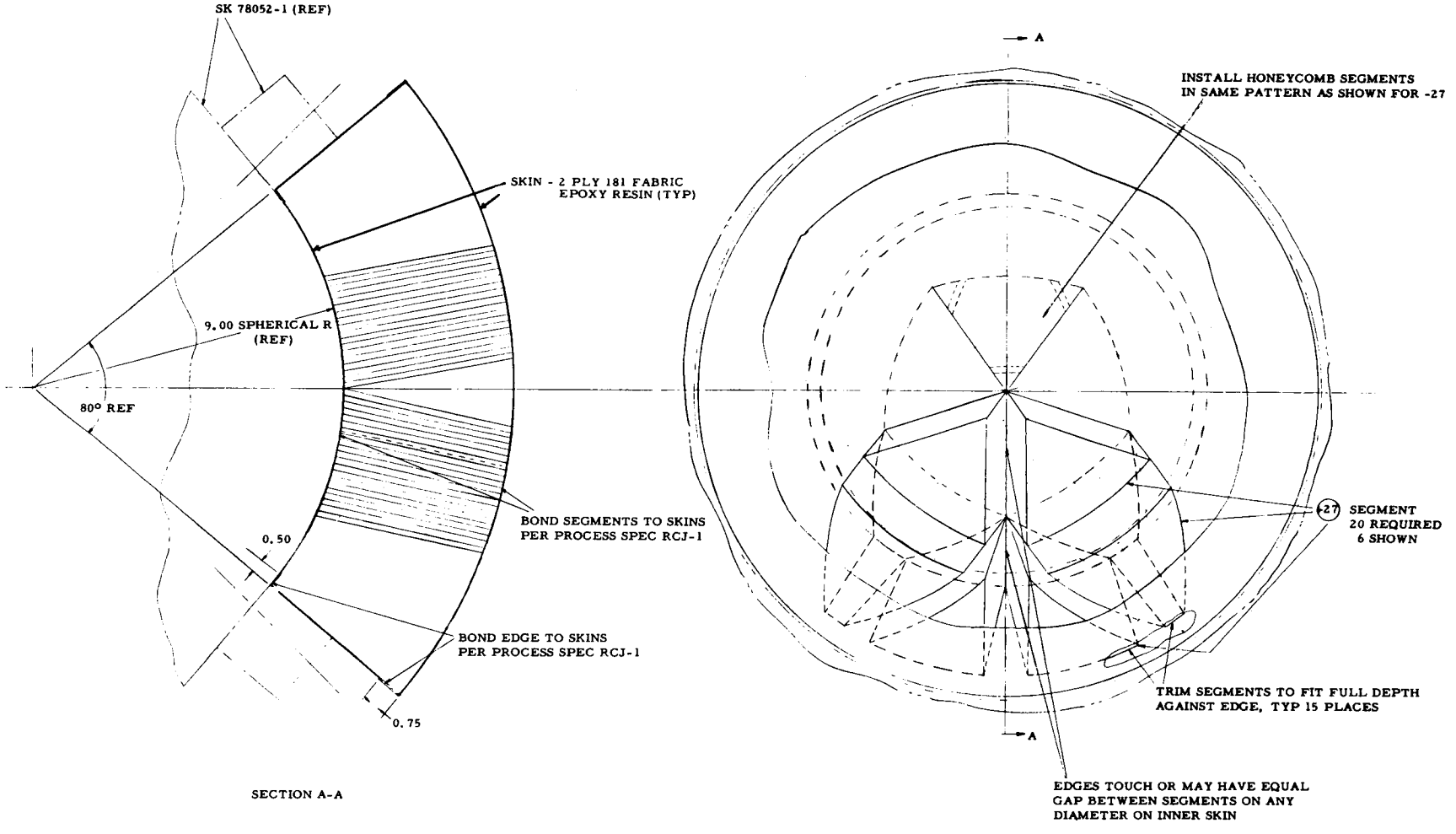

SK78054 - TEST SEGMENTS, HONEYCOMB AND COMPOSITE, ENERGY ABSORBTION

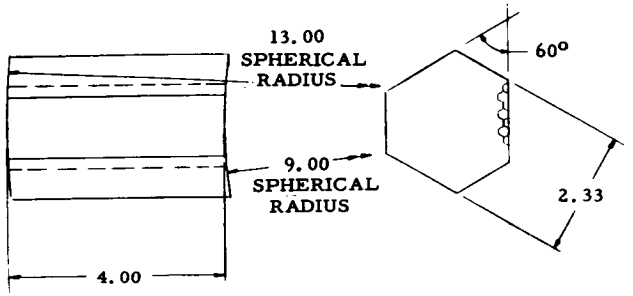

DETAIL -33

FOAM FILLED 6.5 LB/FT^3 HRP HONEYCOMB

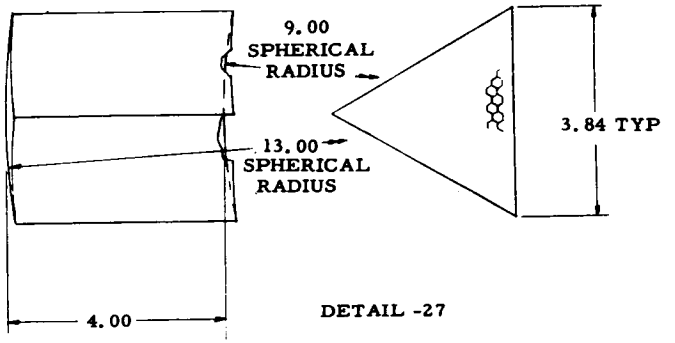

DETAIL -27

6.5 LB/FT^3 HRP HONEYCOMB

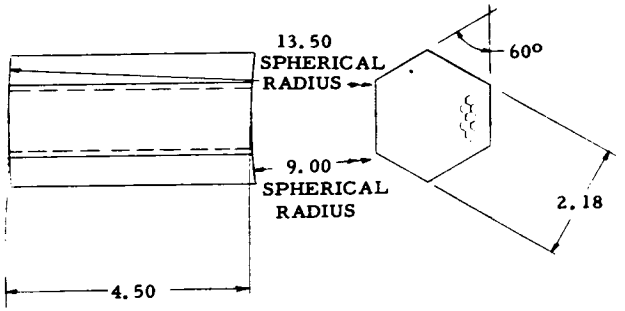

DETAIL -35

FOAM FILLED 6.5 LB/FT^3 HRP HONEYCOMB

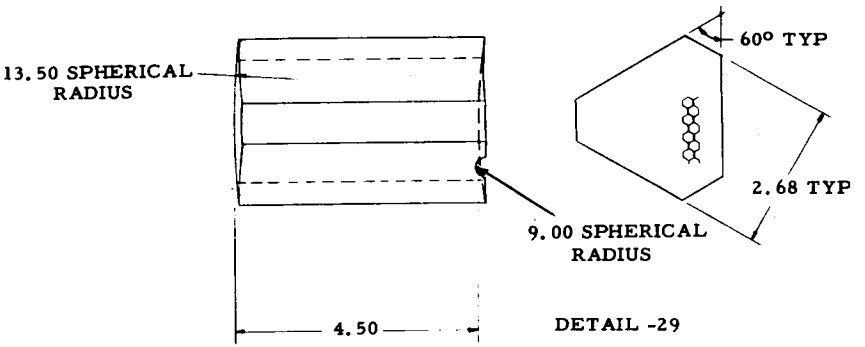

DETAIL -29

6.5 LB/FT^3 HRP HONEYCOMB

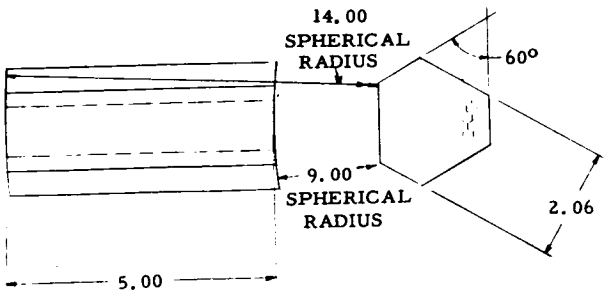

DETAIL -37

FOAM FILLED 6.5 LB/FT^3 HRP HONEYCOMB

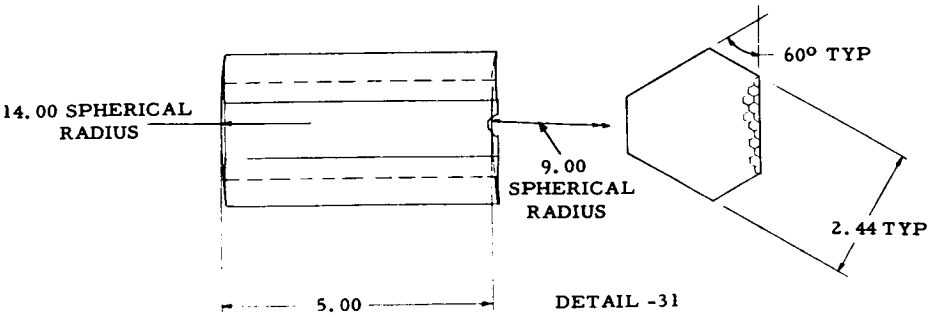

DETAIL -31

6.5 LB/FT^3 HRP HONEYCOMB

SK78054 - CONTINUED

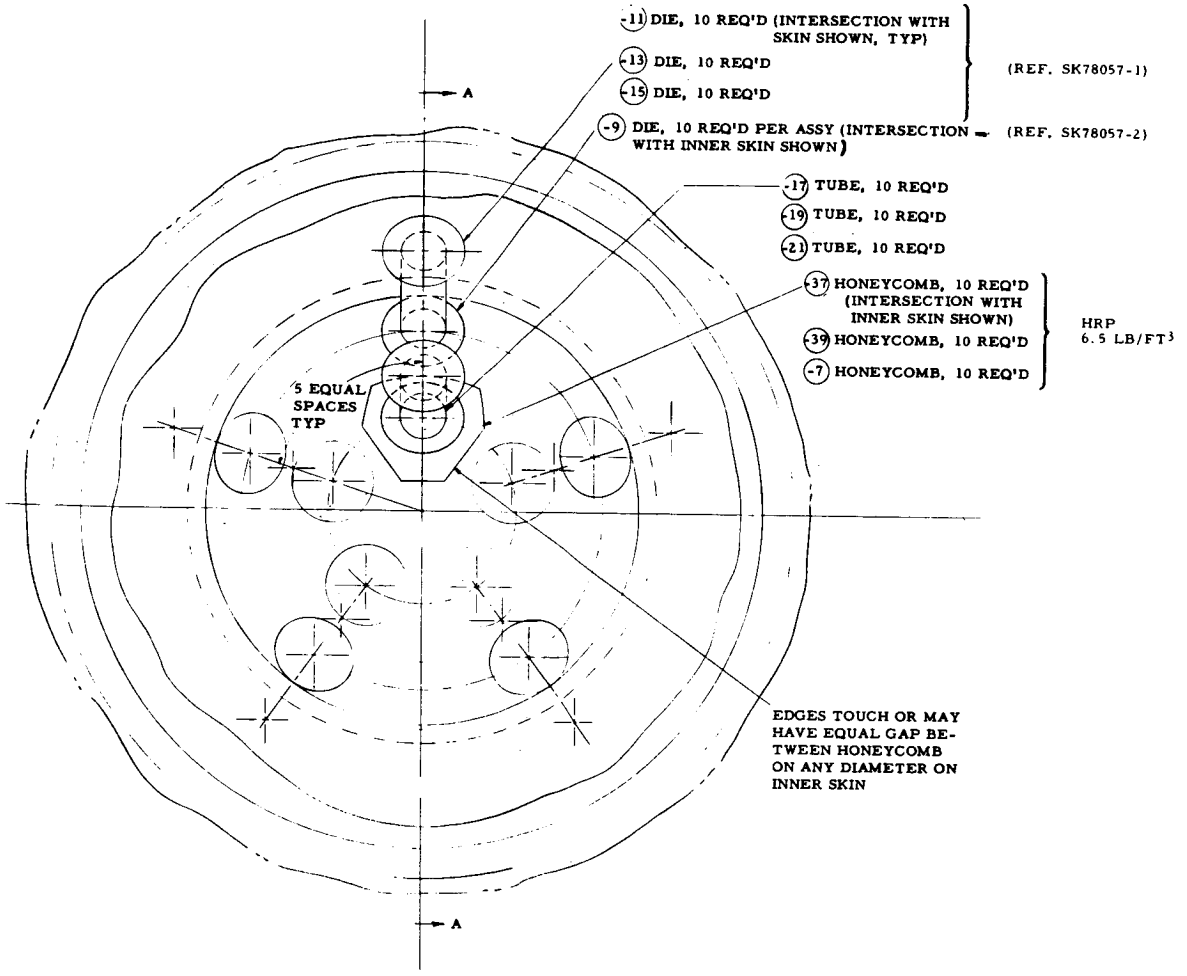

SK78055- TEST SEGMENTS, TUBE AND HONEYCOMB, ENERGY ABSORBTION

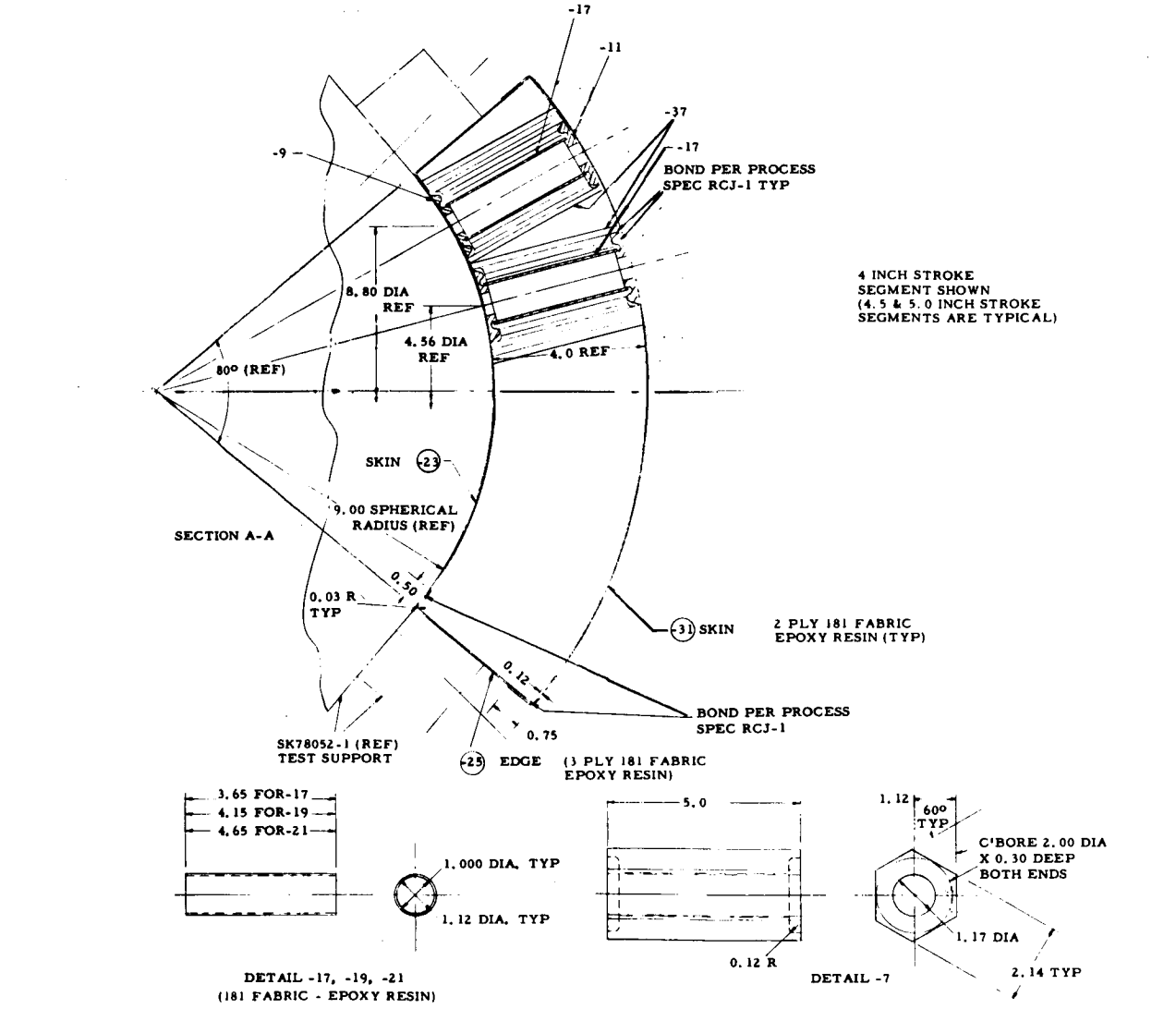

SK 78055 - CONTINUED

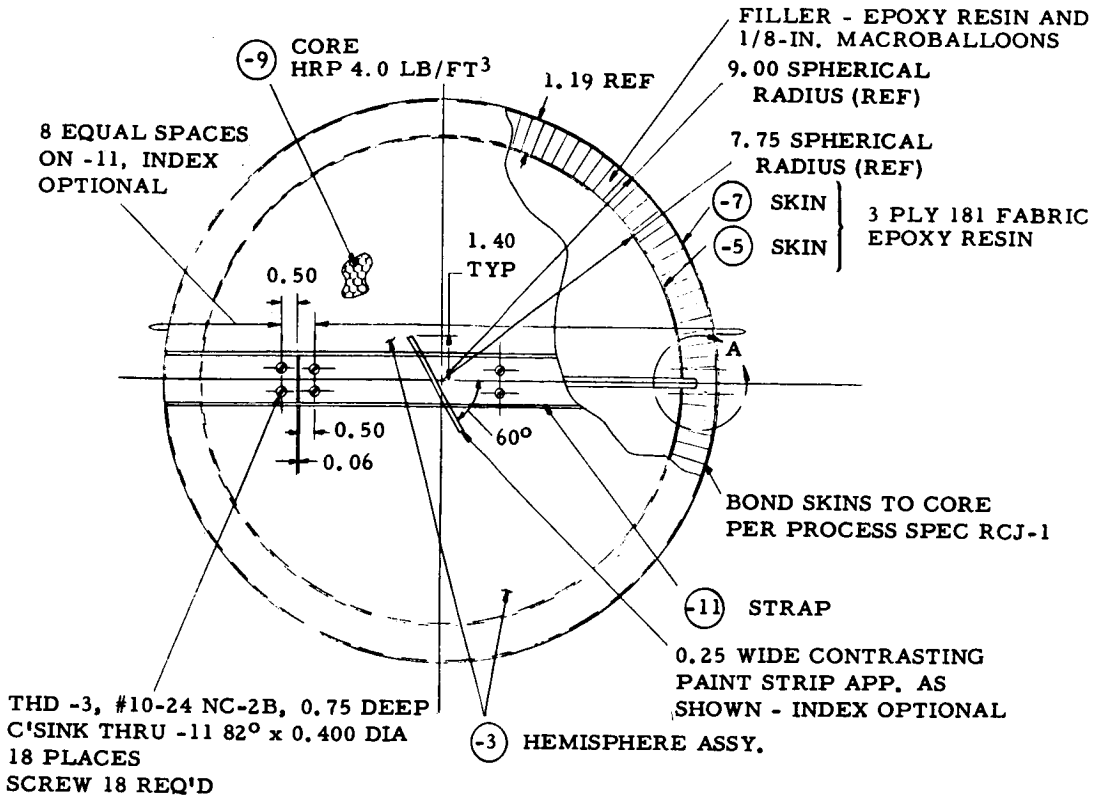

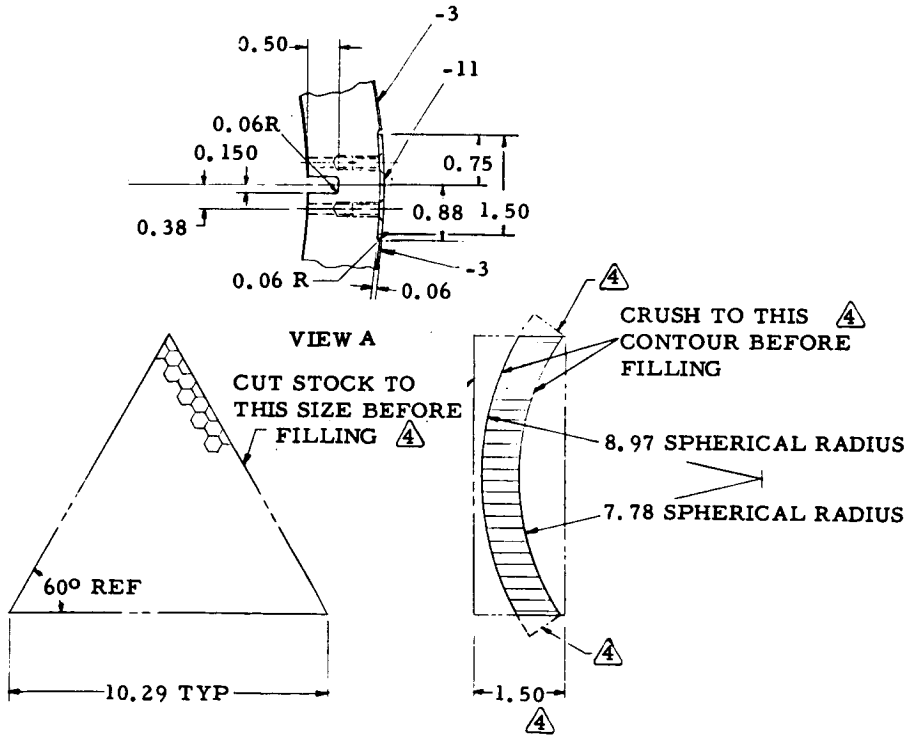

DETAIL -9

SK78056 - TEST VEHICLE SHELL, ENERGY ABSORBTION

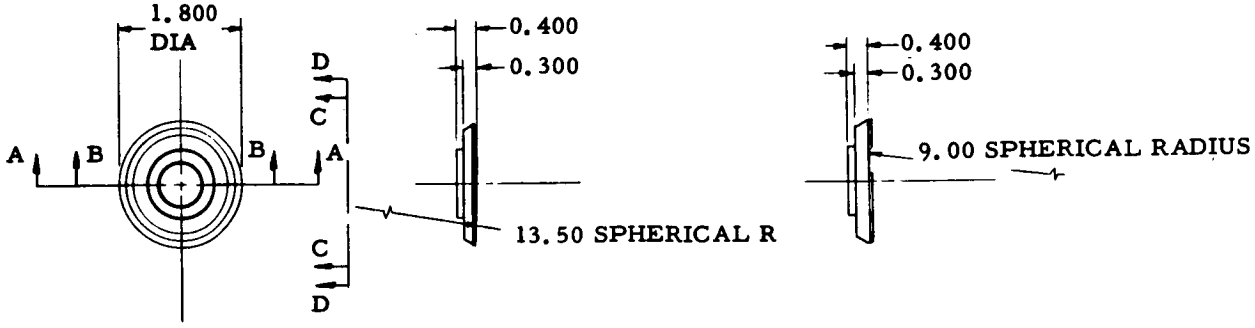

VIEW C-C
FOR -1 ONLY

VIEW D-D
FOR -3 ONLY

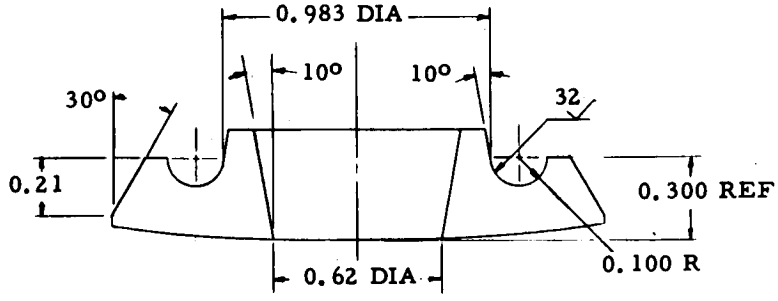

SECTION A-A
SCALE $\frac{4}{1}$
FOR -1 ONLY

MATERIAL:
PHENOLIC RESIN WITH
CHOPPED GLASS REINFORCEMENT
MIL-M-19833

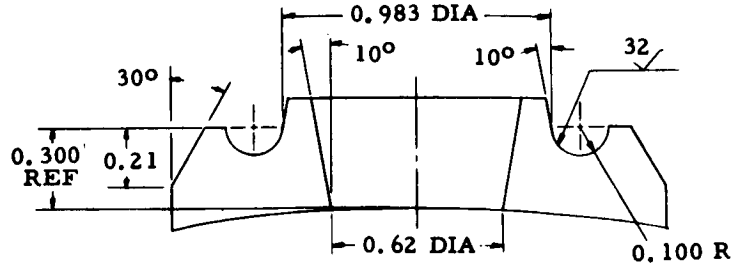

SECTION B-B
SCALE $\frac{4}{1}$
FOR -3 ONLY

SK78057 - DIE, ENERGY ABSORBTION